Fall | 2011

BCI Telemeter: Final Design

Washington University in St. Louis

Jessi Mischel, Lindsey Moses, Osasuyi Tongo

BME 401 Senior Design
Presented to: Dr. Klaesner, Dr. Yin, Dr. Anastasio
12/07/2011

Table of Contents

1.0 ABBREVIATIONS 5

2.0 NEED AND SPECIFIC REQUIREMENTS 6

2.1 NEED FOR BCI TELEMETER 6

2.2 PROJECT SCOPE AND DESIGN REQUIREMENTS 6

2.2.1 Project Scope 6

2.2.2 Design Requirements 7

3.0 OVERVIEW OF ANALYSIS USED TO CHOOSE DESIGN 8

3.1 ASIC 8

3.1.1 Multiplexer 8

3.1.2 ASP Block 10

3.1.3 ADC 12

3.1.3.1 Resolution 12

3.1.3.2 ADC Architecture 13

3.1.3.3 Overview 14

3.1.4 DSP Microchip 14

3.2 TELEMETER 15

3.2.1 Modulation Formats 15

3.2.2 Antenna 16

3.3 BATTERY 17

3.3.1 Battery Type 17

3.3.2 Recharging 19

3.4 CASING 20

4.0 OVERVIEW OF DESIGN 21

5.0 ANALYTIC EFFORTS NEEDED FOR DESIGN 22

5.1 ASIC 22

5.1.1 Resolution 22

5.1.2 Noise 23

5.1.2.1 Quantization Noise 26

5.1.2.2. Noise Shaping 27

5.1.3 Bandwidth and Sampling Speed 29

5.1.4 Anti-Aliasing Filter 30

5.2 TELEMETER 32

5.2.1 Modulation 32

5.2.2 Antenna 33

5.3 BATTERY 34

5.3.1 Current Consumption 35

5.3.2 Capacity 37

5.3.3 Voltage 38

5.3.4 TET System for Recharging 39

5.4 CASING 39

6.0 SPECIFIC DETAILS OF CHOSEN DESIGN 40

6.1 ASIC 40

6.1.1 ASP Block Wiring Diagrams 40

6.1.2 Printed Circuit Board 42

6.1.3 ASIC Components 44

6.1.3.1 Analog Switch 44

6.1.3.2 Instrumentation Amplifiers 45

6.1.3.3 Operational Amplifier for AA filter 46
6.1.3.4 Resistors for AA filter 47
6.1.3.5 Capacitors for AA filter 48
6.1.3.6 DSP Microchip with integrated 24-bit Delta-Sigma ADC 50
6.1.4 TI CC1101 Transceiver Specifications 54
6.1.5 Antenna 57
6.2 BATTERY 59
6.3 RECHARGING: TRANSCUTANEOUS ENERGY TRANSFER SYSTEM 61
6.4 CASING 64
6.4.1 Design Drawings 64
6.4.2 Polymer Coating: Parylene 64
6.5 SAFETY 65
7.0 SPECIFIC MATERIAL AND MANUFACTURING DEFINITIONS 67
7.1 ASIC 67
7.1.1 ASIC Components 67
7.1.2 Printed Circuit Board 68
7.2 CASING 68
7.2.1 Parylene Coating 69
7.2.3 TET System 70
7.3 OVERALL EXPENSES 70
8.0 CONCLUSIONS 71
9.0 REFERENCES 76
APPENDIX A. DESIGN SCHEDULE 77
LIST OF TASKS TO BE COMPLETED 77
Task 1: Project Scope - Due September 14 77
Task 3: Headstage Circuit Design 77
Task 4: Telemeter Circuit Board 78
Task 5: Case Design 78
Task 6: Web Page 78
Task 7: Progress Report and Presentation - Due October 26 78
Task 8: Risk Assessment 79
Task 9: Final Report and Presentation - Due December 7 79
Task 10: Senior Design Poster 79
DESIGN SCHEDULE 80
APPENDIX B. CONTACT INFORMATION AND TEAM ORGANIZATION 81
CONTACT INFORMATION 81
TEAM ORGANIZATION 81
APPENDIX C. COMPANY CONTACT INFORMATION 82
APPENDIX D. DESIGNSAFE 83
APPENDIX E. CODE USED FOR CIRCUIT ANALYSIS 85
ANALOG TO DIGITAL CONVERTER 85
ANTI-ALIASING FILTER 86
APPENDIX F. ADDITIONAL CAD DRAWINGS 89
APPENDIX G. COMPONENT DATA SHEETS 91
Analog Switch – TS3A4751 91
Instrumentation Amplifier – AD8236 93
Operational Amplifier – OPA2333 96

High Stability Thin Film Flat Chip Resistor *98*
Ceramic Chip Capacitor *99*
Microchip - MSP430AFE2x2 ..... *100*
Telemeter – TI C1101 ..... *102*
Antenna – 0868AT43A0020 ..... *104*
Li-Ion Battery – QL0200IA *107*
Titanium Alloy *108*

1.0 Abbreviations

AA - Antialiasing
ADC – Analog to digital converter
AIWN – Additive Independent White Noise
ASIC – Application Specific Integrated Circuit
ASP – Analog Signal Processing
BCI – Brain-Computer Interface
CMOS - Complementary metal–oxide–semiconductor
CMRR – Common Mode Rejection Ratio
DSP – Digital Signal Processing
ECoG – Electrocorticography
ENOB – Effective Number of Bits
ESR – Equivalent Series Resistance
IC – Integrated Circuit
IP – Intellectual Property
LSB – Least Significant Bit
MLCC – Multi Layer Ceramic Circuit
MCU – Microcontroller Unit
Op-Amp – Operational Amplifier
OSR – Oversampling Ratio
RF – Radio Frequency
RM - Receiving Mode
SNR – Signal-to-Noise Ratio
TCR – Temperature Coefficient of Resistance
TI – Texas Instruments
TM – Transmitting Mode

2.0 Need and Specific Requirements

2.1 Need For BCI Telemeter

Brain-computer interfaces (BCI) allow subjects to control devices using their own brain signals. The signals are sent through a series of filters and amplifiers to a digital signal processor where they are converted into an output communicating the user's intent. BCI is very useful for patients with severe motor disabilities because it gives them a way to communicate and interact with their environment. Current BCI technology requires a wired connection in which external cords are used to carry the brain signals from an electrocorticography (ECoG) electrode array on the dura of the brain to a digital signal processor. The presence of this external wiring poses two major problems: the subject has limited mobility and the exposed leads carry a risk of infection.

2.2 Project Scope and Design Requirements

2.2.1 Project Scope

To address the problems of percutaneous leads leading to CNS infection and limited subject mobility leading to limited recording time, a modular system was designed to process signals from the brain and wirelessly transmit them to an external receiver. A multi-channel Application Specific Integrated Circuit (ASIC) containing an Analog Signal Processing (ASP) module amplifies and filters the ECoG signals. The output of this module goes through an Analog-to-Digital converter (ADC) and is then sent to a Digital Signal Processing (DSP) unit where a power spectrum is produced. A telemetry module will transmit the processed signals to a receiving agent. When the computer or intermediate device receives the transmitted power spectrum, an algorithm will compare

the signal to baseline recordings and modulations from baseline will be used to establish brain control. The ASP, ADC, DSP, and telemetry modules will be contained in a casing with a biocompatible film on the outside to allow for implantation in the body. An implanted rechargeable battery will serve as the power source for the device.

2.2.2 Design Requirements

The proposed system will support the following features:

- Able to record signals with amplitude 1-10 μV with ability to distinguish modulation down to 300 nV
- Telemetry to PC for 8 ECoG channels in either raw (2000 Hz) or processed (20 Hz) modes
- Each of the 8 channels chosen from one of eight groups of 4 electrodes with reference chosen from one of four electrodes
- Bidirectional RF (radio frequency) link for system configuration, control, and data telemetry
- Low-noise electronics offering high Signal-to-Noise Ratio (SNR) and Common Mode Rejection Ratio (CMRR)
- Low-power, rechargeable battery-operated
- Variable RF data rates (and power consumption) of up to 500 kHz
- One week of typical use between recharge cycles
- Transmit signals at least 50 feet
- MSP430 Microcontroller
- TI CC1101 Transceiver
- Cost < $5,000

3.0 Overview of Analysis Used to Choose Design

3.1 ASIC

The ECoG signals recorded from the brain are transmitted through fiber optics to the BCI Telemeter. At this initial point of the system, the signals begin to be processed using the headstage module. The term "headstage" refers to processing block in which the signals are filtered and amplified. The purpose of the headstage module is to consolidate multiple analog integrated circuits along with the required digital signal processing (DSP) functions into a custom Application Specific Integrated Circuit (ASIC). This multi-channel ASIC will be paired with a commercially available Radio Frequency (RF) telemetry chip to transmit brain signals to an external computer.

The ASIC receives input from a 32-channel µECoG electrode array implanted epidurally on the subject's brain. The 32 electrodes are organized into eight groups of four electrodes. One electrode from each bank of four can be selected for processing and telemetering, leading to a total of 8 processed channels.

3.1.1 Multiplexer

An electronic multiplexer allows for several signals to share one device or resource, such as an ADC or communication line, instead of requiring one device per input signal. An analog switch selects one of several analog signals and forwards the selected input on to the next component.

Eight channels are chosen from the 32 channels of the µECoG electrode array, one from each of the eight groups of four electrodes that share a reference. Analog switches select

these channels before the signals are sent to the ASP block. From this point there are two options: eight separate ASP blocks can process the analog signals individually and send them to eight ADCs, or a multiplexer can be used to allow all eight channels to be processed by one ASP block and go on to one ADC.

Table 1 contains a Pugh Chart that compares options for multiplexer configurations. The input values range from 1-100 and are weighted based on the priority of the design specifications.

Table 1: Pugh chart comparing options for multiplexer configurations

Multiplexer		
	8 Separate ASP Blocks	**Multiplex Signals Before ASP**
Signal Fidelity (x10)	95	35
Speed (x5)	85	65
Space (x3)	35	98
Cost (x2)	45	95
Total	**1570**	**1159**

Even though using eight separate ASP blocks and eight separate ADCs is more expensive and requires more space, the speed and signal quality that result from this configuration makes it the desirable choice for the BCI telemeter.

The schematic for the chosen option is shown in Figure 1 below.

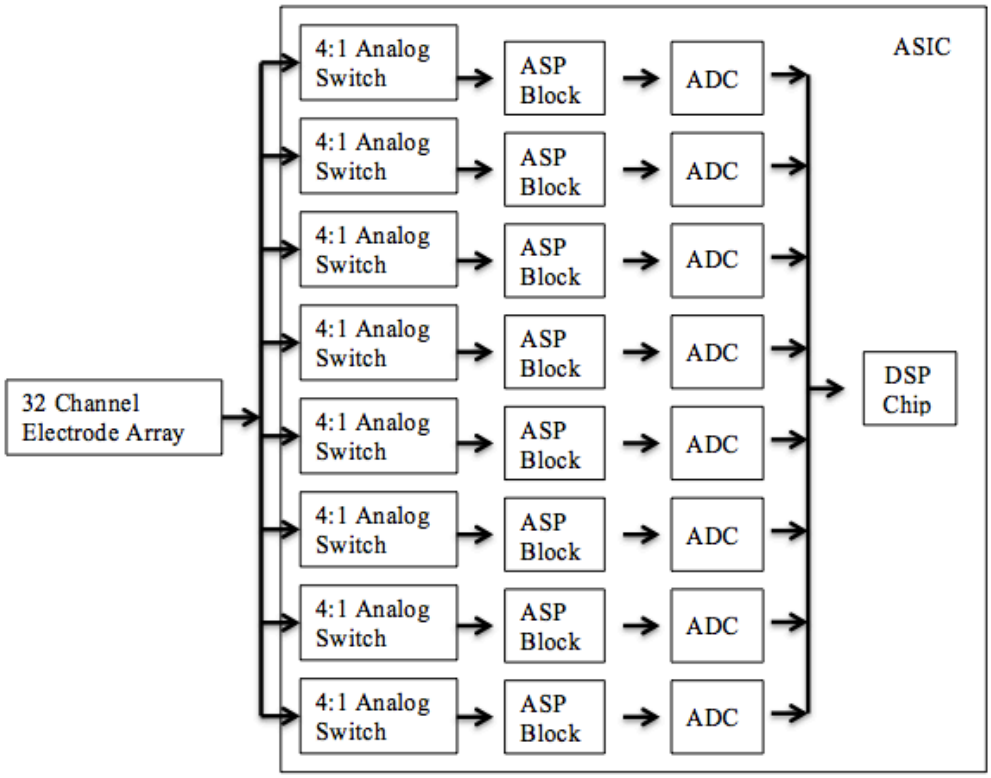

Figure 1: Schematic for first ASIC option using eight 4:1 analog switches, eight ASP blocks, and eight ADCs leading to one DSP chip with eight inputs

3.1.2 ASP Block

Two factors must be considered in choosing amplifiers to use in the ASP Block:

1. ECoG signals are in the microvolt range so even a small amount of noise dramatically influences control. Caution must be taken to amplify the signal of interest while attenuating the noise.
2. The electrodes used for ECoG are small and have large electrical impedances, on the order of a mega-ohm in the frequency band of interest [1].

The input voltage coming into an op-amp sees an impedance load composed of the impedances of the input components and the amplifier input impedance. When the signal

source has significant resistance, as the ECoG electrodes do, the external load on the input signal will have detrimental effects on the amplifier performance. Figure 2 models the transmission of a brain signal to the ASP block.

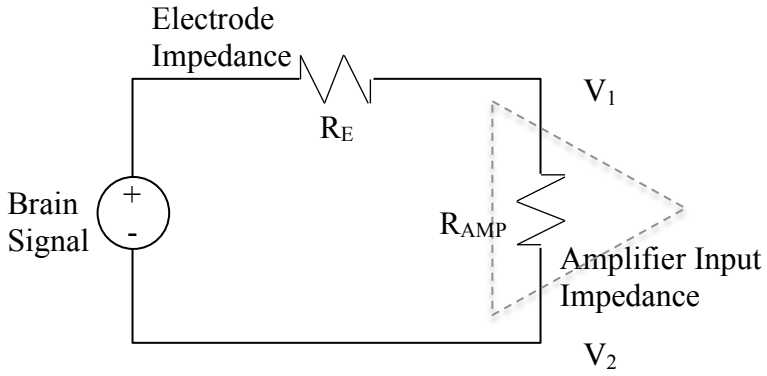

Figure 2: Circuit model of the transmission of a recorded brain signal to the ASP block

To accurately measure voltage, the input impedance of the amplifier should be considerably larger than the impedance at the recording site, or the electrode impedance. If this is not the case the signal could be attenuated and distorted.

Table 2 contains a Pugh Chart that compares options for the front end of the ASP block. The input values range from 1-100 and are weighted based on the priority of the design specifications.

Table 2: Pugh chart comparing options for the front end of the ASP block

Front End of ASP Block			
	Buffer	**Differential Amplifier**	**Instrumentation Amplifier**
Common Mode Rejection (x8)	0	98	98
Input Impedance (x5)	95	50	95
Cost (x2)	95	65	50
Total	665	1164	**1359**

An instrumentation amplifier is a type of differential amplifier that has been outfitted with buffers before each of its inputs, effectively lowering the source impedance and eliminating the need for higher input impedance in the differential amplifier. The input buffers lower the impedance of the inputs V_1 and V_2 from one mega-ohm to around 50 ohms; the input impedance of the differential amplifier is then sufficiently larger than the source impedance and is effective for common mode rejection.

3.1.3 ADC

An ADC is a device that converts a continuous signal to a discrete-time digital representation. In the BCI Telemeter, analog brain signals must be digitized before being transferred to the DSP block.

3.1.3.1 Resolution

Resolution indicates the number of discrete values that can be produced over the range of analog values. Electrical resolution is expressed in volts; the minimum change in voltage required to guarantee a change in the output code level. Table 3 contains a Pugh Chart that compares options analog to digital converter resolution. The input values range from 1-100 and are weighted based on the priority of the design specifications.

Table 3: Pugh chart comparing options for ADC resolution

Analog to Digital Converter			
	<16-Bit ADC	**16-Bit ADC**	**24-Bit ADC**
Resolution (x6)	10	80	98
Need for additional Analog Processing (x2)	0	60	90
Cost (x1)	90	65	50
Total	150	665	**818**

Although 24-bit ADCs are more expensive than their 16-bit counter parts, the cost of additional op-amps, resistors, and capacitors necessary in the 16-bit configuration for signal amplification raise the cost of the 16-bit ADC above that of the 24-bit ADC.

3.1.3.2 ADC Architecture

ADCs can be classified into two main categories based on the sampling rate of the input analog signal: 1) Nyquist-rate ADCs and 2) over-sampling ADCs. Table 4 contains a Pugh Chart that compares options analog to digital converter architectures. The input values range from 1-100 and are weighted based on the priority of the design specifications.

Table 4: Pugh Chart comparing options for ADC architectures

Analog to Digital Converter – Type		
	Nyquist-Rate ADC	**Oversampling ADC**
Resolution (x10)	65	100
Accuracy (x5)	55	95
Speed (x1)	80	45
Cost (x2)	30	80
Total	1065	**1680**

Oversampling ADCs can provide resolution as fine as 24 bits by trading off resolution for speed. ECoG recordings, for example, have magnitudes in the microvolt range, meaning that for accurate digital processing the signal must be amplified significantly before it is digitized, or it must be digitized with corresponding microvolt resolution. Physiological signals propagate relatively slowly so using an oversampling ADC is ideal for recording ECoG signals.

3.1.3.3 Overview

Table 5 contains a Pugh Chart that compares options for overall ADC configurations. The input values range from 1-100 and are weighted based on the priority of the design specifications.

Table 5: Pugh chart comparing overall ADC configurations

Analog to Digital Converter - Overall				
	Nyquist-Rate 16-Bit ADC	**Oversampling 16-Bit ADC**	**Nyquist-Rate 24-Bit ADC**	**Oversampling 24-Bit ADC**
Resolution (x10)	65	80	90	95
Need for Additional Amplifiers (x3)	60	60	85	95
Cost (x1)	40	98	15	85
Total	870	1078	1170	**1320**

While the 24-bit Nyquist-rate ADC and the 24-bit oversampling are comparable in most of their characteristics, the lower cost of using an oversampling ADC makes it the better choice for the BCI Telemeter.

3.1.4 DSP Microchip

Digital signal processing algorithms typically require a large number of mathematical operations to be performed quickly and repetitively on a set of data. The DSP software for the BCI Telemeter is encoded on a microchip that uses the output of the ADC as its input. As a specification for this project, the DSP software required for the BCI Telemeter has been provided, and preliminary testing has been done using a low power microcontroller.

The microcode written for the BCI Telemeter is compatible with the Texas Instruments (TI) MSP430 Microcontroller given in the design specifications. The MSP430 MCU is designed specifically for ultra-low-power applications. Its flexible clocking system, multiple low-power modes, instant wakeup and intelligent autonomous peripherals enable true ultra-low-power optimization, dramatically extending battery life. The MSP430 family offers over 25 packages to ensure that it fits the needs of the device in which it is being used; it also supports devices as small as 3x3 mm [4]. The MSP430 Microcontroller nicely addresses the BCI Telemeter's power consumption specifications and limited space requirements.

3.2 Telemeter

3.2.1 Modulation Formats

Signal modulation allows the transmission of the processed signals at a specific frequency while keeping the frequency response of the ECoG data intact. The signal is sent from the transmitter to receiver in a carrier wave; once it reaches the receiver it is demodulated and the original signal is reproduced. Table 6 is a Pugh chart outlining the parameters used to determine what modulation format is best for the BCI Telemeter. The input values range from 1-100 and are weighted based on their priority.

Table 6: Pugh chart comparing parameters of modulation format

Modulation Formats		
	Frequency Modulation	**Amplitude Modulation**
Cost (x2)	60	90
Signal Quality (x5)	90	90
Transmission Distance (x1)	80	95
Total	650	**725**

Transmission distance is greater for AM than FM, but signals will not need to be transmitted large distances in the applications the BCI Telemeter is intended for, so transmission distance was given the lowest weighting. Cost is a factor in all decisions regarding the design, but in this case signal quality is much more important than cost. The result of the Pugh chart in Table 4 determine that amplitude modulation will be used to transmit signals from the ASIC to an external computer in BCI applications.

3.2.2 Antenna

The most critical component of a wireless transmission system is the antenna. An antenna has two modes: the transmit mode in which it transforms electrical signals into RF electromagnetic waves propagating into free space, and the receiving mode in which it transforms RF electromagnetic waves back into electrical signals [2]. The antenna in the BCI Telemeter is responsible for communicating ECoG data from the ASIC to an external computer by sending electromagnetic waves in a specific frequency band. Table 7 is a Pugh chart comparing various parameters that must be considered when choosing an antenna. The input values range from 1-100 and are weighted based on their priority in the design.

Table 7: Pugh chart comparing parameters of different antenna types

Antenna Type				
	PCB	**Chip**	**Whip**	**Wire**
Size (x8)	50	95	30	85
Cost (x2)	95	85	30	99
Performance (x5)	60	75	95	50
Total	890	**1305**	775	1128

The chip antenna offers the best size solution and scores second highest on performance. Overall, the chip antenna is the best option and will be used to transmit signals in the BCI Telemeter.

3.3 Battery

The device is fully implantable so it needs to have a rechargeable battery that can be charged from an external source as stated in the specifications. A rechargeable battery is crucial so that surgery is not required to repower the system once the charge has been depleted. High levels of power are continuously available between charges, and once the battery's charge is depleted an external power source can reverse the electrochemical reaction and recharge the battery from outside the body. As a result the battery system does not restrict the lifetime of the device.

3.3.1 Battery Type

To meet the specifications of low power consumption and continuous power delivery, the battery must balance characteristics such as voltage, power delivery, discharge rate, efficiency, cycle life and energy density. Tables 8 and 9 contain Pugh Charts that compare battery types. The input values range from 1-100 and are weighted based on the priority of the design specifications.

Table 8: Pugh Chart comparing battery types (1-6)

Battery Type						
	Lead Acid	**Alkaline**	**Nickel-Iron**	**Nickel-Cadmium**	**Nickel-Hydride**	**Nickel-Zinc**
Safety (x10)	5	60	55	25	30	45
Size (x7)	5	60	60	70	75	70
Energy Density (x5)	20	55	40	30	60	50
Power (x3)	30	10	32	50	70	98
Efficiency (x3)	80	65	65	75	50	66
Discharge Rate (x3)	30	95	5	10	12	20
Cycles (x3)	70	50	65	70	100	30
Life (x1)	90	75	100	60	10	50
Voltage (x1)	90	80	70	70	80	8
Totals	995	2110	1841	1635	1911	1890

Table 9: Pugh Chart comparing battery types (1-6)

Battery Type					
	Lithium-Ion	**Lithium-Ion-Polymer**	**Silver Zinc**	**Zinc Bromide**	**Zinc-Carbon**
Safety (x10)	90	95	80	75	75
Size (x7)	90	100	80	80	80
Energy Density (x5)	95	100	92	90	65
Power (x3)	95	100	50	65	70
Efficiency (x3)	85	95	75	80	77
Discharge Rate (x3)	75	35	60	65	40
Cycles (x3)	75	65	75	40	30
Life (x1)	25	20	75	70	65
Voltage (x1)	85	90	75	80	90
Totals	3105	3145	2790	2660	2441

The scores in the Pugh charts above show that a Lithium-Ion-polymer system would be the most suitable battery for the BCI Telemeter. The scores between the lithium-ion and lithium-ion-polymers systems are the two highest. This is primarily due to the fact that safety is given such a high weight in the Pugh chart. Even though many batteries score well in power and energy categories, they are not suitable for implantation in the body.

Lithium ion batteries and lithium-ion-polymer batteries have similar characteristics, and thus, similar scores in the Pugh chart above. The main difference between the two systems is their size, which is primarily influenced by the difference in the electrolyte used. The lithium-ion-polymer system uses a polymer as an electrolyte, while the lithium-ion system uses a liquid electrolyte gel. The liquid electrolyte of the lithium-ion battery requires secondary packaging to safely contain some flammable active ingredients. As a result, this additional packaging increases the weight and cost and limits the size flexibility. Additional weight and size decrease energy density scores. Lastly, there is no free liquid electrolyte in lithium-ion-polymer batteries, which increases stability and leaves the components less vulnerable to problems caused by overcharging, damage, or leakage. The lithium-ion-polymer battery scores slightly higher in the safety, size, and energy density categories and is the best choice for the BCI Telemeter.

3.3.2 Recharging

Table 10 is a Pugh chart comparing systems for recharging the battery. The input values range from 1-100 and are weighted based on the priority of the design specifications.

Table 10: Pugh chart with values that compare the Transcutaneous Energy Transfer System and the photovoltaic system.

Battery Recharging Systems		
	TET	**Photovoltaic**
Safety (x5)	95	75
Conductivity (x4)	80	80
Toxicity (x3)	90	85
Power Conversion Rate (x2)	95	95
Cost (x2)	95	80
Total	1445	1300

The Pugh chart indicates that the TET system is the best rechargeable system. This is primarily due to differences in safety and toxicity. Since the photovoltaic system has not been fully tested on human subjects, it received a lower safety score. In addition, its cost score incorporates the need for future FDA regulations and cost for approval.

3.4 Casing

The main component of the BCI Telemeter casing is titanium, but design enhancements affect a few of the characteristics such as biocompatibility, safety and strength. The Pugh chart in Table 11 compares casing options. The input values range from 1-100 and are weighted based on the priority of the design specifications.

Table 11: Comparison between three methods for producing the casing

Casing Options			
Casing Material	**Pure Titanium**	**Titanium Alloy**	**Titanium Alloy + Hydrogel**
Safety (x5)	80	90	100
Biocompatibility (x4)	90	80	100
Corrosion Resistance (x3)	90	90	100
Strength (x3)	100	90	80
Durability (x3)	100	100	90
Flexibility (x2)	80	100	90
Weight (x2)	80	100	90
Cost (x1)	90	90	70
Total	2040	2100	2140

The Pugh chart shows that the titanium alloy with a hydrogel polymer biolayer is the best design. The hydrogel combines the best elements of the other two designs, but incorporates a component that enhances the biocompatibility of the design. The biolayer increases the resistance to corrosion, which also makes it safer. Since safety is of the utmost concern in the design of the BCI Telemeter, the high score in the safety category is worth the increases in weight and cost.

4.0 Overview of Design

The final ASIC design includes eight 4:1 analog switches, an instrumentation amplifier at its front end, a 24-bit oversampling ADC, and a MSP430 Microcontroller for digital signal processing. While using a second multiplexer before the analog signal processing block conserves space and money, the potential signal distortion causes this option to be unsuitable for the BCI Telemeter. According to the analysis provided, an instrumentation amplifier is the most expensive option for the front end of the analog signal processing block, but it provides the necessary input impedance and common mode rejection ratio needed for high fidelity ECoG recordings. Using a 24-bit oversampling ADC provides the required resolution for accurate processing while avoiding the use of additional amplifiers in the ASP block. The output of the ADC will be processed by DSP software programmed on a microcontroller. The MSP430 addresses the BCI telemeter's power consumption specifications and limited space requirements.

The output of the ADC will be wirelessly transmitted via the TI CC1101 Transceiver and the signal carried using amplitude modulation. The TI CC101 Transceiver supports several types of antennas, and the BCI Telemeter will incorporate a chip antenna due to its small size and good performance.

The BCI Telemeter will be powered by a thin-filmed lithium ion rechargeable battery, chosen for its exceptional safety standards and small size. The battery is recharged through the skin using a transcutaneous energy transfer system.

All components will be enclosed in a biocompatible titanium-alloy case. This case will be hermetically sealed and implanted subcutaneously in the body.

5.0 Analytic Efforts Needed For Design

5.1 ASIC

5.1.1 Resolution

Resolution indicates the number of discrete values that can be produced over the range of analog values. Electrical resolution is expressed in volts; the minimum change in voltage required to guarantee a change in the output code level is called the least significant bit (LSB) voltage. The resolution Q of the ADC is equal to the LSB voltage. The voltage resolution of an ADC is equal to the full-scale voltage range (FSR) divided by the number of discrete voltage intervals (N):

$$Q = \frac{FSR}{N} \qquad \text{Eqn.1}$$

FSR and N are calculated as follows:

$$FSR = V_{High} - V_{Low} \qquad \text{Eqn.2}$$

$$N = 2^M \qquad \text{Eqn.3}$$

where V_{High} and V_{Low} are the upper and lower limits of voltage that can be recorded and M is the ADC's resolution in bits. An ADC with a resolution of 8 bits, for example, can encode an analog input to one of 2^8 discrete values.

Characteristics of a 24-bit ADC with $\pm$ 1.8V rails are:

$$Voltage\ Steps = N = 2^{24} = 16{,}777{,}216$$

$$Resolution = Q = \frac{3.6\ Volts}{16{,}777{,}216} = 214.6\ nV$$

Using an ADC with this resolution would not require ECoG signals to go through any analog amplification after the common-mode noise has been subtracted and before being digitized. A 10X gain can be added to the initial instrumentation amplifier to bring the resolution down even lower to 20.146 nV. A resolution this low is sufficient for high accuracy data processing and transmission.

Although 24-bit ADCs are more expensive than their 16-bit counter parts, the cost of additional op-amps, resistors, and capacitors necessary in the 16-bit configuration raise the cost of the 16-bit ADC above that of the 24-bit ADC.

5.1.2 Noise

The sampling theorem states that sampling frequency, f_s, must be greater than twice the maximum frequency of the input signal in order for the signal to be uniquely reconstructed without aliasing.

$$f_s > 2 * f_{max} \qquad \text{Eqn. 4}$$

The frequency $2*f_{max}$ is the Nyquist sampling rate, and half of this value, f_{max}, is the Nyquist frequency. Nyquist-rate ADCs operate with an input signal frequency close to half the sampling frequency and require a very sharp cutoff for the preamplifier or anti-aliasing filter. Though Nyquist ADCs are very fast, their resolution is limited by component matching and circuit non-idealities.

Over-sampling ADCs trade off resolution in time for increased resolution in amplitude. Oversampling is implemented in order to achieve cheaper higher-resolution analog to

digital conversion. To get n additional bits of resolution, the oversampling factor must be equal to

$$Oversampling\ Factor = 2^{2n} \qquad \text{Eqn. 5}$$

For instance, to implement a 24-bit converter, it is sufficient to use a 20-bit converter that can run at 256 times the target sampling rate. These ADCs oversample the desired signal and utilize digital filters to remove unwanted frequencies and to reduce the sample rate after the analog-to-digital conversion.

Oversampling ADCs trade off complexity in the analog block for complexity in digital processing. They circumvent the need for a sharp-cutoff (and therefore complex and expensive) continuous time anti-aliasing (AA) filter by sampling initially at an elevated rate, DF_S, when the final sampling rate is still F_S. An AA filter is still necessary, but only for protection against the high initial sampling rate. The large difference between the desired signal bandwidth and the new AA cutoff frequency at $DF_S/2$ means that the transition bandwidth of the filter is many times larger than its pass-band width and that the filter can be realized with less precise circuitry.

To accommodate the same final sampling rate F_S, the oversampled signal must be filtered further to suppress frequencies above $F_S/2$. This additional filtering, however, can occur digitally after the signal has been quantized. The signal is then down-sampled or decimated, completing the sampling process of signal acquisition by returning the sampling rate to F_S.

The frequency response of signal that has been sampled and quantized using a Nyquist frequency ADC is presented below in figure 3. To filter this signal using a low-pass antialiasing filter would require a steep drop-off due to the narrow transition band.

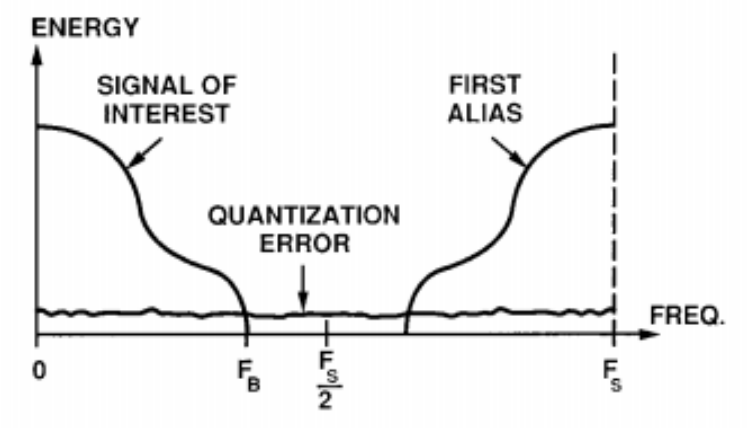

Figure 3: Frequency spectrum of sampled and quantized signal [1]

Figure 4 demonstrates how oversampling a signal removes the necessity for a sharp cut-off antialiasing filter by widening the separation between the signal and the first alias. This reduces the complexity of the analog filter, allowing further filtering to take place digitally.

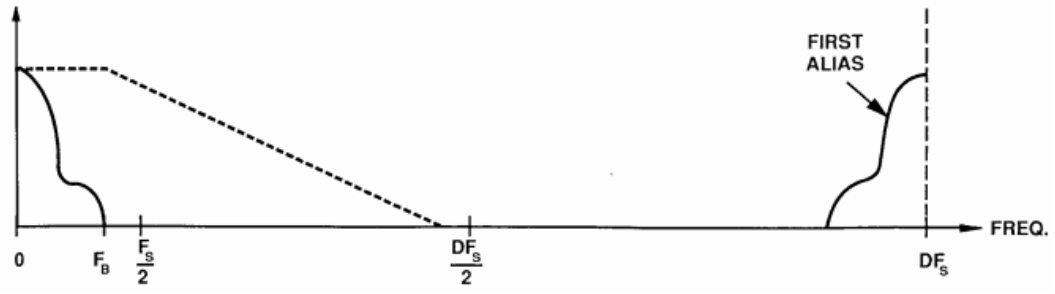

Figure 4: Frequency spectrum of sampled and quantized signal with oversampling [1]

5.1.2.1 Quantization Noise

Oversampling and decimation is also used to increase a quantizer's effective resolution. Quantization converts an analog signal from a continuous set of values to a discrete set of values, whereas sampling discretizes the time scale [1]. Provided that the sampling rate F_s exceeds twice the bandwidth of the analog signal, the original signal may in principle be reconstructed exactly from its samples.

Quantization is the process of mapping a large set of input values to a smaller set – such as rounding values to some unit of precision. When forcing an arbitrary signal value x to its closest quantization level x_q, this x_q value can be seen as x plus some error. We will denote that error as e_q (for quantization error):

$$x_q = x + e_q \quad \Leftrightarrow \quad e_q = x_q - x \qquad \text{Eqn. 6}$$

The quantization error is restricted to the range $-\frac{\Delta}{2}$ to $\frac{\Delta}{2}$, where Δ is the step size of the converter, so e_q will never be larger than half of the quantization step size. An ideal N-bit linear ADC tends to introduce a wide-band quantization error resembling additive independent white noise (AIWN) and thus appears to be uniformly distributed.

Figure 3 above shows that quantization noise occupies the same frequency range as the signal of interest when a Nyquist frequency ADC is used. In contrast, when a signal is oversampled, the quantization noise is spread out, occurring at an oversampled rate of DF_S. With the signal of interest occupying $F_S/2$, a digital low-pass filter will reduce the quantization noise power and the quantizer resolution will be increased. This is demonstrated in figure 5 below.

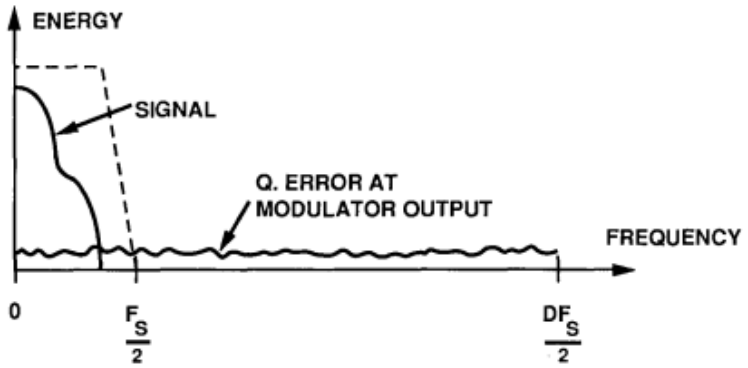

Figure 5: Oversampling for resolution enhancement

5.1.2.2. Noise Shaping

In many oversampling ADCs, a delta-sigma modulator shapes the quantization noise (see figures 6 and 7 below) so that the majority of the noise can be removed using low-pass filters, via a decimator.

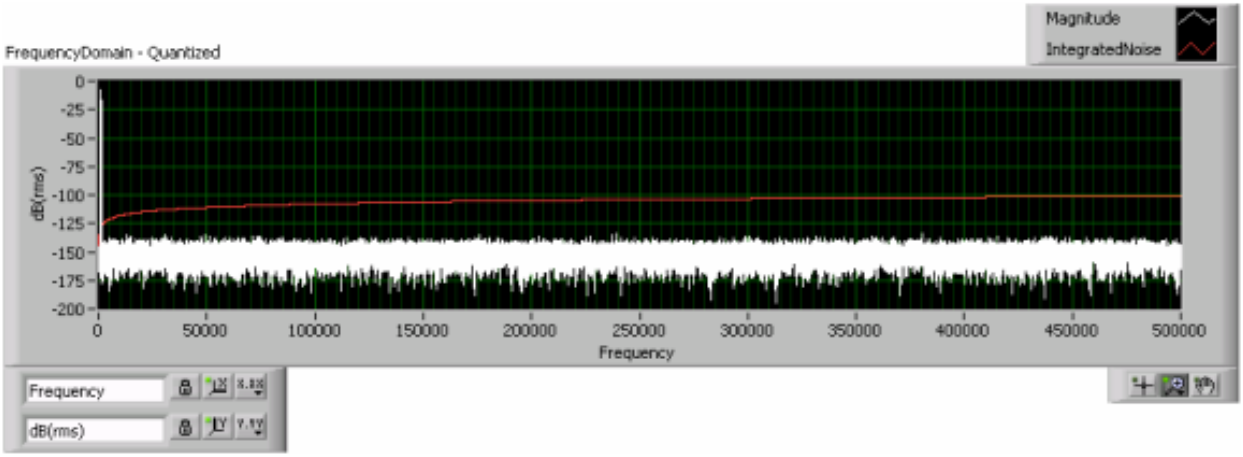

Figure 6: Flat quantization noise and integrated noise outside of signal band

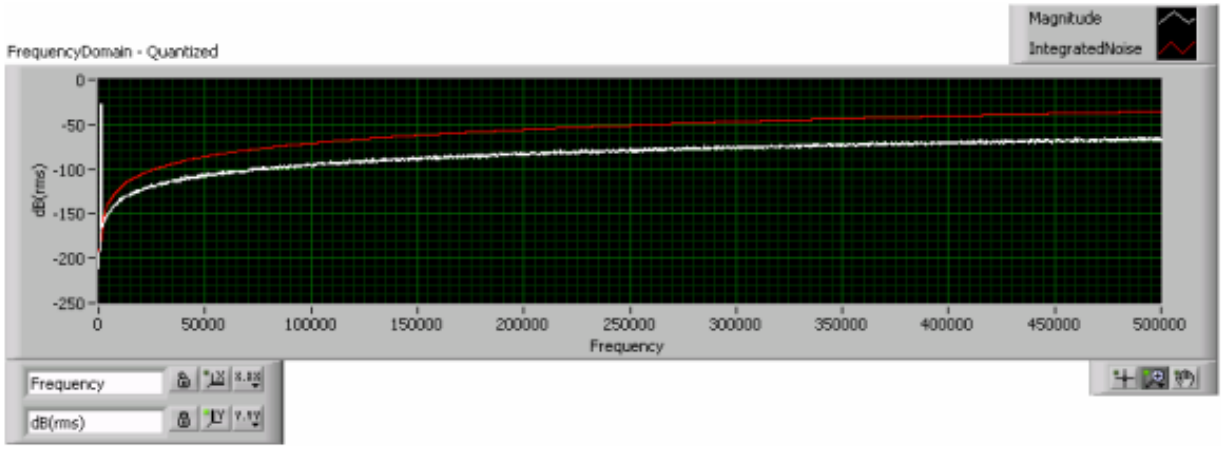

Figure 7: Shaped quantization noise and integrated noise

Shaping the quantization noise with a delta-sigma modulator provides the quantized noise power spectrum as demonstrated in figure 7. In this case, a low pass filter would be much more effective at removing quantized noise.

For a 2nd order delta-sigma modulator, about 2 ½ bits of resolution are gained per octave of oversampling, whereas if the quantization noise is flat, only ½ bit of resolution is gained per octave. This is demonstrated in figures 8 and 9 below. The LabVIEW code to produce these figures is provided in Appendix E.

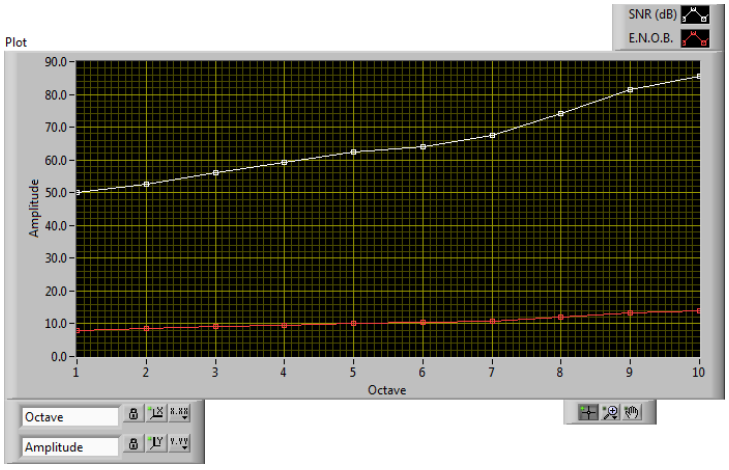

Figure 8: Plot demonstrating that in an N-bit Linear ADC (without noise shaping), resolution (Effective Number Of Bits, ENOB) increases by about ½ bit per octave of oversampling

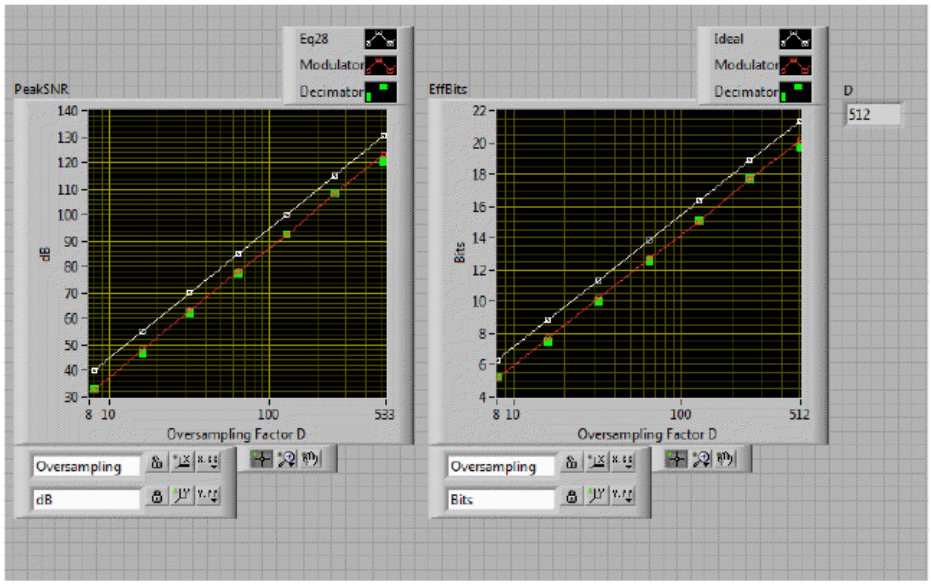

Figure 9: Plot demonstrating that in an Delta-Sigma modulator oversampling ADC (with noise shaping), ENOB increases by about 2½ bit per octave of oversampling (plot on the right)

Using a LabVIEW VI to measure the SNR and the ENOB, the trend of these parameters was observed as a function of the Oversampling Ratio (OSR). Figure 8 demonstrates that the SNR increase by about 3dB/octave and that the ENOB increase by about ½ bit/octave for the designed 8-bit ADC. Both the increase in SNR and ENOB do not appear to be linear, which is likely due to the fact that the quantization noise is not white.

Figure 9 demonstrates that the SNR value increases by about 15 dB/octave, plotted on the left axes, and that the ENOB increases by about 2.5 dB/octave, plotted on the right axes.

5.1.3 Bandwidth and Sampling Speed

It has been shown that the best frequencies for discrimination in control tasks are centered on the 75-105 Hz control band [2]. To capture the signal of interest, a base band of 200Hz is sufficient. For oversampling yielding 24-bit resolution, and with a delta-sigma ADC yielding 2.5 bits of resolution per octave of oversampling,

$$24\ bits * \frac{Octave}{2.5\ bits} = 9.6\ Octaves$$

$$D = Oversampling\ Factor = 2^{10} = 1024$$

Thus, we will need to oversample by 10 octaves, yielding a sampling frequency within the analog to digital converter of F_S = 204,800 Hz. The calculations are presented below.

$$200Hz * 1024 = 204{,}800\ Hz$$

Therefore, an ADC that samples at 1 MHz is sufficient for the BCI telemeter.

5.1.4 Anti-Aliasing Filter

A unity gain Sallen-Key topology second order low-pass butterworth filter was designed for anti-aliasing and implemented using the configuration below.

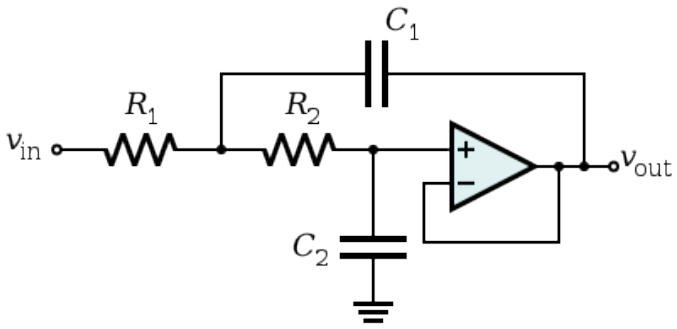

Figure 10: Sallen-Key topology second order low-pass filter schematic

The transfer function for this second-order unity gain low-pass filter is

$$H(s) = \frac{(2\pi f_c)^2}{s^2 + \frac{2\pi f_c}{Q} * s + (2\pi f_c)^2} \qquad \text{Eqn 7}$$

where the cut-off frequency f_c and the Q factor are given by

$$f_c = \frac{1}{2\pi\sqrt{R_1 R_2 C_1 C_2}} \qquad \text{Eqn. 8}$$

$$Q = \frac{\sqrt{R_1 R_2 C_1 C_2}}{C_2(R_1+R_2)} \qquad \text{Eqn. 9}$$

The BCI Telemeter requires a cut-off frequency for the anti-aliasing filter corresponding to the bandwidth, so the second order Sallen-Key anti-aliasing filter will be designed with a cut-off frequency of 200 Hz. A butterworth filter is chosen due to its maximally flat frequency response. In a butterworth filter, the quality factor is $Q = \frac{1}{\sqrt{2}}$ and the other variables can be solved for when the value of one element, R or C, is known. Matlab code presented in Appendix E calculated the resistor and capacitor values, given that $C_1 = 100\,nF$. The provided code solves for butterworth filters of several orders, and while higher order corresponds to a steeper cut-off, due to oversampling, the attenuation does not need to be steep and a second-order filter provides the necessary cut-off. The output of the program printed:

2-order Butterworth Lowpass at 200 Hz
Sallen-Key parameters:
C1: 1e-007
C2: 2e-007
R1: 5626.92301
R2: 5626.92301

To check these values, $R_1 = R_2 = 5.627\,K\Omega, C_1 = 100\,nF, and\ C_2 = 200\,nF$ were plugged into the equation 8 above and the cut-off frequency was calculated.

$$f_c = \frac{1}{2\pi\sqrt{(5.627 * 10^3)^2(100 * 10^{-9})(200 * 10^{-9})}}$$

$$f_c = 200\,Hz$$

5.2 Telemeter

The role of the telemeter is to wirelessly send brain signals from a transmitter on the ASIC to an external receiver. The specifications of the BCI Telemeter require implementation of the TI CC1101 Transceiver, which is compatible with the TI MSP430 Microcontroller being used. This is a low-power Sub-1 GHz RF Transceiver designed for wireless applications. RF Transmission uses radio waves to transmit signals from a transmitter to a receiver, and an antenna is used to send and receive signals.

5.2.1 Modulation

Modulation allows the transmission of the processed signals at a specific frequency while keeping the frequency response of the ECoG data intact. The signal associated with brain activity is transposed to a higher frequency where there is significantly less 1/f noise, amplified, then demodulated back to its original frequency band. The original signal is thus reproduced at the receiver. The equation for a sine wave is:

$$e(t) = A * \sin(\omega t + \emptyset) \qquad \text{Eqn. 9}$$

Varying A in the carrier wave results in amplitude modulation (AM). Amplitude modulation involves varying the strength of the carrier signal in relation to the signal of interest. An AM wave is the vector sum of three or more sine waves of different amplitudes, giving the appearance of a sine wave with varying amplitude in the time domain [3]. The TI CC1101 supports two types of amplitude modulation, On-Off Keying (OOK) and Amplitude Shift Keying (ASK) [4]. OOK modulation simply turns the power amplifier on or off to modulate ones and zeros respectively; it is the most basic type of

AM. ASK is a method of AM in which a finite number of amplitudes are each assigned a unique pattern of binary digits. Each pattern of bits forms a symbol represented by a particular amplitude and recognized by the demodulator, which determines the amplitude of the received signal and maps it back to the symbol it represents, uncovering the original data [5]. The advantage of ASK over OOK is that ASK allows programming of the modulation depth (the difference between 1 and 0), and shaping of the pulse amplitude [4]. The BCI Telemeter will use ASK modulation to send and receive brain signals.

5.2.2 Antenna

The most critical component of a wireless transmission system is the antenna. An antenna has two modes: the transmit mode in which it transforms electrical signals into RF electromagnetic waves propagating into free space, and the receiving mode in which it transforms RF electromagnetic waves back into electrical signals [6]. The antenna in the BCI Telemeter is responsible for communicating ECoG data from the ASIC to an external computer by sending electromagnetic waves in a specific frequency band.

The size of an antenna is based on the wavelength of the signal being transmitted; maximal power transfer occurs when the antenna is half -wavelength. A half-wavelength antenna is commonly referred to as a dipole antenna. One way to reduce antenna size is to place a quarter-wavelength antenna on a ground plane, which acts as the other quarter-wavelength and produces an effective half-wavelength antenna. A quarter-wavelength antenna is referred to as a monopole antenna. The TI CC1101 Transceiver is a low-power device operating below 1 GHz. The smallest size antenna that could be used with this transceiver is calculated below using equation 10.

$$Wavelength = \lambda = \frac{speed\ of\ electromagnetic\ wave}{frequency} \qquad \text{Eqn. 10}$$

$$\lambda = \frac{3 * 10^8 \frac{m}{s}}{1 * 10^9 \frac{1}{s}} = 0.3\ m$$

$$Antenna\ Length = \frac{\lambda}{4} = 0.075\ m = 7.5\ cm \qquad \text{Eqn. 11}$$

Factors to consider when choosing an antenna include size, cost, and performance. The BCI Telemeter has significant size restrictions since it must be fully implantable, but high performance is crucial for transmitting high fidelity signals. The TI CC1101 Transceiver can support several types of antennas; a chip antenna will be used for the BCI Telemeter. A chip antenna is an excellent option when board space is limited because it supports small solution sizes even for frequencies below 1 GHz.

5.3 Battery

The BCI Telemeter is powered by a lithium-ion-polymer based battery. The performance requirements for the battery are determined by the needs of the ASIC and Telemeter. Voltage (Volts), current (Amps) and charge capacity (amps-hour) are characteristics that must be considered when choosing an appropriate battery. Other factors such as the discharge rate, recharge rate, and life cycles are values that should be optimized, however, they are dependent on how the battery is used. To analyze the efforts of the battery, the following calculations determine how the device will utilize power.

5.3.1 Current Consumption

The internal components of the system use different amounts of current depending on the mode the device is in. To save power, the design incorporates a step down converter (TPS62730) that adjusts the amount of current used in order to minimize power consumption. The converter allows the telemeter to be in two different modes: ON and SLEEP. Another factor controlling how much current is being used is whether the device is transmitting a signal to the external computer or receiving feedback from the computer. This results in two additional modes: transmitting mode (TM) and receiving mode (RM). Table 12 shows the amount of current consumed by the Telemeter in each mode.

Table 12: Current Caluclation for the 2 main modes that the Telemeter

Current Calculations		
	Transmitting Mode (TX)	Receiving Mode (RX)
ON	34 mA	17 mA
Sleep	30 nA	30 nA

Equation 12 estimates the amount of current used during typical operations incorporating the amount of time the telemeter is ON (measured in seconds), the fraction of time spent in TM and the fraction of time spent in RM. Equation 13 is a simplification of equation 12 in which the current used in sleep mode is neglected since it is six orders of magnitude smaller than the current used in ON mode. The parenthetical value represents the average current while the Telemeter is in the ON mode. To calculate the average current, 5 different values of TM and RM fractions were used.

$$Current = ON(h) * (TM * 34mA + RM * 17mA) + Sleep(h) * nA \quad \text{Eqn. 12}$$

$$Current = ON(h) * (TM * 34mA + RM * 17mA) \quad \text{Eqn. 13}$$

Table 13 below shows estimated values of average current that the Telemeter may use and Table 14 shows the estimated amount of current that would be needed in a given 16 hour time period based on 5 different ratios of ON/Sleep. These ratios are based on the assumption that at peak activity moments the highest ON/Sleep ratios are about 25% per hour [9].

Table 13: The average current is calculated using 5 different ratios of transmitting/receiving modes of the Telemeter

TM Ratio	RM Ratio	Average Current (mA)
0.25	0.75	21.25
0.35	0.65	22.95
0.5	0.5	25.5
0.65	0.35	28.05
0.75	0.25	29.75

Table 14: Using the average current, the current consumption per hour is calculated based on varying ratios of ON/Sleep modes. These calculations use an average current while the unitless ratios account for the amount of time the battery in the ON/SLEEP mode.

ON (hours)	Sleep (hours)	Current (mA/hr)
0.8	15.2	2.04
1.6	14.4	4.08
2.4	13.6	6.12
3.2	12.8	8.16
4	12	10.2

To calculate the total current needed by the BCI Telemeter, the current needed for the ASIC must be considered. The current of the ASIC changes based on the signals that are being filtered and amplified. Simulations indicate that the current needed for the amplifiers of the ASIC model will vary between 100-220 uA. The total current is calculated using the highest value of 220uA.

Table 15: Total current is calculated based summing the currents from the Telemeter and the ASIC. The ASIC current calculations are based on an average current consumption of 22 mA, which is an estimation that is slightly above the mean value of the simulation range. Since the device can be in the either ON or SLEEP mode, the current calculations for both the Telemeter and ASIC components are based on similar estimations of ON/SLEEP ratios per hour in Table 14

Telemeter Current (mA)	ASIC Current (mA)	Total Current (mA)
2.04	0.22	2.26
4.08	0.22	4.3
6.12	0.22	6.34
8.16	0.22	8.38
10.2	0.22	10.42

5.3.2 Capacity

The capacity (mAmp-hours) is a measurement of how much charge is stored in the battery, and is the most important factor to consider when choosing the appropriate battery for a design. A higher capacity will increase the amount of time the device can run between charges. The analytical effort calculations of capacity are based on the amount of charge needed to run the device for a 24-hour period, recharging once a day. The following equations are needed to calculate the required capacity and use the estimated quantities for current usage calculated above.

Equation 14 is the starting equation that measures capacity using the estimated current over a 16 hour time period. (This assumes the device is inactive for at least 8 hours during the day).

$$Capacity(mA-H) = Current(mA) * Time(hours) \qquad \text{Eqn. 14}$$

Equation 15 adjusts the calculated capacity by incorporating a cutoff point at which the battery needs to be recharged. To increase the life of the battery and the safety of the device, the battery should not be run down to 0% of its capacity before being recharged. The variable F represents the percentage of charge depleted when a “low battery” signal

goes off to tell the user that the battery needs to be recharged. For the calculations in Table 16, F = .90 (90%). When the capacity is about 90% the user will need to recharge the battery using the TET recharging system.

$$Capacity' = Capacity/F \qquad \text{Eqn. 15}$$

Equation 16 adjusts for varying discharge rates when the battery is not in use. Depending on the type of battery this may affect the capacity of the battery. D represents a variable used to compensate for the additional required capacity. The lower the value of D the more the battery discharges when it's not in use. Since the BCI Telemeter utilizes a lithium-ion battery the discharge rate is very low and D is about 0.99.

$$Capacity'' = Capacity/D \qquad \text{Eqn. 15}$$

Table 16 contains the calculated capacities needed for the device to run over the specified 24 hour time period.

Table 16: The required capacity of the battery is calculated based on the estimated current consumption calculation in Table (#) and equations (#-#). The calculations indicate that an optimal battery would have a capacity between 25-115 mA-hours. This would allow the device to operate for a 24-hour period while recharging once a day. Although the range is somewhat large, this is based on the estimation of current consumption.

Total Current (mA)	Time	Capacity (mA-H)	Capacity/F	Capacity/(F*D)
2.26	16	36.16	40.18	40.58
4.3	16	68.8	76.44	77.22
6.34	16	101.44	112.71	113.85
8.38	16	134.08	148.98	150.48
10.42	16	166.72	185.24	187.12

5.3.3 Voltage

Thin-Filmed lithium Ion batteries for implantable devices generally operate with a voltage of 3.6-3.7 Volts. This value is standardized to accommodate a wide range of devices. When choosing the appropriate battery for a device, designers can adjust the

internal components to be compatible with the 3.6 Volts. The analog-to-digital converter in the ASIC design depends on this value, so the power-rail will be (+/-) 1.8 volts.

5.3.4 TET System for Recharging

The device will use a Transcutaneous Energy Transfer System to recharge the lithium ion battery. The TET system has been successfully implemented by a number of research teams, most notably by T. Dissanayake et al. from the Auckland Bioengineering Institute. With collaboration, the TET system will be modeled according to their previous work. The analytical effort has been documented and published [11]. Using this information, the manufacturing details will be determine along with the specification of the design and how it will be configured.

Some of the analytical effort calculations that were considered include: the capacitance, inductance, and resistance of the internal components, the size and material of the magnetic coils and optimal separation between the coils. These calculations are beyond the scope of the BCI Telemeter, but the research papers are located in the appendix. The results of the papers are used to determine the manufacturing costs and configuration.

5.4 Casing

The casing encloses the entire device so the calculations needed to determine the dimensions of the case are based on the dimensions of the PCB and battery. The PCB is 7.0 cm x 6.0 cm with a thickness of 2 mm. The 5.5 mm thick battery sits on top of the PCB, making the total thickness of the internal components 7.5 mm. The casing will be 7.3cm x 6.1cm x 1.2 cm to give 5-10 mm of room to the internal components on all sides.

6.0 Specific Details of Chosen Design

6.1 ASIC

6.1.1 ASP Block Wiring Diagrams

Figure 11 below presents an overview of the Multisim circuit schematic. This figure does not include grounds, power sources or specific values. These are presented in the Multisim schematic in figure 12.

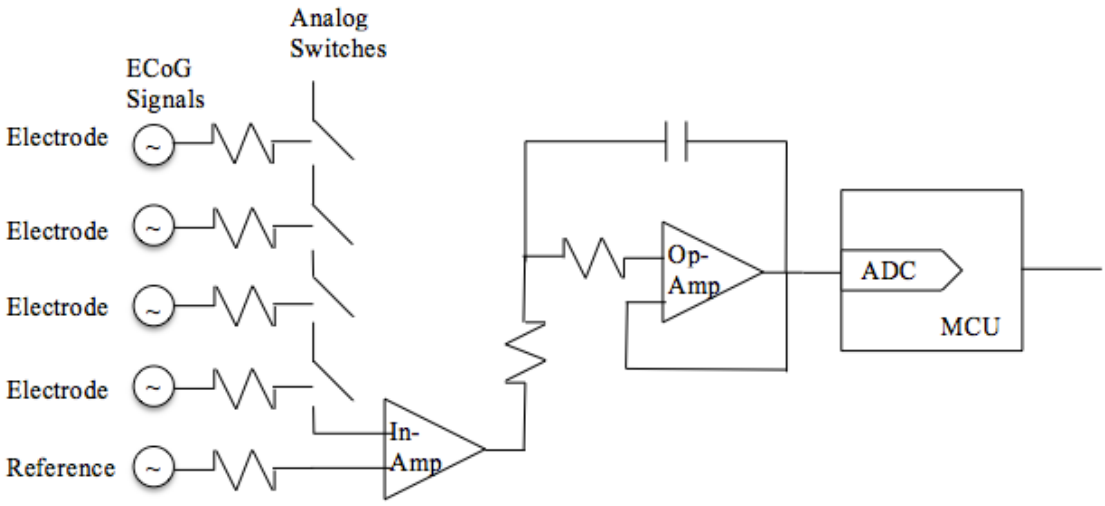

Figure 11: Overview of Multisim circuit schematic

The resistors between the recording electrodes and the analog switches represent the high source impedance of the electrode-tissue interface. The analog switches allow the user to chose eight of 32 channels for further processing. After the instrumentation amplifier removes the noise from the recorded signal and amplifies the signal by a factor of ten, a Sallen-Key topology anti-aliasing filter is implemented to prevent signal distortion from high frequency noise during quantization. The microcontroller unit contains a 24-bit Delta-Sigma ADC that digitizes the signal and digitally processes it before sending it to the telemeter.

Figure 12 below shows the Multisim circuit schematic for one channel.

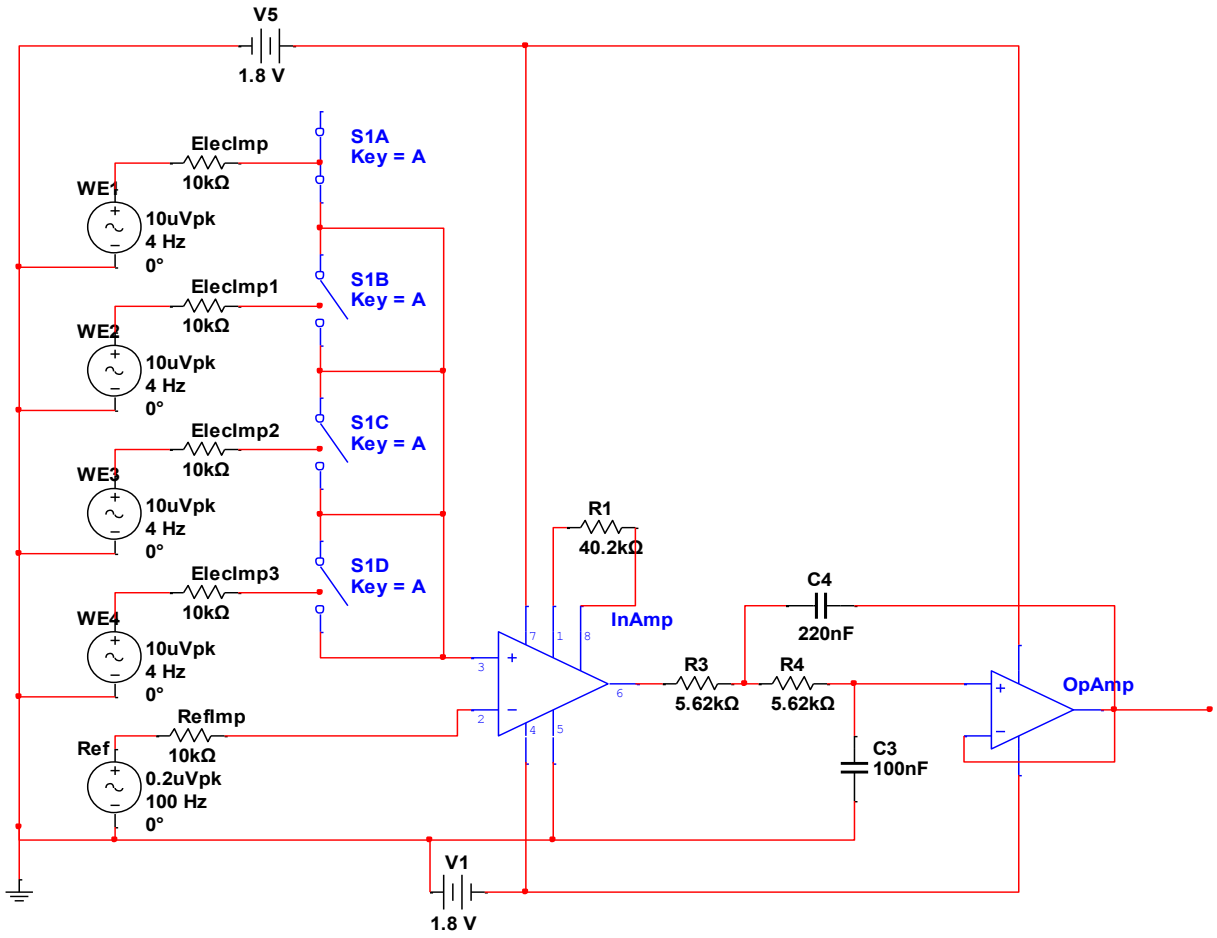

Figure 12: Multisim circuit diagram for one channel of the ASIC

The bode plot below in figure 13 demonstrates that the frequency components beyond 200 Hz are attenuated before digitizing.

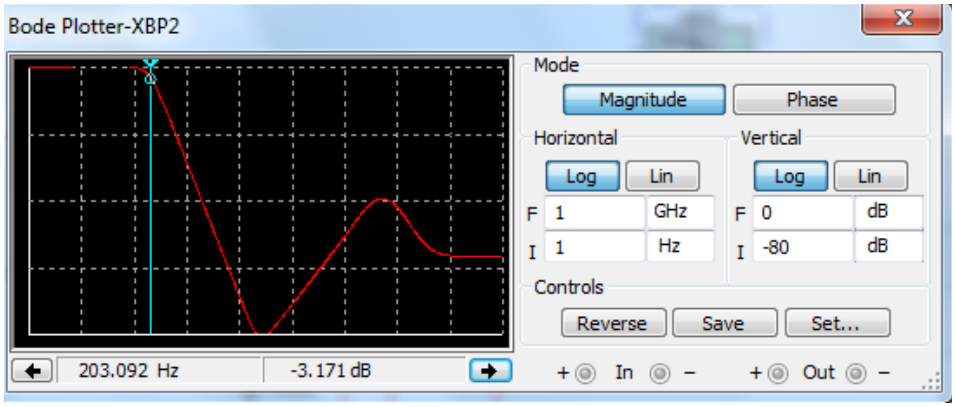

Figure 13: Bode plot demonstrating attenuation beyond 200Hz

6.1.2 Printed Circuit Board

Using Ultiboard 11.0 software, a printed circuit board (PCB) was designed to fit the needs of the BCI Telemeter. The printed circuit board for the ASIC is a 6cm (2.362in) x 7cm (2.756in) board that is 0.5mm (0.0197in) thick. With such a small working area, designing a circuit layout that accomplished the goals of the BCI telemeter was a difficult task. The three dimensional figures of the PCB are presented below in figures 14 and 15.

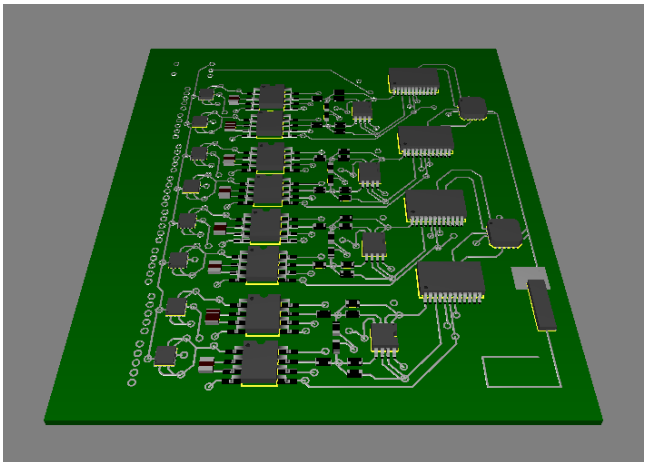

Figure 14: Three Dimensional CAD drawing of the printed circuit board. This is the front side of the circuit board, containing all of the amplifiers, microchips, and the telemeter.

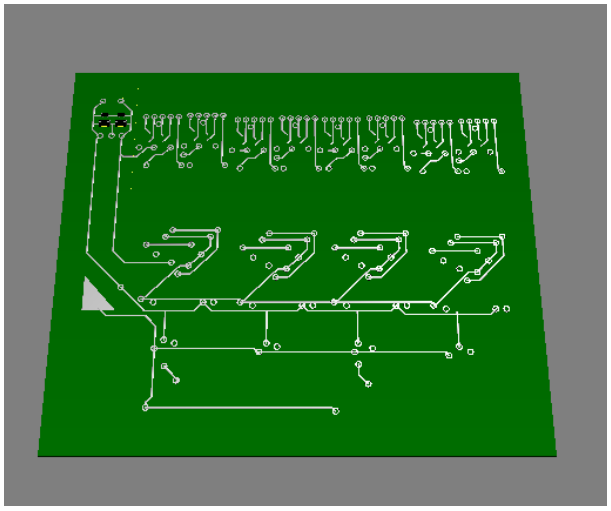

Figure 15: Back side of the printed circuit board. The battery would sit on the backside, connecting into the terminals in the upper left end corner. This acts as a voltage divider, creating a 1.8V port, a -1.8V port and a virtual ground.

The connections made on the reverse side of the PCB enable the creation of a space efficient design. The absence of integrated circuit components on the backside of the PCB provides space for the battery to be placed. The diagram below depicts trace layouts for the PCB (see figure 16).

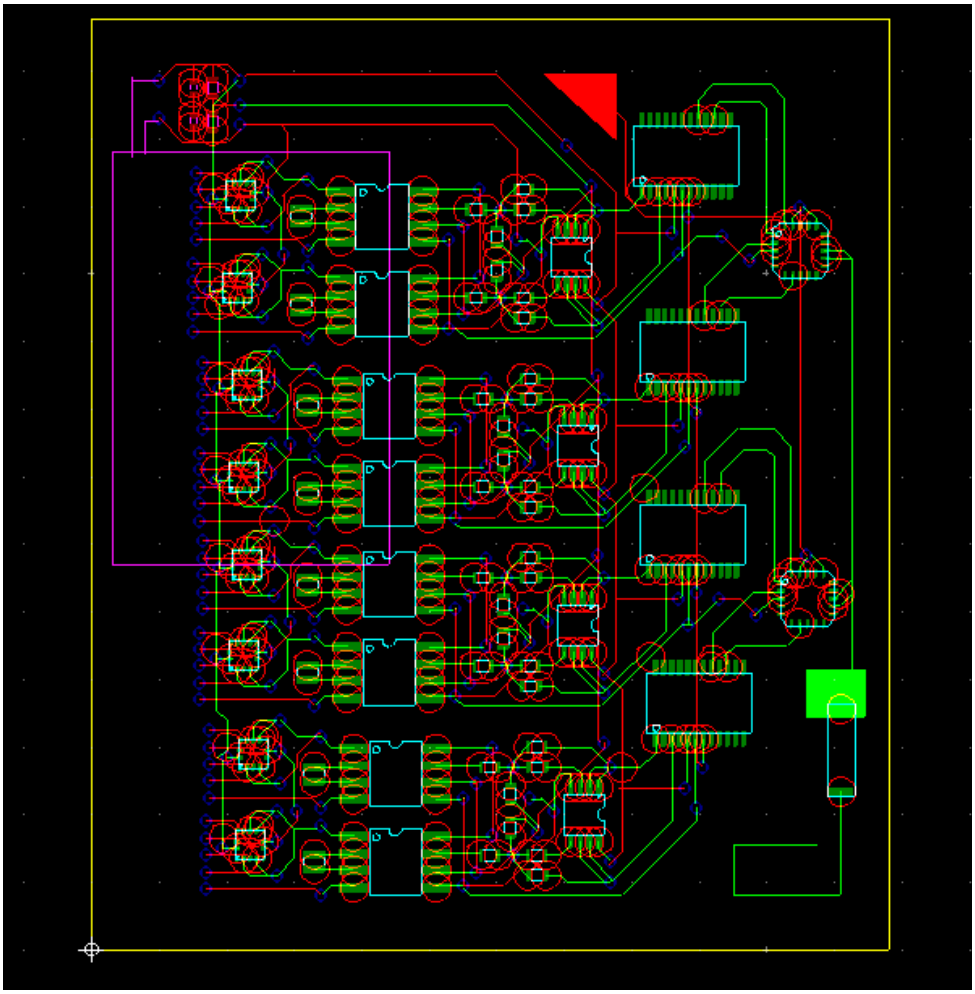

Figure 16: Full printed circuit board for the ASIC

The red traces indicate wires located on the backside of the PCB whereas the green traces indicate wires laid out on the front. The blue circles are “vias” and allow communication between the copper traces on each side of the board. The pink outline indicates the placement of the battery on the reverse side of the PCB. A voltage divider using resistors and capacitors is employed to transform the 3.6V lithium ion battery into a 1.8V positive

source, a negative 1.8V source, and a virtual ground between the two. This allows for the use of both single source and dual source circuit components. A closer image of two channels is presented below in figure 17.

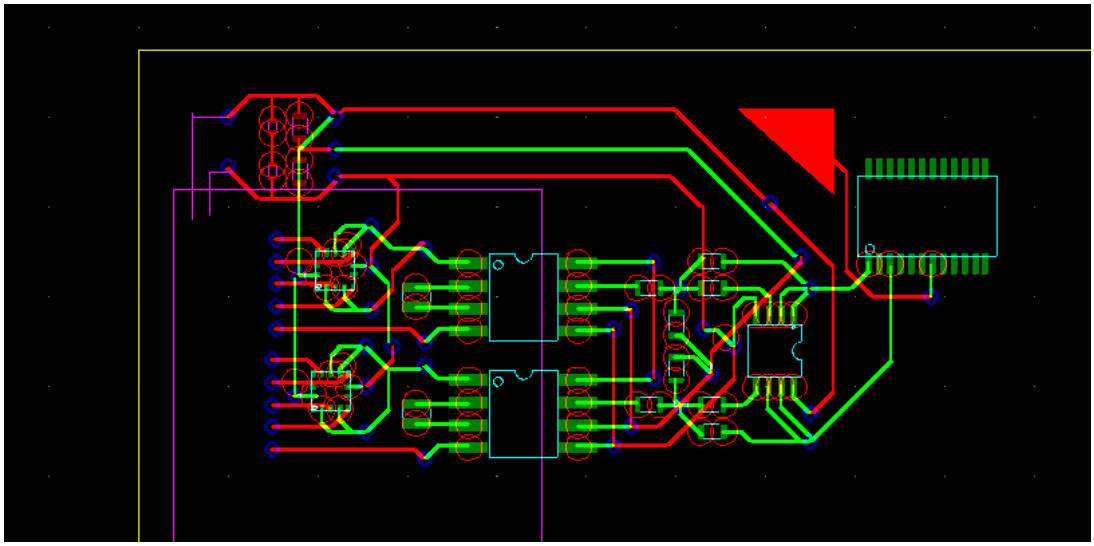

Figure 17: Two channels represented on the printed circuit board. This figure is the PCB representation of the Multisim schematic in figure 13

6.1.3 ASIC Components

6.1.3.1 Analog Switch

The TS3A4751 is a low ON-state resistance (R_{on}), low-voltage, quad, single-pole/single-throw (SPST) analog switch that operates from a single 1.6-V to 3.6-V supply. This device has fast switching speeds, handles rail-to-rail analog signals, and consumes very low quiescent power. The digital input is 1.8-V, which is compatible with the BCI Telemeter's battery specifications. The TS3A4751 is available in a 14-pin micro QFN (RUC) package, demonstrated below in figure 18, saving space on the PCB.

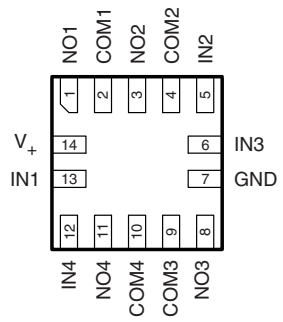

Figure 18: RUC Package for the analog switch (bottom view)

The RUC package has length L = 2.05mm (0.081in), width W = 2.05mm (0.081in), and thickness T = 0.40mm (0.016in) making it an ideal size to be used in a device with strict space requirements. The data sheet for this type of switch is provided in Appendix G.

6.1.3.2 Instrumentation Amplifiers

The AD8236 is the lowest power instrumentation amplifier in the industry. It has rail-to-rail outputs and can operate on voltages as low as 1.8 V, which makes it an ideal choice for BCI telemeter. Its 40 µA maximum supply current supports low current consumption in battery-powered applications. The internal differential amplifier and high input impedance leads to an extremely high CMRR and high SNR.

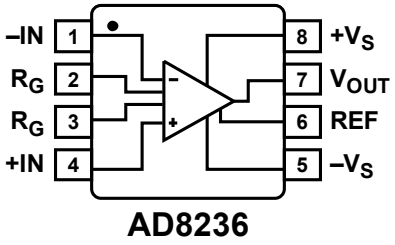

Figure 19: Pin diagram from AD8236

The gain of the AD8236 is set with one resistor, and in the BCI Telemeter, is set to a gain of G=10 with a 84.5 $k\Omega$ resistor. The table of standard gain and resistor values is presented below in table 17.

Table 17: Gains achieved using 1% resistors

1% Standard Table Value of R_G (Ω)	Calculated Gain
422 k	6.0
210 k	7.0
140 k	8.0
105 k	9.0
84.5 k	10.0
28 k	20.0
9.31 k	50.1
4.42 k	100.0
2.15 k	200.3

The AD8236 defaults to G = 5 when no gain resistor is used. The inclusion of an external gain resistor increases the gain drift of the instrumentation amplifier. Using a 24-bit ADC negates the need for significant amplification, thus keeping the gain small reduces the amount a drift due to the instrumentation amplifier.

The AD8236 instrumentation amplifier is supplied by analog devices and is 5mm (0.197in) (including the pins) by 3mm (0.118in) and is specified for operation from –40°C to +125°C. The data sheet for this amplifier is supplied in Appendix G.

6.1.3.3 Operational Amplifier for AA filter

The OPA333 series of complementary metal–oxide–semiconductor (CMOS) operational amplifiers uses a proprietary auto-calibration technique to simultaneously provide very low offset voltage and near-zero drift over both time and temperature. These small, high precision amplifiers provide high-impedance inputs and uses single or dual supplies as low as +1.8V, or ± 0.9V. Their small size, precision, and optimization for low-voltage operations makes it perfect for use in the BCI Telemeter. The OPA333 family offers excellent CMRR, results in superior performance for driving analog-to-digital converters

without degrading the signal integrity. The data sheet for the operation amplifier is supplied in Appendix G.

The BCI Telemeter employs the OPA2333-AID (Texas Instruments) is the dual version of the OPA333 and contains two operational amplifiers in one SO-8 package. This saves space, enabling a smaller printed circuit board construction. The pin diagram is presented below in figure 20.

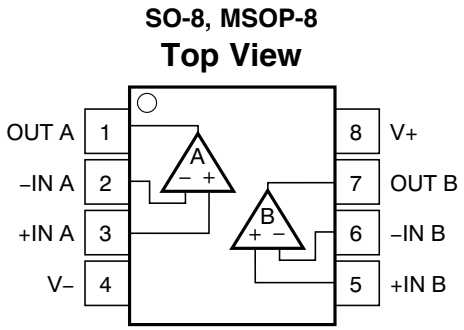

Figure 20: Pin diagram for OPA2333

The OPA2333 is 5mm (0.197in) (including the pins) by 3mm (0.118in) and is specified for operation from –40°C to +125°C.

6.1.3.4 Resistors for AA filter

High Stability Thin Film Flat Chip Resistors will be used when implementing the ASIC design. TNPW e3 Precision Thin Film Flat Chip Resistors designed by Vishay are typical in many medical applications. Figure 21 depicts standard high stability thin film flat chip resistors.

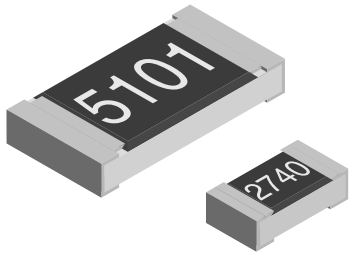

Figure 21: High stability thin film flat chip resistors

A homogeneous film of metal alloy is deposited on a high grade Al_2O_3 ceramic substrate and conditioned to achieve the desired temperature coefficient. Specially designed inner contacts are deposited on both sides and a special laser is used to achieve the target value by smoothly fine trimming the resistive layer without damaging the ceramics. The result of production is then verified by an extensive testing procedure. The data sheet for this type of resistor is provided in Appendix G.

The 5.62 kΩ resistor (KEMET, TNPW06035K62BEEA) and the 665Ω resistor (KEMET, TNPW06035K62BEEA) that will be used to apply a gain to the instrumentation amplifier both have length L = 1.60mm (0.063in) ± 0.10mm (0.004in), width W = 0.85mm (0.034in) ± 0.10mm (0.004in), and thickness T = 0.35mm (0.014in) ± 0.05mm (0.002in). These resistors have tolerance of 0.1% and a temperature coefficient of resistance (TCR) of ± 25 ppm/K.

6.1.3.5 Capacitors for AA filter

Ceramics are non-polar devices that offer unsurpassed volumetric efficiency, delivering the highest capacitance in the smallest package sizes in the market. Multi Layer Ceramic Capacitors (MLCCs) offer very low equivalent series resistance (ESR), exhibit excellent

high frequency characteristics and are extremely reliable. Figure 22 depicts a standard surface mount MLCC.

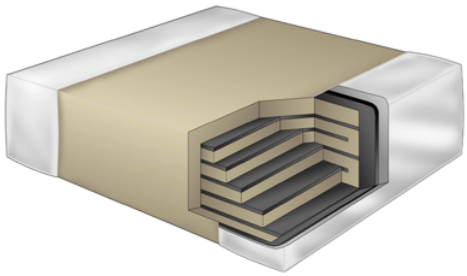

Figure 22: Surface mount multi layer ceramic chip capacitor

MLCCs are monolithic devices that consist of laminated layers of specially formulated, ceramic dielectric materials interspersed with a metal electrode system. The layered formation is then fired at high temperature to produce a sintered and volumetrically efficient capacitance device. A conductive termination barrier system is integrated on the exposed ends of the chip to complete the connection. The data sheet for this type of capacitor is provided in Appendix G.

Both capacitors contain the dielectric material X7R. X7R formulations are called "temperature stable" ceramics and fall into EIA Class II materials. It is the most popular of these intermediate dielectric constant materials, with temperature variation of capacitance within ±15% from -55°C to +125°C. This change in capacitance is non-linear.

The 100nF capacitor (KEMET, C0402C104J4RACTU) has length L= 1.00mm (0.040in) ± 0.05mm (0.002in), width W= 0.50mm (0.020in) ± 0.05mm (0.002in), and thickness T = 0.50mm (0.020in) ± 0.05mm (0.002in). This capacitor has a DC voltage rating of 16 V and a capacitance tolerance of 5%. The 220nF capacitor (KEMET,

C0603C224J4RACTU) has length L = 1.60mm (0.063in) ± 0.15mm (0.006in), width W = 0.80mm (0.032in) ± 0.15mm (0.006in), and thickness T = 0.50mm (0.020in) ± 0.05mm (0.002in). This capacitor has a DC voltage rating of 16 V and a capacitance tolerance of 5%.

6.1.3.6 DSP Microchip with integrated 24-bit Delta-Sigma ADC

The MSP430 MCU is designed specifically for ultra-low-power applications. Its flexible clocking system, multiple low-power modes, instant wakeup and intelligent autonomous peripherals enable true ultra-low-power optimization, dramatically extending battery life. The pin diagram for this microchip is presented below in figure 23.

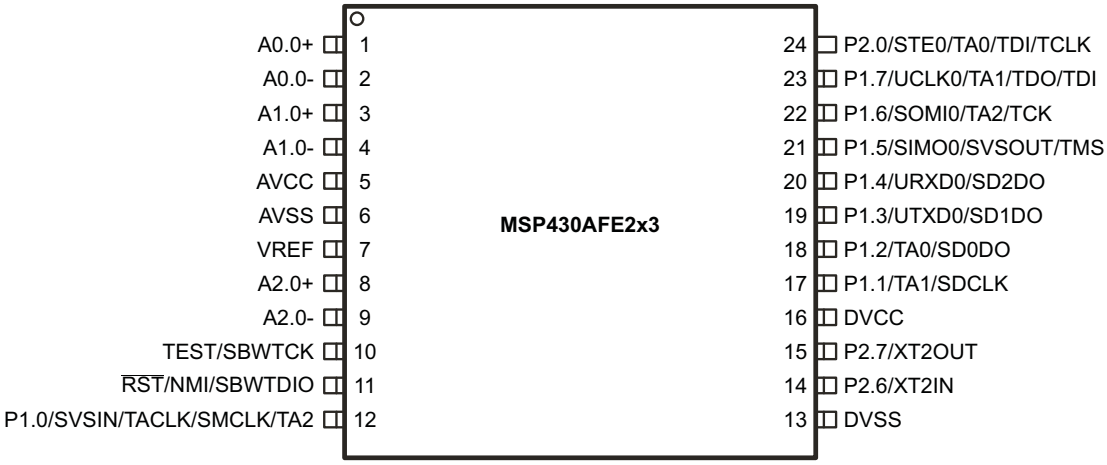

Figure 23: MSP430AFE 2x2 pin layout for ASIC. Each chip processes two analog channels

The MSP430AFE252 is an ultra-low-power mixed signal microcontrollers integrating two independent 24-bit sigma-delta A/D converters, one 16-bit timer, one 16-bit hardware multiplier, USART communication interface, watchdog timer, and 11 I/O pins. It requires a low supply voltage, between 1.8V and 3.6V, and has length L = 7.90mm (0.311in), width W = 6.60mm (0.26in) including the pins, and a thickness T = 1.20mm

(0.047in). The microchip has five power-saving modes and is able to transition to active mode from standby-mode in less than 1us. In active mode the device uses 220uA at 1MHz, whereas in standby mode is uses 0.5uA. The data sheet for this type of microchip in Appendix G.

Two 24-bit delta-sigma ADC are included on the MSP430 Microchip. To simulate the 24-bit delta-sigma converter, a virtual instrument (VI) was created in LabVIEW (see figure 24). The subVIs that were used in this schematic are presented in Appendix E.

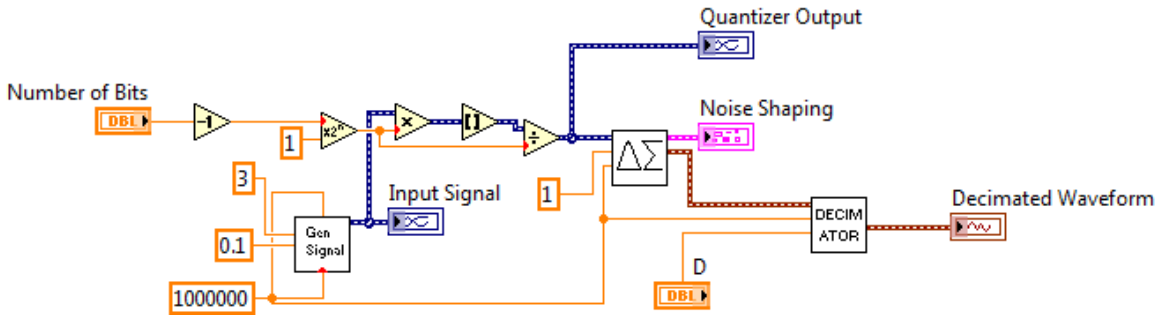

Figure 24:Overall VI that will act as the Delta-Sigma ADC in the Multisim simulation

In order to quantize the input signal into 24-bit integers, the input signal was multiplied by 2^{23}, rounded, and divided by 2^{23} before being referred to the input of the ADC. The quantized signal was then sent to the delta-sigma modulator, which implements a second order noise shaping feedback loop. Hauser's proposed one-bit delta-sigma modulator configuration of second order is presented below in figure 25.

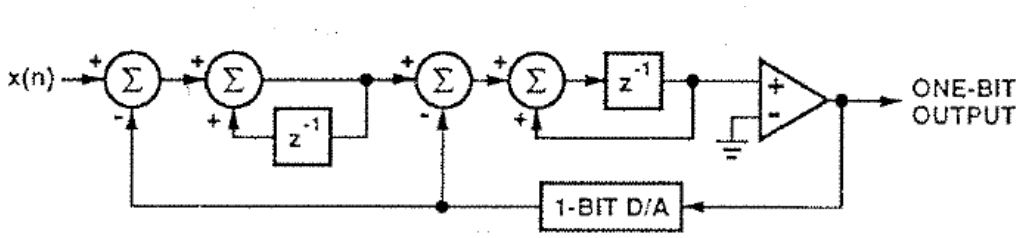

Figure 25: Second order delta sigma modulator configuration

Each sample of the signal is passed into the modulator and through a series of summations and feedback loops. After the final integrator, the value of the sample is compared to zero. If the sample's value is above zero, V_{ref} (in this case + 1V) is passed out of the modulator. If the sample's value is below zero, $-V_{ref}$ (in this case -1V) is passed out of the modulator. Hence, the output waveform consists of only $\pm V_{ref}$, representing a string of one-bit binary code that is sent to the decimator, where it is low pass filtered and down-sampled.

Decimation is the process by which ADCs digitally filter out high frequency noise (this also serves an anti-aliasing function) and resample the quantized signal at a more desirable frequency. To lower the number of taps, and hence improve the performance of the ADC, the decimation scheme was designed with two FIR filters. The first stage filters the modulated signal with the stop band starting at $\frac{4Fs}{D} - \frac{Fs}{2D}$ Hz, where D is the oversampling factor and F_s is the oversampling frequency of the incoming, modulated signal. As this represents a reduction of bandwidth by about a factor of D/8, the digital signal is subsequently down sampled by the same factor, meaning 1 in every D/8 samples is allowed to pass through the rest of the ACD. This design feature serves to prevent

aliased components to impinge upon the region from 0 to $\frac{Fs}{2D}$ Hz, which is the desired bandwidth at the output of the ADC.

The second stage of the decimator involves filtering out frequencies above F_s/2D, meaning the new sampling frequency at the output of the decimator is F_s/D. This represents a further reduction of bandwidth by a factor of 8, so the digital signal is subsequently down sampled by the same factor. Again, this means 1 in every 8 samples is allowed to pass through the rest of the ACD. The LabVIEW code for both the modulator and the decimator are presented in Appendix E.

Figure 26 below demonstrates the output at each component of the delta sigma modulator. It can be seen that the output of the decimator (and in the designed circuit the output of the ADC) is an accurate representation of the original signal.

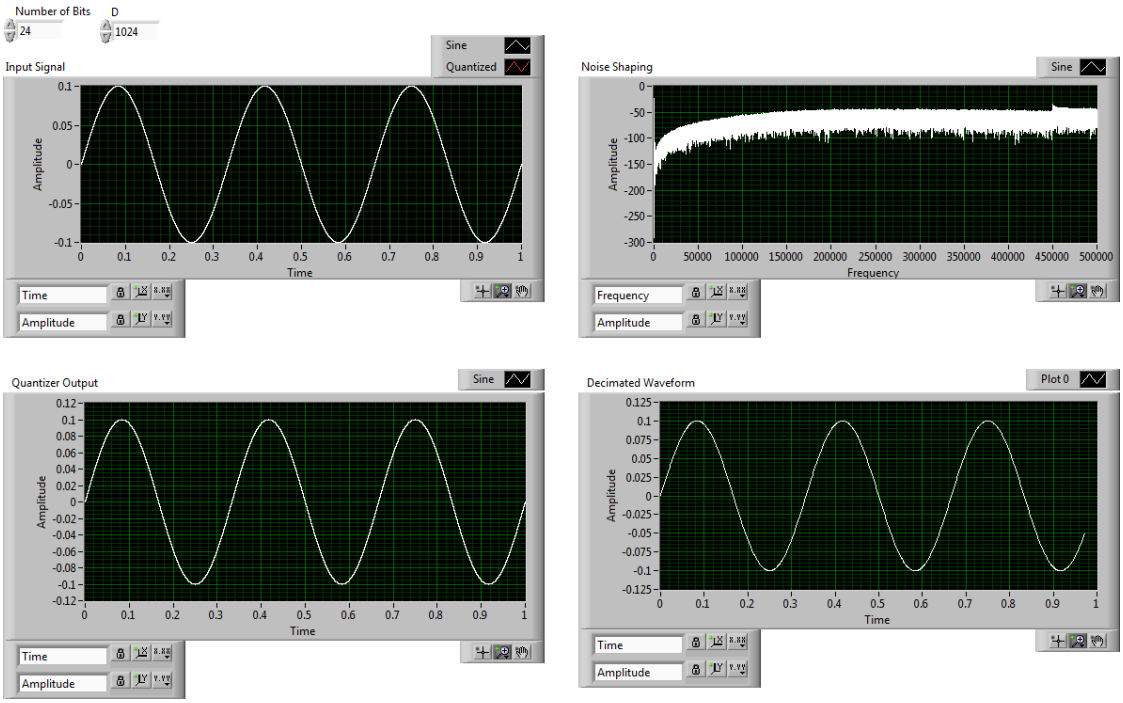

Figure 26: Front panel of ADC Block demonstrating noise shaping and appropriate reconstruction

The output of the analog Delta-Sigma modulator is a 1-bit 512 kHz data stream. This high-speed 1-bit data is then processed by a digital signal-processing (DSP) block to yield a 16-bit, 2000 samples/sec output stream. The DSP microcode required for the BCI Telemeter has been provided as a specification for this project, and preliminary testing has been done using MSP430 experimentation board.

The BCI Telemeter will employ four MSP430AFE252 chips. Each microchip contains two 24-bit Delta-Sigma converters that can digitize analog channels simultaneously. It is important that each channel can be processed at the same time because control is based on visual feedback to the subject and because using an oversampling Delta-Sigma ADC is already compromising speed.

6.1.4 TI CC1101 Transceiver Specifications

The TI CC1101 is a low-power sub-1 GHz RF transceiver ideal for ultra low-power wireless applications operating in the 300-348 MHz, 387-464 MHz, and 779-928 MHz Industrial, Scientific, and Medical (ISM) frequency bands. The BCI Telemeter will be programmed to operate in the highest of these, the 779-928 MHz band. Key features of the TI CC1101 include high sensitivity, -112 dBm at 1.2 kBaud and 868 MHz with a 1% packet error rate, as well as a low current consumption of 14.7 mA in receiving mode at 868 MHz. Small size and low-power features of the transceiver make it particularly useful for the applications of the BCI Telemeter. The transceiver chip has dimensions of 4mm (0.157in) x 4mm (0.157in) and a 200 nA current consumption in sleep mode with a startup time of 240 μs from sleep to transmitting or receiving mode. In addition, the TI CC1101 contains a completely on-chip frequency synthesizer, removing the need for

external filters or RF switches. A block diagram of the CC1101 Transceiver is shown below in figure 27.

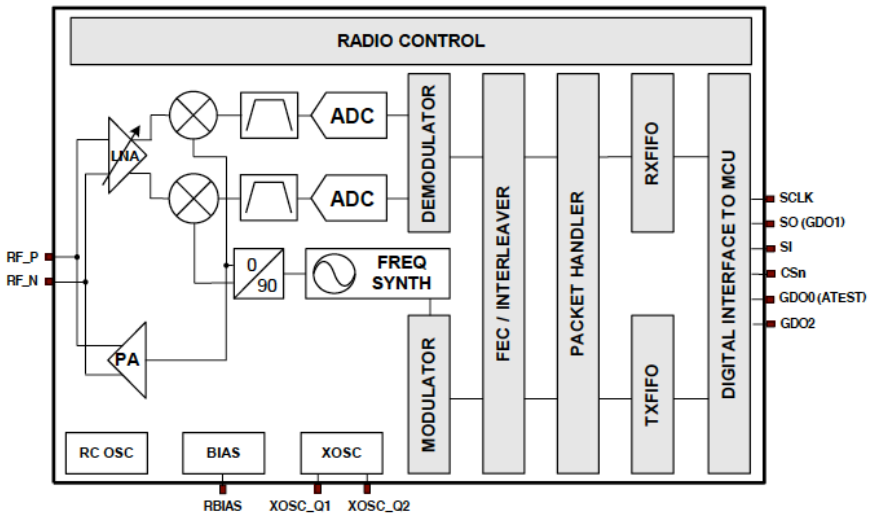

Figure 27: Simplified block diagram of CC1101

The received RF signal is amplified by the low-noise amplifier (LNA) and down converted to the intermediate frequency (IF). The signals are then digitized by the ADCs. Automatic gain control (AGC), fine channel filtering, demodulation, and bit/packet synchronization are performed digitally. A crystal oscillator connected to XOSC_Q1 and XOSC_Q2 generates a reference frequency for the frequency synthesizer as well as clocks for the ADC. Loading capacitors for the crystal are required and come with the TI CC1101. For the crystal to oscillate at the specified frequency, either 26 or 27 MHz, the values of the loading capacitors depend on the total load capacitance C_L specified for the crystal.

$$C_L = \frac{1}{\frac{1}{C_{81}} + \frac{1}{C_{101}}} + C_{parasitic}$$

C_{81} and C_{101} are the loading capacitors from TI, and $C_{parasitic}$ is constituted by pin input capacitance and PCB stray capacitance and is typically around 2.5 pF. The crystal oscillator is amplitude regulated. A high initial current is used to start the oscillations, then reduced once the amplitude has built up to ensure a fast start-up and keep the drive level to a minimum. A circuit diagram of the CC1101 including the C81 and C101 capacitors and crystal is shown below in figure 28.

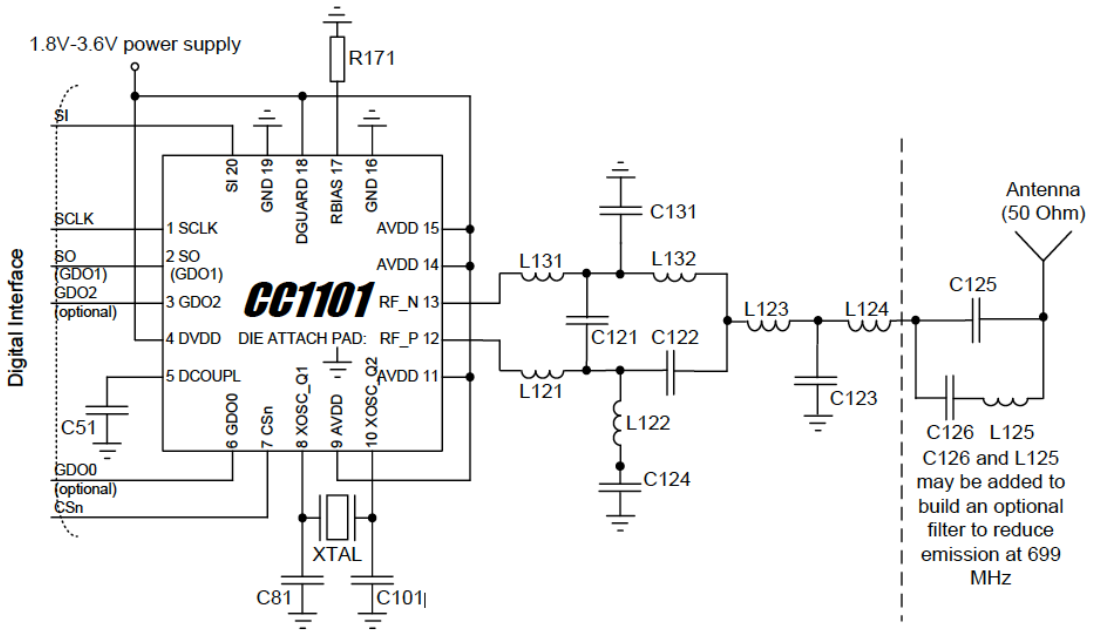

Figure 28: Typical application and evaluation circuit 868/915 MHz

The TI CC1101 RF Transceiver can operate between -40°C and +85°C and with an operating supply voltage between 1.8 V and 3.6 V given that all supply pins have the same voltage. Figure [x] below shows a top view of the transceiver chip with 20 pins labeled. The data sheet for the telemeter is presented in Appendix G.

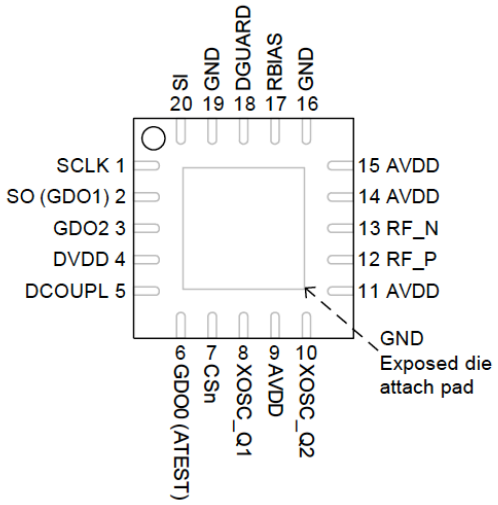

Figure 29: Pinout top view of TI CC1101 RF Transceiver

6.1.5 Antenna

The antenna chosen for use in the BCI Telemeter is an RF Antenna (0868AT43A0020, Johanson Technology) that is compatible with the TI CC1101 RF Transceiver and optimized for operation in the 868 MHz band. It is a ceramic chip antenna with size requirements of 8.5mm (0.335in) x 7.8 mm (0.307in). The high performance antenna solution consists of a chip antenna in conjunction with a special PCB trace. Figure 30 below provides a top view of the chip antenna, while Figure 31 and Table 18 show the recommended dimensions of the PCB trace for a center frequency at 866.5 MHz. The data sheet for the antenna is presented in Appendix G.

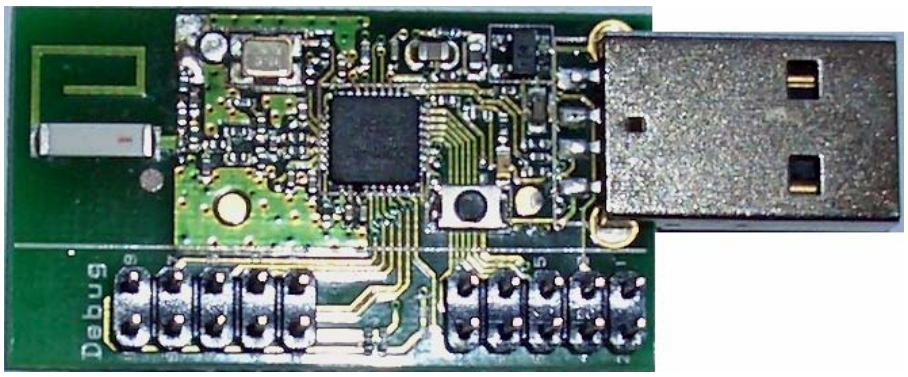

Figure 30: RF Chip Antenna from Johanson Technology

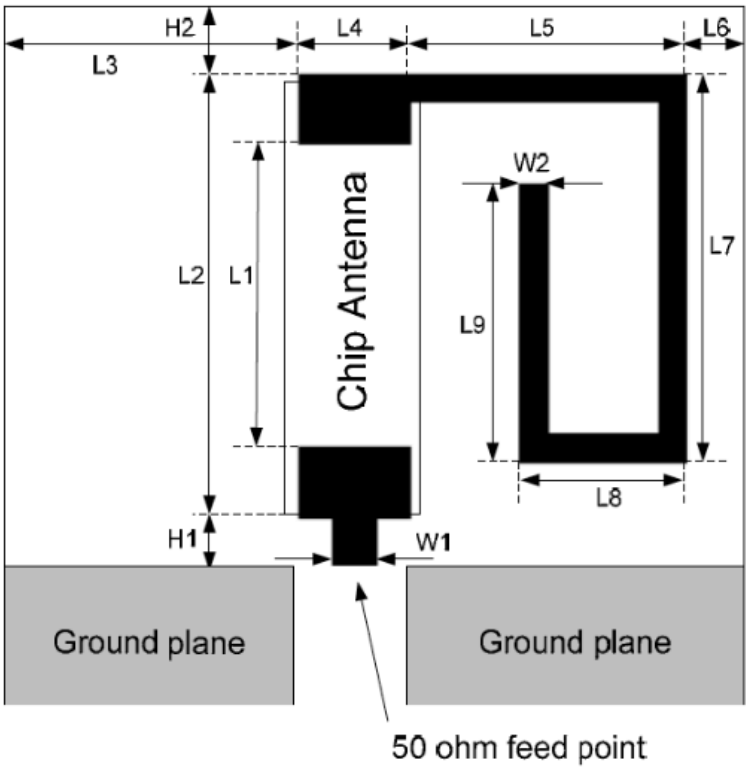

Figure 31: Figure of Antenna with specified dimensions

Table 18: Antenna Dimension

H1	1.0 mm (0.039in)	**L6**	2.7 mm (0.106in)
H2	1.3 mm (0.051in)	**L7**	7.0 mm (0.276in)
L1	5.5 mm (0.217in)	**L8**	3.0 mm (0.118in)
L2	8.0 mm (0.335in)	**L9**	5.0 mm (0.197in)
L3	12.8 mm (0.504in)	**W1**	0.5 mm (0.02 in)
L4	2.0 mm (0.079in)	**W2**	0.8 mm (0.031in)
L5	5.0 mm (0.197in)		

6.2 Battery

Quallion's QL00200I-A rechargeable lithium-ion battery is a surface-mount, solid state, energy storage device rated for 200 mA-h nominal capacity and 3.6 V nominal voltage. The maximum current discharge is 210 mA, well above the amount needed for the BCI Telemeter. Figure 32 shows a picture of the battery with its dimensions. The physical characteristics of this battery make it the ideal shape for an implantable device. Table 19 lists these characteristics. The data sheet for this battery is included in Appendix G.

Figure 32: Quallion's QL00200IA Lithium Ion battery

Table 19: Physical Characteristics of the battery

Physical Characteristics	
Width	17 mm
Height	35 mm
Thickness	5.5 mm
Weight	8 g
Volume	3.27 cc
Weight Energy Density	148 Wh/kg
Volume Energy Density	289 Wh/L

The biocompatible battery has a low discharge life and a long calendar life. Its compact, light weight and hermetically sealed. It employs Quallion's Zero Volt™ and SaFE-LYTE™ technologies, which are safety features. All together, these characteristics create a fully implantable biocompatible battery.

Quallion's patented Zero Volt™ technology allows long storage periods in a deep discharged state with no permanent capacity loss due to low voltage. The ability to discharge a battery to zero volts offers a number of important advantages. Most importantly, it allows batteries to be stored for long periods of time without requiring maintenance. In addition, the charge can be completely removed when connecting batteries to volatile systems or implanting cells inside the human body as in the case of the BCI Telemeter. In all applications, the batteries are guaranteed to function at peak capacity levels, even after long storage periods without any maintenance. This is particularly valuable in applications where frequent maintenance is not possible, and offers a large advantage over conventional Li-ion batteries that cannot survive a deep discharge.

SaFE-LYTE™ technology enhances battery safety without compromising electrochemical performance. In general, lithium ion batteries are intrinsically less safe than other battery chemistries such as Ni-MH and lead acid, because Li-ion batteries contain a flammable non-aqueous electrolyte. For that reason, piercing and compression may cause a battery to ignite and catch fire. The SaFE-LYTE™ technology integrates into the battery a liquid halogen compound that is flame-retardant and immiscible in the electrolyte. This solution significantly lowers the risk of combustion, and makes batteries that are far safer than conventional Li-ion options.

6.3 Recharging: Transcutaneous Energy Transfer System

The Transcutaneous Energy Transfer (TET) enables power transfer across the skin without direct electrical connectivity. This is implemented through a transcutaneous transformer where the primary and the secondary coils of the transformer are separated by the patient's skin providing two electrically isolated systems. A TET system is illustrated in figure 33. The electromagnetic field produced by the primary coil penetrates the skin and produces an induced voltage in the secondary coil.

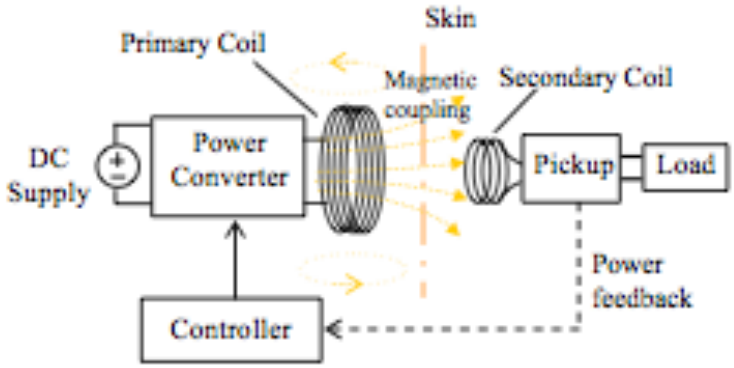

Figure 33: Block Diagram of a TET system. Load is the lithium-ion battery. The Secondary Coil is incorporated into the PCB board to allow for magnetic coupling

The TET system is designed to deliver power in the range of 5W to 25W. Figure 34 illustrates the architecture of the overall system. A DC voltage is supplied to the system with an external battery pack. A current fed push pull resonant converter is used to generate a high frequency sinusoidal current across the primary coil. The magnetic coupling between the primary and the secondary systems produces a sinusoidal voltage in the secondary coil which is rectified by the power conditioning circuit in the pickup to provide a stable DC output to the implanted load. As shown in figure 34, a DC inductor is added to the secondary pick up following the rectifier bridge in order to maximize the

power transfer to the load. The DC inductor aids in sustaining a continuous current flow in the pick up.

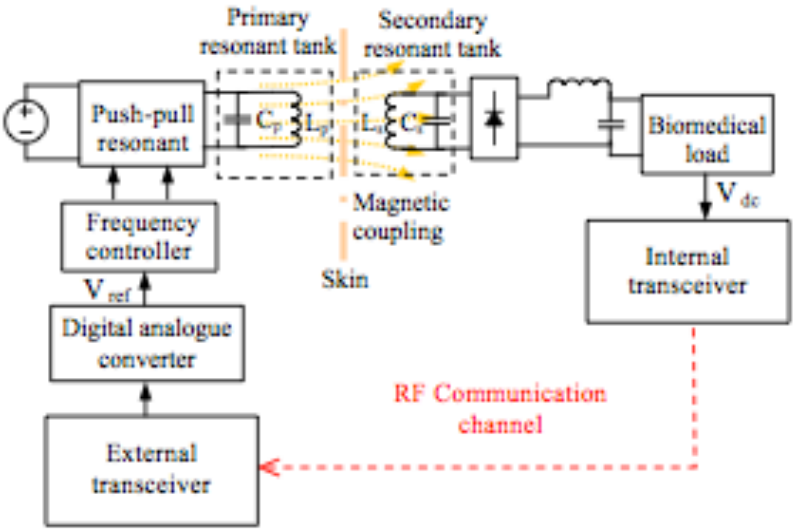

Figure 34: System architecture with more specifics. The frequency controller, Digital analogue converted and external receiver work together to adjust the amount of delivered power.

Two nRF24E1 Nordic transceivers are used for data communication. The DC output voltage of the pickup is detected and transmitted to the external transceiver. The external transceiver processes the data and adjusts the duty cycle of the output PWM signal in order to vary the reference voltage (V_{ref}) of the frequency control circuitry. The PWM signal is passed through a Digital to Analog Converter (DAC), in order to obtain a variable reference voltage. This variable reference voltage is then used to vary the frequency of the primary resonant converter, which in turn varies the power delivered to the implantable system. The response time of the system is approximately 360ms.

The frequency controller employs a switched capacitor control method. The controller varies the overall resonant frequency of the primary resonant tank in order to tune/detune to the secondary resonant frequency. The frequency of the primary circuit is adjusted by

varying the effective capacitance of the primary resonant tank. This is illustrated below in figure 35.

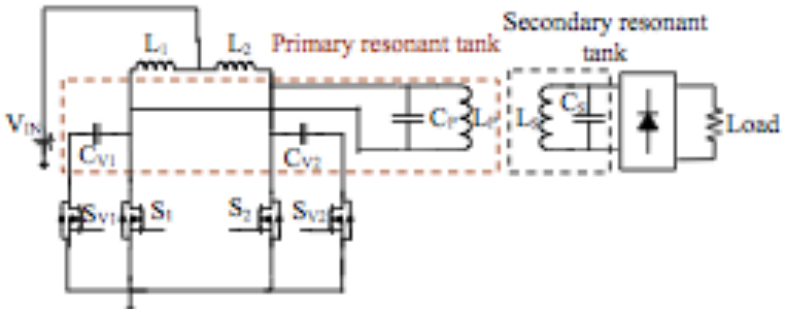

Figure 35: System architecture of primary frequency control

Inductor LP, capacitor CP and switching capacitors CV1 and CV2 form the resonant tank. The main switches S1 and S2 are switched on and off alternatively for half of each resonant period and changing the duty cycle of the detuning switch SV1 and SV2 varies the effective capacitances of CV1 and CV2 by changing the average charging or discharging period. This in turn will vary the operating frequency of the primary converter. Each CV1 and CV2 is involved in the resonance for half of each resonant period. The variation in reference voltage (Vref) obtained from the DAC is used to vary the switching period of these capacitors. This method of frequency control maintains the zero voltage switching condition of the converter while managing the operating frequency. This helps to minimize the high frequency harmonics and power losses in the system. As shown in figure 35 above, the pickup circuitry is tuned to a fixed frequency using the constant parameters LS and CS. The operating frequency of the overall system is dependent on the primary resonant tank, which can be varied by changing the equivalent resonant capacitance, therefore the tuning condition of the power pickup can be controlled.

6.4 Casing

6.4.1 Design Drawings

The Titanium alloy casing is manufactured and assembled by Hudson Technologies. Based on their recommendations pertaining to implantable medical devices, the titanium alloy will be Grade 5 (6% aluminum, 4% vanadium). The casing is formed by hermetically sealing two halves of the dimensioned casing together. Figure 36 approximates how the actual casing will look like with an imperceptible line sealing the two halves together and the CAD drawings are presented in Appendix F. The dimensions are based on the size of the PCB and internal components.

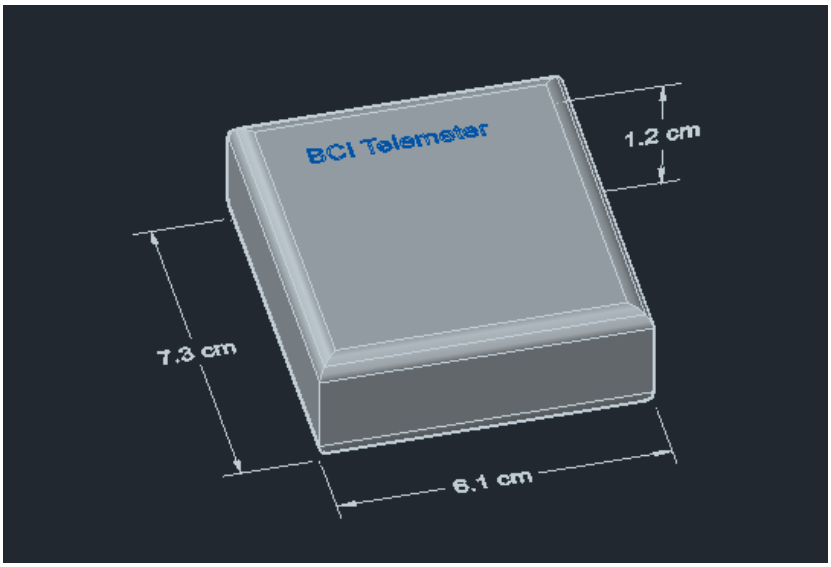

Figure 36: Final representation of the BCI telemeter titanium casing

6.4.2 Polymer Coating: Parylene

Parylene is a conformal protective polymer coating material utilized to uniformly protect any component configuration on such diverse substrates as metal, glass, paper, resin, plastic, ceramic, ferrite and silicon. Because of its unique properties, Parylene conforms

to virtually any shape, including sharp edges, crevices, points, or flat and exposed internal surfaces.

Parylene is applied at room temperature with specialized vacuum deposition equipment that permits control of coating rate and thickness. The deposition process takes place at the molecular level as the chemical, in dimer form, is converted under vacuum and heat to dimeric gas, pyrolized to cleave the dimer, and deposited as a clear polymer film. Coating thicknesses ranging from 0.100 to 76 microns can be applied in a single operation. Typical coating thickness for a circuit board is 0.001-in. No catalysts or solvents are required and no foreign substances that could be introduced will degrade the coated surface.

6.5 Safety

The BCI Telemeter poses a safety risk to the user since it must be surgically implanted into the body and remains there for an extended period of time. There is an initial risk to the patient due to the fact that invasive surgery is required to implant the ECoG electrode array on the dura of the brain and place the BCI Telemeter in the chest with internal wires connecting the two in order for the device to function. The specific risks of implanting the BCI Telemeter are the risks of undergoing any operation, as well as the risk of having a foreign object implanted in the body. The surgery for implantation is a standard procedure used to implant pacemakers and deep brain stimulators, and carries with it the risks of any surgery including side effects from anesthesia. Once the device has been implanted, the primary safety concern is the body's reaction to the foreign object. To help alleviate this risk, the casing containing the device is coated in parylene, a biocompatible

film that interacts safely with the internal environment of the body. The internal circuit components of the BCI Telemeter are contained in the hermetically sealed casing and will never come into direct contact with the body. The battery poses a few safety risks of its own that are accounted for by the Zero Volt™ and SaFE-LYTE™ technologies provided with the Quallion battery. These technologies are discussed in depth on page 59 in conjunction with the specific details of the battery. Zero Volt™ technology allows the battery to be safely implanted in the body and remain there for an extended period of time without maintenance while still performing at peak capacity. SaFE-LYTE™ technology reduces the risk of combustion of the electrolyte in the battery to negligible, making it safe to operate inside the body. Additional safety precautions include training the physicians and researchers using the BCI technology. A DesignSafe Analysis of the BCI Telemeter can be found in Appendix D.

7.0 Specific Material and Manufacturing Definitions

7.1 ASIC

7.1.1 ASIC Components

The BCI Telemeter's ASIC includes several integrated circuit components. These elements are presented below in table [x].

Table 20: Specific Devices used in the ASIC design

Part Description	Part Number	Brand	Supplier	#	Price per Unit	Total Price
4:1 Analog Switch	TS3A4751-RUCR	Texas Instruments	Digi-Key	8	$1.47	$11.76
Instrumentation Amplifier	AD8236-BRZ	Analog Devices	Digi-Key	8	$7.61	$60.88
Operation Amplifier	OPA2333-AID	Texas Instruments	Digi-Key	4	$5.04	$20.16
MCU (including ADC)	MSP430-AFE252	Texas Instruments	Digi-Key	4	$5.74	$22.96
Telemeter	CC1101-RTK	Texas Instruments	Digi-Key	2	$5.17	$10.34
Antenna	0868AT43-A0020	Johanson Technology	Digi-Key	1	$1.18	$1.18
5.62 kΩ Resistor	TNPW0603-5K62BEEA	Vishay	Digi-Key	16	$0.47	$7.52
84.5 $k\Omega$ Resistor (R_G)	TNPW1206-665RBEEA	Vishay	Digi-Key	8	$0.55	$4.40
100 nF Capacitor	C0402C104-J4RACTU	Kemet	Digi-Key	8	$0.79	$6.32
220 nF Capacitor	C0603C224-J8RACTU	Kemet	Digi-Key	8	$0.55	$4.40
TOTAL COST OF ASIC COMPONENTS						$152.63

The 200nF capacitor was replaced by a 220nF capacitor due to the limitations of commercially acceptable devices. Plugging this value into equation 8 yields the following cut-off frequency.

$$f_c = \frac{1}{2\pi\sqrt{(5.627 * 10^3)^2(100 * 10^{-9})(220 * 10^{-9})}}$$

$$f_c = 190.69\ Hz$$

This cut-off frequency is beyond the signal of interest (75-105) Hz and is thus sufficient for the AA filter.

7.1.2 Printed Circuit Board

After placing the components and the routed traces on the PCB in Ultiboard 11.0, the design can be exported to a file that will be provided to the board manufacturer. This file contains complete information describing how the finished board is to be manufactured.

The PCB will be ordered from Sunstone Circuits using their ValueProto Option. This option is ideal for prototype boards and small quantity orders. Sunstone requires that uploaded files include 6 Gerber RS-274X formatted files be uploaded, one for each copper layer, solder mask, and legend layer as well as the board outline. Ultiboard supports exporting files to Gerber format, and thus the BCI Telemeter ASIC can be manufactured by Sunstone. The PCB for the BCI telemeter is quoted at $31.92 and will be shipped within two weeks of the order being placed.

7.2 Casing

The PCB will be shipped to Hudson Technologies where it will be hermetically sealed within a titanium alloy (6% aluminum, 4% vanadium) casing. They have quoted the price

of this to be $22.53 plus shipping. The device will be shipped to the coating center located in Katy, Texas. An average shipping rate from Ormond Beach, FL to Katy Texas for a package that is less than 10 lbs. is $11.22.

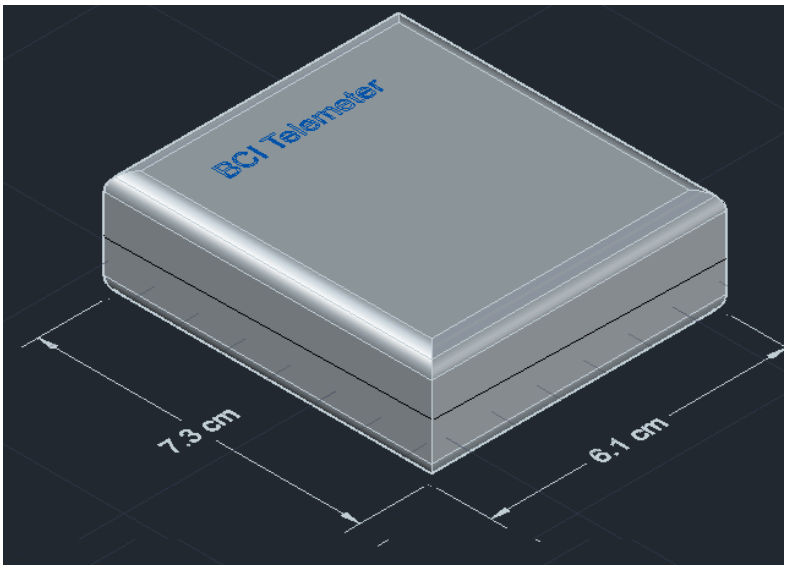

Figure 37: Manufactured BCI Telemeter

7.2.1 Parylene Coating

The device within the titanium coating will be sent to Parylene Coating Service Inc. located in Katy, Texas [13]. At their site the Parylene coating is applied through a mechanized process. The process consists of four stages that occur in four different chambers that alter the temperature of the mixture.

Stage 1: a dimer is added to the machine and heated to 150 ° C.

Stage 2: In this vaporized state, the dimer is then set through a channel in which its converted to a monomer and heated to 660° C

Stage 3: The monomer mixture is cooled to room temperature forming a polymer mixture. The device is contained in the room temperature chamber and polymer bonds to the titanium surface.

Stage 4: Excess gas is expelled and the device is removed.

After this process, the device will be ship to the lab center, free of charge.

7.2.3 TET System

TET systems are not available for purchase commercially. The design of the TET system was not a part of the original project scope for the BCI Telemeter, however, and details of its manufacturing will not be discussed here. The TET system used with the BCI Telemeter will be modeled after a system designed by the Wong lab [source].

7.3 Overall Expenses

Table 21: Overall Expenses to build the BCI Telemeter prototype

Overall Expenses	
ASIC Components	$149.92
PCB Manufacturing	$31.92
Battery	$11.78
Casing	$22.53
Paralyne Coating	$11.22
TOTAL COST	$227.37

8.0 Conclusions

The problem we were given to solve was a challenging one, requiring a great deal of forethought, careful planning, and perseverance throughout the design process. We took on the task of creating a fully implantable device that can wirelessly transmit brain signals from an ECoG electrode array placed on the dura of a subject's brain to an external computer. This device offers solutions to some of the current limitations of BCI technology, resulting from use of percutaneous leads and cables to connect the electrode array to an external computer. As a result, the subject's mobility is limited and the recording time is restricted because the device can only function when the subject is plugged into the computer. Eliminating the need for external wiring gives the subject free range of motion and greatly reduces the risk of infection posed by the exposure of percutaneous leads to the environment. A rechargeable lithium-ion battery system allows for 24 hour recording and can be recharged through the skin using a transcutaneous energy transfer system. The combination of these innovative technologies allows the device to be implanted within the subject, thus the BCI Telemeter solves the problems faced by current methods of BCI technology.

Future uses of BCI technology include continued research in neural prosthetics as well as clinical applications to study disease states in patients with neurological disorders such as Parkinson's disease. The ability to record brain signals for 24 hours straight in a research setting would allow for a much greater understanding of how the brain controls normal daily behaviors, providing vital information for the development of effective neural prosthetics. In addition, insight into the specific areas of the brain responsible for neurological diseases could give rise too much more effective treatments and change the

lives of patients suffering from these conditions. The design of the BCI Telemeter is a step toward making these applications possible, but there is much to be done before BCI technology can be widely used. The size of the BCI Telemeter is larger than we originally planned; reducing the size would be the next step in making the device more practical for implantation. A great deal of testing would also need to be done to ensure the device is safe and approved for human use.

When designing a device intended for implantation in the body, safety must be a priority. Before starting the design of the BCI Telemeter we had to consider whether the benefits that could come from the device were worth the risks involved with brain surgery that will be required to hook up the BCI Telemeter to an electrode array on the brain. The purpose of the BCI Telemeter in a clinical setting is to give patients with severe motor disabilities the ability to communicate with their environment by controlling prosthetic devices and wheelchairs with their own brain signals. To a patient without the ability to move on his own, the benefits of this technology certainly outweigh the risks. The purpose of the BCI Telemeter in a research setting is to gain valuable insight into the way in which the brain controls normal behaviors and to learn about disease states of the brain in patients with neurological diseases. The application of this knowledge in designing neural prosthetics and developing treatments for neurological diseases could change the lives of patients suffering from these conditions. Since BCI technology is already used in research labs with monkeys, the added risk of implanting the BCI Telemeter is small compared to the initial risks of placing the electrode arrays on the monkeys' brains. The BCI Telemeter will actually make this research safer by eliminating the need for percutaneous leads that cause infection. A great deal of thought and effort were put into

ensuring the BCI Telemeter is safe enough to be implanted inside of a monkey or a human. Throughout the design process, safety was emphasized and each component of the system required careful consideration to make sure the device is biocompatible. Since the casing is the primary component of the device in direct contact with the body, it was one of the most important safety hazards to consider. A biocompatible parylene film covers the casing that surrounds the ASIC where all the signal processing and transmission takes place. The casing is hermetically sealed so that the circuit elements of the ASIC never come into contact with the body. The main safety hazard inside of the device comes from the lithium-ion battery. The battery we have chosen uses trademarked SaFE-LYTE^{TM} technology to significantly lower the risk of combustion thus producing a battery that is much safer than conventional Li-ion batteries. In addition, Zero Volt^{TM} technology allows for safe implantation of the battery in the body and keeps the battery running at full capacity without maintenance for long periods of time. Safety was not one of the main factors we considered when originally conceptualizing our design, but throughout the process of choosing the specific components that make up the BCI Telemeter, particularly the battery and casing, we realized how vital of a role safety played in making our device practical for use.

The BCI Telemeter is designed as a prototype that can be used for very specific research and clinical needs. The unique combination of the signal processing components on the ASIC with the wireless transceiver comprises an original design that we believe is patentable. Using ECoG for BCI is a relatively new technology that has been around for less than 10 years and there are currently no existing solutions on the market that allow for the wireless transmission of brain signals. Before the BCI Telemeter can be used in a

clinical setting it will require FDA approval due to the safety concerns surrounding implanting the device in a human. At this stage in the design process we are only planning to build one prototype of the BCI Telemeter that will be tested and improved upon before submitting a request for FDA approval.

Coming up with a design for the BCI Telemeter was much more difficult than we anticipated, particularly when it came to the very specific details contained in this final report. We were proactive at the beginning of the semester and started working on our project right away; we were all excited about it and did not want to make the mistake of waiting until the last minute to start putting it together. It was difficult to coordinate schedules and to find time to meet with our mentor each week and we quickly learned that there was a great deal of background research to do before we could begin coming up with design ideas. Some of the frustrations we ran into were limited access to the programs we needed and the constant realization that there is always more to be done to improve our design. It was crucial that each member of the group pulled his or her weight and stayed in constant communication with the other team members to prevent any conflict or disagreement. A valuable lesson that we learned from this experience is that the best way to motivate other people is to lead by example. When one group member would do a significant amount of work toward the next design report, the other members were motivated to do the same out of a mutual respect for one another and a desire to contribute to the project. This mindset helped us stay on schedule and kept our design process moving forward, even during the busiest times in the semester.

In retrospect, we may have taken on a project that required a greater amount of knowledge, skills and time than we possess. In order for this project to be successful, we

had to be constantly working and researching to understand the intricate components of device, while simultaneously brainstorming ways to make the design better. If we had the chance to do something differently we would have considered the difficulty level of our project at the very beginning of the semester and altered the scope or chosen a different need that we were more capable of addressing using the skill sets we have each acquired through our engineering curriculum. We have all benefited greatly from going through this experience and will come away from it having learned that a design is never complete, but it is constantly being developed through an ongoing process of thought and innovation.

9.0 References

[1] Mancini, Ron. *So Many Amplifiers to Choose From: Matching Amplifiers to Application*. Tech. Texas Instruments Incorporated. Print. Amplifiers: Op Amps.

[2] A. Rouse and D. Moran, "Neural adaptation of epidural electrocorticographic (EECoG) signals during closed-loop brain computer interface (BCI) tasks," in Engineering in Medicine and Biology Society, 2009. EMBC 2009. Annual International Conference of the IEEE, pp. 5514-5517, 2009.

[3] "Frequency Modulation." *Webtools.delmarlearning.com*. Thomson Delmar Learning, 22 Oct. 2002. Web. 22 Oct. 2011.

[4] "Low Power Sub 1 GHz RF Transceiver." *www.ti.com*. Texas Instruments, 2011. Web. 23 Oct. 2011.

[5] Salz, Jack, Fair Haven, and Jean J. Werner. Amplitude and Frequency Modulation System. Bell Telephone Laboratories, Incorporated, Murray Hill, NJ, assignee. Patent 4,170,764. 9 Oct. 1979. Print.

[6] "Antenna Selection Guide." *www.ti.com*. Texas Instruments. Web. 22 Oct. 2011.

[7] CIRCUITRY FOR A REMOTELY POWERED BIO- IMPLANTABLE GASTRIC ELECTRICAL STIMULATION SYSTEM, Satish Kona B.S., Andhra University, India, 2001 December 2003

[8] "How to Calculate Battery Run-time When Design Equipment Using Batteries." *PowerStream Power Supplies and Chargers for OEMs in a Hurry*. Web. 06 Dec. 2011. <http://www.powerstream.com/battery-capacity-calculations.htm>.

[9] Transcutaneous Energy Transfer System for Powering Implantable Biomedical Devices, T. Dissanayake1, D. Budgett1, 2, A.P. Hu3, S. Malpas2,4 and L. Bennet4, Auckland Bioengineering Institute, University of Auckland, Auckland, New Zealand

[10] Product Specifications: *Rechargeable Lithium-ion Batteries, QL0200IA* <http://www.quallion.com/sub-sp-main.asp >

[11] "Our Process | Parylene Coatings Services Inc." *Home | Parylene Coatings Services Inc.* Web. 06 Dec. 2011. <http://www.paryleneinc.com//Our-Process.php>.

[12] Qianhong Chen, Siu Chung Wong, Chi K. Tse, and Ruan. "7.) Analysis, Design and Control of a Transcutaneous Power Regulator for Artificial Heart." Web. 3 Dec. 2011. <http://repository.lib.polyu.edu.hk/jspui/bitstream/10397/729/1/artificial-heart_08.pdf>.

Appendix A. Design Schedule

The tasks outlined in this section are to be completed throughout the semester to yield a cohesive final design. In addition to maintaining this schedule, each group member is required to keep a design notebook that will convey logical and chronological evidence of the progress of the design. Also, a weekly report will be submitted each week outlining the progress made during the previous week and goals for the following week.

List of Tasks to Be Completed

Task 1: Project Scope - Due September 14

The project scope identifies the problem to be addressed and discusses the basic requirements of the design. It presents an overview of the project and lists foreseen challenges that will need to be addressed during the design process.

Task 2: Preliminary Report and Presentation - Due September 28

The preliminary report focuses on defining the scope of the project. It includes background information about previous technologies and an in-depth analysis of the need for the design. The preliminary report includes detailed project specifications, taking into account both the consumer perspective and the eventual marketing potential.

Task 3: Headstage Circuit Design

The headstage circuit board must retain the ability to amplify and filter ECoG signals and have a low noise floor in order to accommodate extremely small brain signals. The design for this circuit board will be completed using the specifications given by Dr. Moran. While most of the data processing algorithm is already finished and can be easily

programmed onto a chip, the hardware that will make this compatible with multiple channels of ECoG recording needs to be designed.

Task 4: Telemeter Circuit Board

The telemeter circuit board must transmit both raw and processed signals to an external receiver to be used for brain control tasks. Brain control is established in ECoG by using power modulation in the frequency domain, so transmitting the processed signal with the frequency response intact is essential.

Task 5: Case Design

The material that encases the BCI Telemeter circuit board and battery must be biocompatible and must include a section that is transparent to the scanning radio-frequency beam that activates the telemetry chip. This design must be large enough to encase all the necessary hardware and small enough to fit comfortably in the chest.

Task 6: Web Page

The project web page provides a clear representation of our project for public access. It includes an overview of the project, all weekly reports, presentations, design safe outputs, and other relevant information. This website will be used primarily to track progress of the project and will be kept active for a significant length of time to be used on resumes.

Task 7: Progress Report and Presentation - Due October 26

The progress report outlines several possible solutions to the problem presented by our mentor. Each of these solutions will be examined and one will be presented as the best choice based on benefits and trade offs of each option. For this report, preliminary circuit

designs will be completed and simulations in PSpice will be prepared for presentation. The information in this report will also be presented to the class in the form of a 12-minute oral presentation.

Task 8: Risk Assessment

The risk assessment evaluates the potential dangers associated with our design and discusses ways to mitigate these risks. During the risk evaluation, the ways in which the design might malfunction as well as possible user errors that could contribute to product failure will be examined. The likelihood of these errors occurring and the significance of each risk will be evaluated. To mitigate these shortcomings of the design, ways to eliminate the cause, lower the probability, or protect against the effect of each risk will be determined. A safety assessment will be completed using DesignSafe software. The output of this evaluation will be posted on the project website.

Task 9: Final Report and Presentation - Due December 7

The final report presents the complete solution and an evaluation of the design process. Circuit simulations for both the headstage circuit board and the telemeter circuit board will be completed and the results, matching the specifications of our mentor, will be presented. The information in this report will also be presented to the class in the form of a 12-minute oral presentation.

Task 10: Senior Design Poster

The senior design poster presents the final design project in a succinct manner to be displayed to other students and faculty at the Undergraduate Research Symposium.

Design Schedule

In order to complete this project in the allotted 16 weeks, a strict schedule was developed and has been maintained. The cells that are in black have been completed and the cells in grey have been started and are in progress.

Table 22: Updated Design Schedule

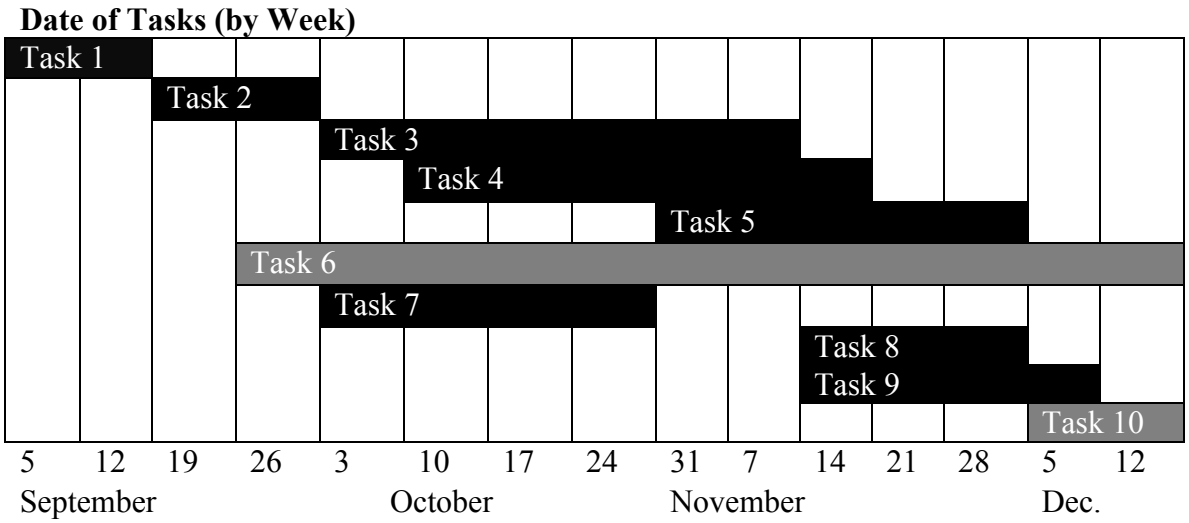

Appendix B. Contact Information and Team Organization

Contact information

Jessica Mischel	jmischel@wustl.edu
Lindsey Moses	Lindseymoses@go.wustl.edu
Osasuyi Tongo	oit1@cec.wustl.edu

Team Organization

Tasks will be assigned to team members based on particular strengths. The tables below outlines the specific work needed to be done to complete each task and how these tasks will be distributed amongst team members.

Table 23: Oraganization of Tasks

Tasks	**Report**	**Presentation**	**Multisim**	**CAD**	**Web Design**	**DesignSafe**
Task 1	☒					
Task 2	☒	☒				
Task 3			☒			
Task 4			☒			
Task 5				☒		
Task 6					☒	☒
Task 7	☒	☒				
Task 8						☒
Task 9	☒	☒				
Task 10			☒	☒		

Table 24: Distribution of Tasks

Lindsey	**Suyi**	**Jessi**	**Group Tasks**
Preliminary Presentation	Progress Presentation	Final Presentation	Project Scope
Web Page Design	CAD Drawing	Circuit Design	All written reports
Design Safe Analysis	Battery Specifications	Primary contact with mentor	

Appendix C. Company Contact Information

Hudson Technologies Contact Information
Main Tel: (386) 672-2000
Fax: (386) 676-6212
E-mail: sales@hudsontool.com
Address: 1327 North US Highway 1, Ormond Beach, FL 32174-2900
Sales Engineer: **Farley Fitzpatrick** | Tel: (386) 676-6216
Director of Sales: **John Marfiak** | Tel: (386) 676-6207

Parylene Coating Services Inc.
6819 Highway Blvd, Suite 510
Katy, Texas 77494

Digi-Key Corporation
www.digikey.com
Phone: 1-800-344-4539
701 Brooks Avenue South Thief River Falls, MN 56701 USA

Appendix D. DesignSafe

designsafe Report

Application:	BCI Telemeter
Description:	
Analyst Name(s):	Lindsey Moses
Company:	Braintech
Facility Location:	
Product Identifier:	
Assessment Type:	Detailed
Limits:	
Sources:	
Risk Scoring System:	ANSI B11.0 (TR3) Two Factor

Guide sentence: When doing [task], the [user] could be injured by the [hazard] due to the [failure mode].

Item Id	User / Task	Hazard / Failure Mode	Initial Assessment Severity Probability	Risk Level	Risk Reduction /Comments	Final Assessment Severity Probability	Risk Leve	Status / Responsible / /Reference
1-1-1	operator normal operation	noise / vibration : equipment damage	Serious Remote	Low	restricted users	Serious		
2-1-1	engineer modify parts / components	electrical / electronic : improper wiring	Minor Remote	Negligible		Minor		
2-2-1	engineer conduct tests	None / Other : Not a hazard						
2-3-1	engineer design components / systems	electrical / electronic : improper wiring Flaw in PCB manufacturing	Minor Remote	Negligible		Minor		
2-4-1	engineer trouble shooting	None / Other : Not a hazard						
2-5-1	engineer adjust software program / controls	None / Other : Not a hazard						
2-6-1	engineer inspect machinery	None / Other : Not a hazard						
2-7-1	engineer normal operation	None / Other : Not a hazard						
3-1-1	patient normal operation	foreign object in body : rejection by body Body does not respond well to foreign object being placed inside of it	Serious Unlikely	Medium	monitor patient regularly	Serious		
3-1-2	patient normal operation	foreign object in body : battery malfunction inside body	Minor Unlikely	Negligible	Zero Volt Technology, SaFE-LYTE	Minor		
3-2-1	patient undergo surgery	risks of surgery : side effects of anesthesia Anesthesia from surgery can have unpleasant after effects	Minor Likely	Low		Minor		

Item Id	User / Task	Hazard / Failure Mode	Initial Assessment Severity Probability	Risk Level	Risk Reduction /Comments	Final Assessment Severity Probability	Risk Leve	Status / Responsible / /Reference
3-2-2	patient undergo surgery	risks of surgery : complications Inherent risks when undergoing any surgery	Serious Unlikely	Medium	standard procedures, restricted users	Serious		
3-2-3	patient undergo surgery	risks of surgery : infection Inherent risk of infection at site where body was opened to implace device	Moderate Unlikely	Low	Experienced surgeon implanting device, monitor patient regularly	Moderate		
4-1-1	physician perform surgery to implant device	None / Other : Not a hazard						
4-2-1	physician operate device inside patient	None / Other : Not a hazard						

Appendix E. Code Used For Circuit Analysis

Analog to Digital Converter

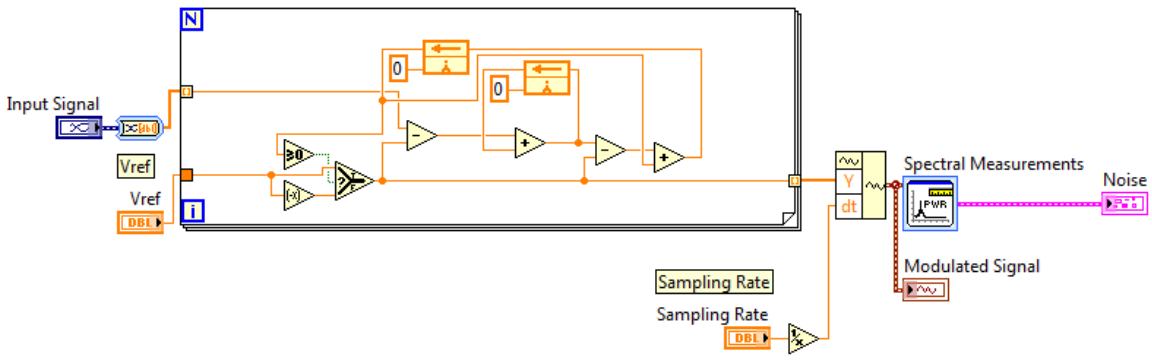

Figure 38: LabVIEW VI used to implement a Delta-Sigma modulator for noise shaping.

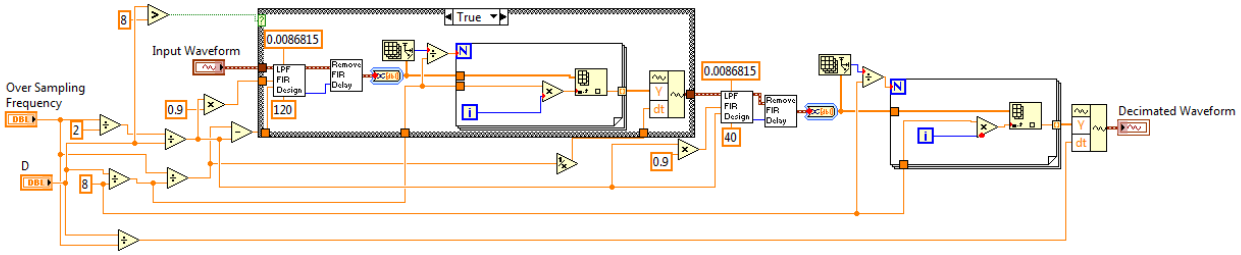

Figure 39: LabVIEW VI used to decimate the modulated signal of the Delta-Sigma modulated signal

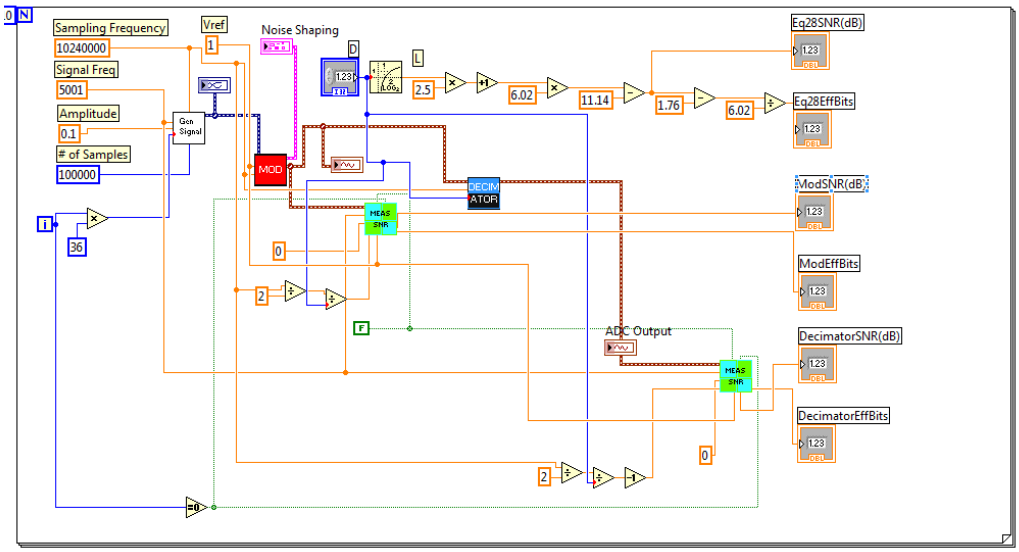

Figure 40: LabVIEW VI used to demonstrate the increase in SNR and ENOB

To combine the modulator and the decimator VIs into one module, the DeltaSigma VI was created and represents an oversampling ADC with a sampled input. The input signal is a sinusoid of 5001 Hz, and amplitude 0.1 V. The oversampling frequency is set at 10.24 MHz. As shown in figure 39, this signal is passed through the Modulator VI and then the Decimator VI, and after each, the SNR is tested using Meas SNR VI (see figure 41).

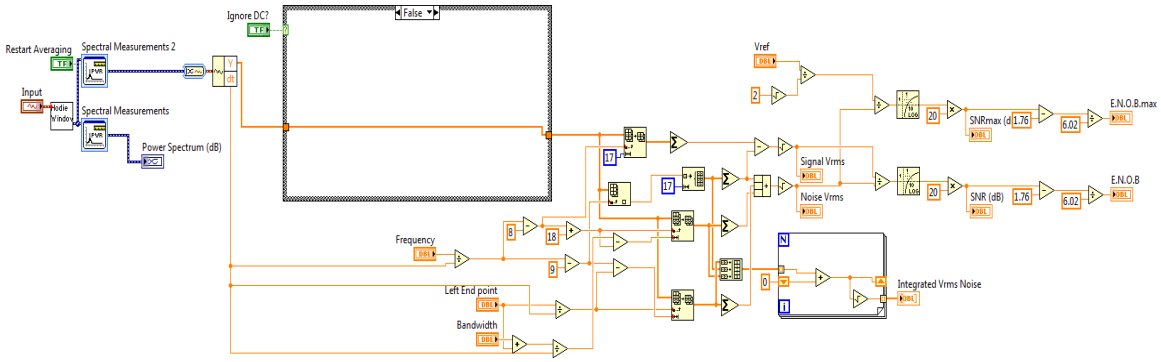

Figure 41: Meas SNR VI used to calculate SNR and ENOB

Anti-Aliasing Filter

Matlab Code for Filter Elements

```
% Low-pass butterworth implemented with cascaded Sallen-Key topologies
% 05-June-11

n   = 2;    % order (1-10)
C1  = 1e-8;    % capacitor value (Farads)
Fc  = 200;    % cutoff (Hz)

switch(n)
   case(1)
      table = [1.0000 0 1.000 NaN];
   case(2)
      table = [1.4142 1 1.000 0.71];
   case(3)
```

```
        table = [1.0000 0 1.000 NaN; ...
                 1.0000 1 1.272 1.00];
    case(4)
        table = [1.8478 1 0.719 0.54; ...
                 0.7654 1 1.390 1.31];
    case(5)
        table = [1.0000 0 1.000 NaN; ...
                 1.6180 1 0.859 0.62; ...
                 0.6180 1 1.448 1.62];
    case(6)
        table = [1.9319 1 0.676 0.52; ...
                 1.4142 1 1.000 0.71; ...
                 0.5176 1 1.479 1.93];
    case(7)
        table = [1.0000 0 1.000 Nan; ...
                 1.8019 1 0.745 0.55; ...
                 1.2470 1 1.117 0.80; ...
                 0.4450 1 1.499 2.25];
    case(8)
        table = [1.9616 1 0.661 0.51; ...
                 1.6629 1 0.829 0.60; ...
                 1.1111 1 1.206 0.90; ...
                 0.3902 1 1.512 2.56];
    case(9)
        table = [1.0000 0 1.000 NaN; ...
                 1.8794 1 0.703 0.53; ...
                 1.5321 1 0.917 0.65; ...
                 1.0000 1 1.272 1.00; ...
                 0.3473 1 1.521 2.88];
    case(10)
        table = [1.9754 1 0.655 0.51; ...
                 1.7820 1 0.756 0.56; ...
                 1.4142 1 1.000 0.71; ...
                 0.9080 1 1.322 1.10; ...
                 0.3129 1 1.527 3.20];
end
num_stages = size(table,1);
a = table(:,1);
b = table(:,2);
if size(C1,1) == 1
    C1 = C1.*ones(num_stages,1);
end
C2 = C1.*4.*b./a.^2;
R1 = (a.*C2-sqrt((a.^2).*(C2.^2)-4.*b.*C1.*C2))./(4.*pi.*Fc.*C1.*C2);
R2 = (a.*C2+sqrt((a.^2).*(C2.^2)-4.*b.*C1.*C2))./(4.*pi.*Fc.*C1.*C2);
display(' ');
```

```
display([num2str(n) '-order Butterworth Lowpass at ' num2str(Fc) ' Hz']);
display('Sallen-Key parameters:');
display(['  C1: ' num2str(C1)]);
display(['  C2: ' num2str(C2)]);
display(['  R1: ' num2str(R1)]);
display(['  R2: ' num2str(R2)]);
```

Appendix F. Additional CAD Drawings

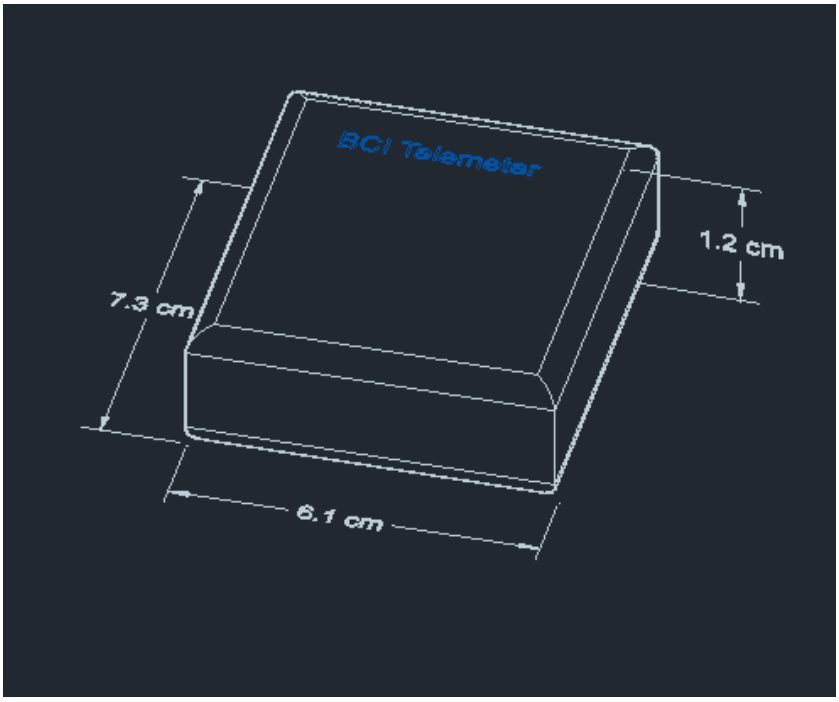

Figure 42: Sketch of 3-D view of BCI Telemeter

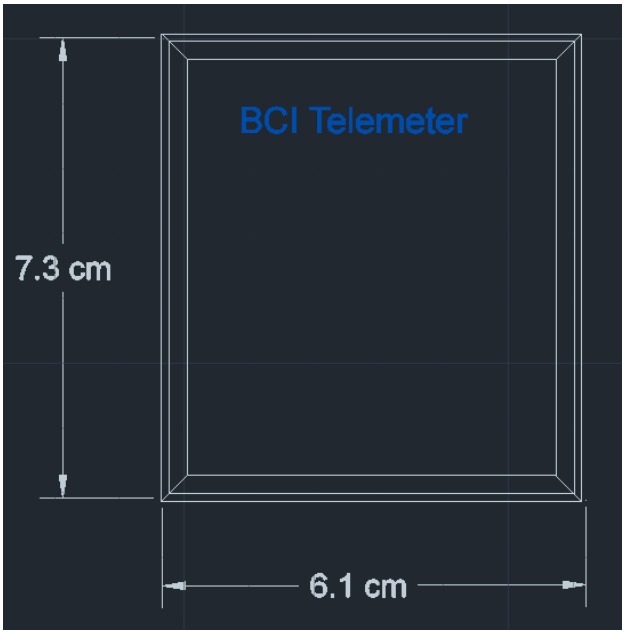

Figure 43: Top View of the BCI Telemeter

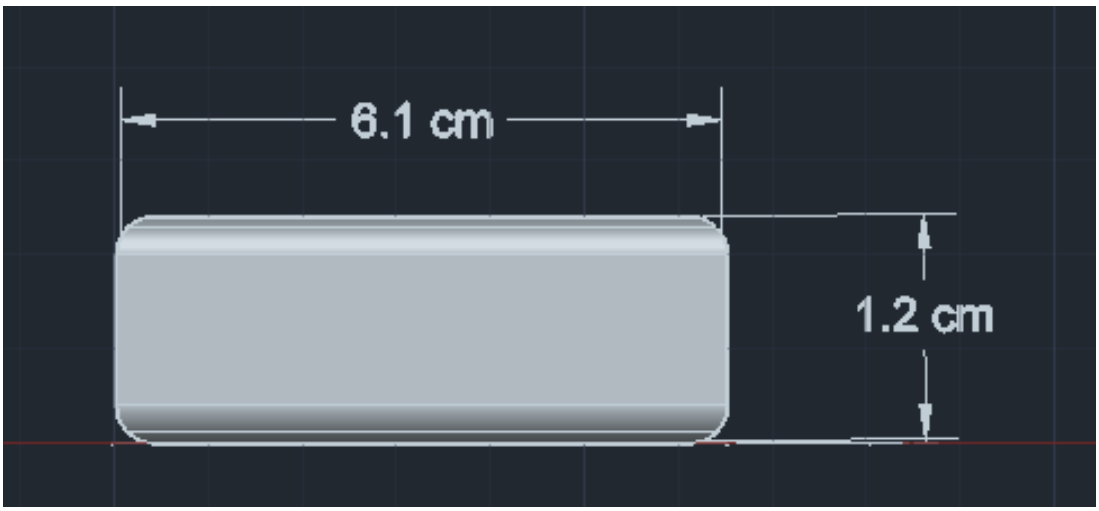

Figure 44: Lateral View of the BCI Telemeter

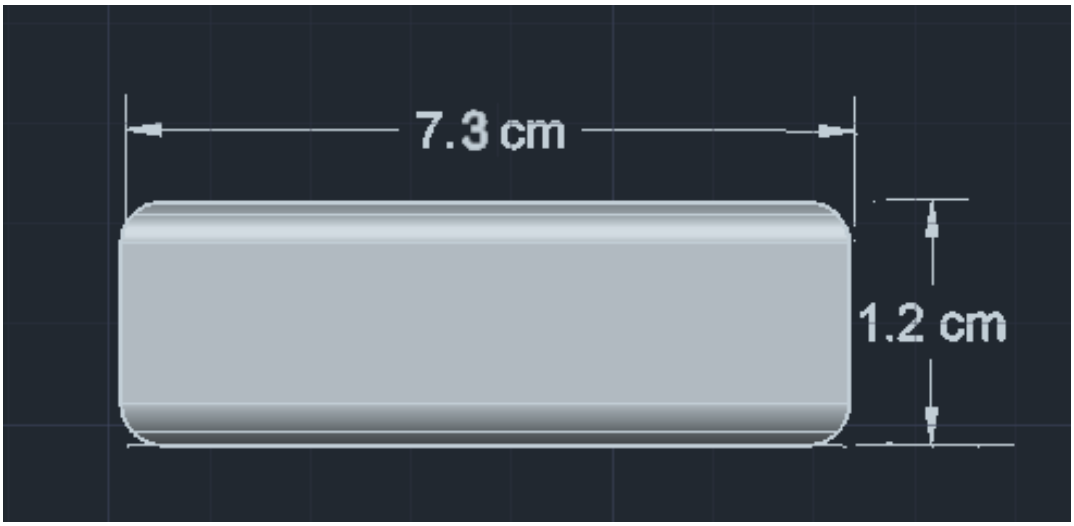

Figure 45: Longitudinal View of the BCI telemeter

Appendix G. Component Data Sheets

Analog Switch – TS3A4751

TEXAS INSTRUMENTS

TS3A4751

0.9-Ω LOW-VOLTAGE SINGLE-SUPPLY QUAD SPST ANALOG SWITCH

FEATURES

- Low ON-State Resistance (r_{ON})
  - 0.9 Ω Max (3-V Supply)
  - 1.5 Ω Max (1.8-V Supply)
- r_{ON} Flatness: 0.4 Ω Max (3-V)
- r_{ON} Matching
  - 0.05 Ω Max (3-V Supply)
  - 0.25 Ω Max (1.8-V Supply)
- 1.6-V to 3.6-V Single-Supply Operation
- 1.8-V CMOS Logic Compatible (3-V Supply)
- High Current-Handling Capacity (100 mA Continuous)
- Fast Switching: t_{ON} = 14 ns, t_{OFF} = 9 ns
- ESD Protection Exceeds JESD-22
  - 4000-V Human Body Model (A114-A)
  - 300-V Machine Model (A115-A)
  - 1000-V Charged Device Model (C101)

APPLICATIONS

- Power Routing
- Battery Powered Systems
- Audio and Video Signal Routing
- Low-Voltage Data-Acquisition Systems
- Communications Circuits
- PCMCIA Cards
- Cellular Phones
- Modems
- Hard Drives

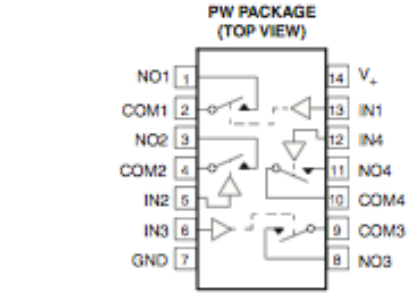

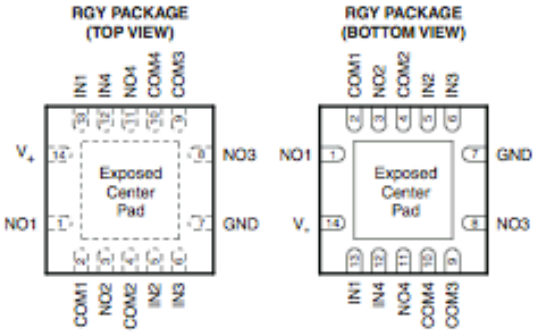

If the exposed center pad is used, it must be connected as a secondary ground or left electrically open.

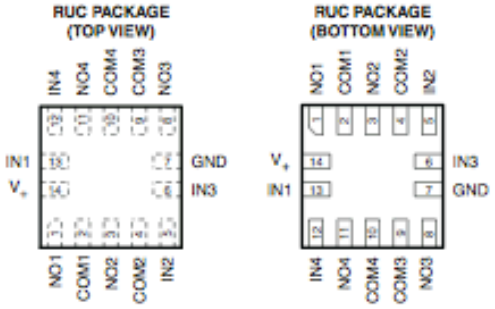

DESCRIPTION/ORDERING INFORMATION

The TS3A4751 is a low ON-state resistance (r_{on}), low-voltage, quad, single-pole/single-throw (SPST) analog switch that operates from a single 1.6-V to 3.6-V supply. This device has fast switching speeds, handles rail-to-rail analog signals, and consumes very low quiescent power.

The digital input is 1.8-V CMOS compatible when using a 3-V supply.

The TS3A4751 has four normally open (NO) switches. The TS3A4751 is available in a 14-pin thin shrink small-outline package (TSSOP) and in space-saving 14-pin SON (RGY) and micro QFN (RUC) packages.

ELECTRICAL CHARACTERISTICS FOR 3-V SUPPLY[1][2]

V_+ = 2.7 V to 3.6 V, T_A = –40°C to 85°C, V_{IH} = 1.4 V, V_{IL} = 0.5 V (unless otherwise noted).

PARAMETER	SYMBOL	TEST CONDITIONS		T_A	MIN	TYP[3]	MAX	UNIT
Analog Switch								
Analog signal range	V_{COM}, V_{NO}				0		V_+	V
ON-state resistance	r_{on}	V_+ = 2.7 V, I_{COM} = –100 mA, V_{NO} = 1.5 V		25°C		0.7	0.9	Ω
				Full			1.1	
ON-state resistance match between channels[4]	Δr_{on}	V_+ = 2.7 V, I_{COM} = –100 mA, V_{NO} = 1.5 V		25°C		0.03	0.05	Ω
				Full			0.15	
ON-state resistance flatness[5]	$r_{on(flat)}$	V_+ = 2.7 V, I_{COM} = –100 mA, V_{NO} = 1 V, 1.5 V, 2 V		25°C		0.23	0.4	Ω
				Full			0.5	
NO OFF leakage current[6]	$I_{NO(OFF)}$	V_+ = 3.6 V, V_{COM} = 0.3 V, 3 V, V_{NO} = 3 V, 0.3 V		25°C	–2	1	2	nA
				Full	–18		18	
COM OFF leakage current[6]	$I_{COM(OFF)}$	V_+ = 3.6 V, V_{COM} = 0.3 V, 3 V, V_{NO} = 3 V, 0.3 V		25°C	–2	1	2	nA
				Full	–18		18	
COM ON leakage current[6]	$I_{COM(ON)}$	V_+ = 3.6 V, V_{COM} = 0.3 V, 3 V, V_{NO} = 0.3 V, 3 V, or floating		25°C	–2.5	0.01	2.5	nA
				Full	–5		5	
Dynamic								
Turn-on time	t_{ON}	V_{NO} = 1.5 V, R_L = 50 Ω, C_L = 35 pF, See Figure 14		25°C		5	14	ns
				Full			15	
Turn-off time	t_{OFF}	V_{NO} = 1.5 V, R_L = 50 Ω, C_L = 35 pF, See Figure 14		25°C		4	9	ns
				Full			10	
Charge injection	Q_C	V_{GEN} = 0, R_{GEN} = 0, C_L = 1 nF, See Figure 15		25°C		3		pC
NO OFF capacitance	$C_{NO(OFF)}$	f = 1 MHz, See Figure 16		25°C		23		pF
COM OFF capacitance	$C_{COM(OFF)}$	f = 1 MHz, See Figure 16		25°C		20		pF
COM ON capacitance	$C_{COM(ON)}$	f = 1 MHz, See Figure 16		25°C		43		pF
Bandwidth	BW	R_L = 50 Ω, Switch ON		25°C		125		MHz
OFF isolation[7]	O_{ISO}	R_L = 50 Ω, C_L = 5 pF, See Figure 17	f = 10 MHz	25°C		–40		dB
			f = 1 MHz			–62		
Crosstalk	X_{TALK}	R_L = 50 Ω, C_L = 5 pF, See Figure 17	f = 10 MHz	25°C		–73		dB
			f = 1 MHz			–95		
Total harmonic distortion	THD	f = 20 Hz to 20 kHz, V_{COM} = 2 V_{P-P}	R_L = 32 Ω	25°C		0.04		%
			R_L = 600 Ω			0.003		
Digital Control Inputs (IN1–IN4)								
Input logic high	V_{IH}			Full	1.4			V
Input logic low	V_{IL}			Full			0.5	V
Input leakage current	I_{IN}	V_I = 0 or V_+		25°C		0.5	1	nA
				Full	–20		20	
Supply								
Power-supply range	V_+				1.6		3.6	V
Positive-supply current	I_+	V_+ = 3.6 V, V_{IN} = 0 or V_+		25°C			0.075	µA
				Full			0.75	

(1) The algebraic convention, whereby the most negative value is a minimum and the most positive value is a maximum.
(2) Parts are tested at 85°C and specified by design and correlation over the full temperature range.
(3) Typical values are at V_+ = 3 V, T_A = 25°C.
(4) $\Delta r_{on} = r_{on(max)} - r_{on(min)}$
(5) Flatness is defined as the difference between the maximum and minimum value of r_{on} as measured over the specified analog signal ranges.
(6) Leakage parameters are 100% tested at the maximum-rated hot operating temperature and specified by correlation at T_A = 25°C.
(7) OFF isolation = $20_{log}10$ (V_{COM}/V_{NO}), V_{COM} = output, V_{NO} = input to OFF switch

Continued at: http://www.ti.com/lit/ds/symlink/ts3a4751.pdf

ANALOG DEVICES

40 µA Micropower Instrumentation Amplifier with Zero Crossover Distortion

AD8236

FEATURES

- Low power: 40 µA supply current (maximum)
- Low input currents
  - 1 pA input bias current
  - 0.5 pA input offset current
- High CMRR: 110 dB CMRR, G = 100
- Space-saving MSOP
- Zero input crossover distortion
- Rail-to-rail input and output
- Gain set with single resistor
- Operates from 1.8 V to 5.5 V

APPLICATIONS

- Medical instrumentation
- Low-side current sense
- Portable devices

CONNECTION DIAGRAM

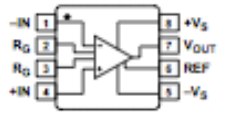

Figure 1.

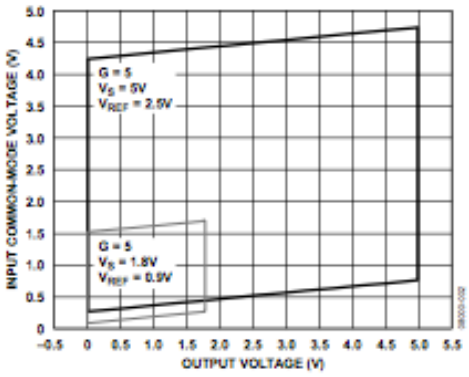

Figure 2. Wide Common-Mode Voltage Range vs. Output Voltage

GENERAL DESCRIPTION

The AD8236 is the lowest power instrumentation amplifier in the industry. It has rail-to-rail outputs and can operate on voltages as low as 1.8 V. Its 40 µA maximum supply current makes it an excellent choice in battery-powered applications.

The AD8236's high input impedance, low input bias current of 1 pA, high CMRR of 110 dB (G = 100), small size, and low power offer tremendous value. It has a wider common-mode voltage range than typical three-op-amp instrumentation amplifiers, making this a great solution for applications that operate on a single 1.8 V or 3 V supply. An innovative input stage allows for a wide rail-to-rail input voltage range without the crossover distortion common in other designs.

The AD8236 is available in an 8-lead MSOP and is specified over the industrial temperature range of −40°C to +125°C.

Table 1. Instrumentation Amplifiers by Category[1]

General Purpose	Zero Drift	Military Grade	Low Power	High Speed PGA
AD8220	AD8230	AD620	AD8236	AD8250
AD8221	AD8231	AD621	AD627	AD8251
AD8222	AD8290	AD624	AD623	AD8253
AD8228	AD8293G80	AD524	AD8223	
AD8295	AD8293G160	AD526	AD8226	
	AD8553			
	AD8556			
	AD8557			

[1] See www.analog.com/inamps for the latest instrumentation amplifiers.

One Technology Way, P.O. Box 9106, Norwood, MA 02062-9106, U.S.A.
Tel: 781.329.4700 www.analog.com
Fax: 781.461.3113

TABLE OF CONTENTS

Features ... 1
Applications ... 1
Connection Diagram ... 1
General Description ... 1
Revision History ... 2
Specifications ... 3
Absolute Maximum Ratings ... 7
Maximum Power Dissipation ... 7
ESD Caution ... 7
Pin Configuration and Function Descriptions ... 8
Typical Performance Characteristics ... 9
Theory of Operation ... 14
Basic Operation ... 14
Gain Selection ... 14
Layout ... 15
Reference Terminal ... 15
Power Supply Regulation and Bypassing ... 15
Input Bias Current Return Path ... 16
Input Protection ... 16
RF Interference ... 16
Common-Mode Input Voltage Range ... 17
Applications Information ... 18
AC-Coupled Instrumentation Amplifier ... 18
Low Power Heart Rate Monitor ... 19
Outline Dimensions ... 20
Ordering Guide ... 20

REVISION HISTORY

5/09—Revision 0: Initial Version

SPECIFICATIONS

$+V_S$ = 5 V, $-V_S$ = 0 V (GND), V_{REF} = 2.5 V, T_A = 25°C, G = 5, R_L = 100 kΩ to GND, unless otherwise noted.

Table 2.

Parameter	Test Conditions	Min	Typ	Max	Unit
COMMON-MODE REJECTION RATIO (CMRR)	V_S = ±2.5 V, V_{REF} = 0 V				
CMRR DC	V_{CM} = −1.8 V to +1.8 V				
G = 5		86	94		dB
G = 10		90	100		dB
G = 100		100	110		dB
G = 200		100	110		dB
NOISE					
Voltage Noise Spectral Density, RTI	f = 1 kHz, G = 5		76		nV/√Hz
RTI, 0.1 Hz to 10 Hz					
G = 5			4		µV p-p
G = 200			4		µV p-p
Current Noise			15		fA/√Hz
VOLTAGE OFFSET					
Input Offset, V_{OS}				3.5	mV
Average Temperature Coefficient (TC)	−40°C to +125°C		2.5		µV/°C
Offset RTI vs. Supply (PSR)	V_S = 1.8 V to 5 V				
G = 5		100	120		dB
G = 10		110	126		dB
G = 100		110	130		dB
G = 200		110	130		dB
INPUT CURRENT					
Input Bias Current			1	10	pA
Overtemperature	−40°C to +85°C			100	pA
	−40°C to +125°C			600	pA
Input Offset Current			0.5	5	pA
Overtemperature	−40°C to +85°C			50	pA
	−40°C to +125°C			130	pA
DYNAMIC RESPONSE					
Small Signal Bandwidth, −3 dB					
G = 5			23		kHz
G = 10			9		kHz
G = 100			0.8		kHz
G = 200			0.4		kHz
Settling Time 0.01%	V_{OUT} = 4 V step				
G = 5			444		µs
G = 10			456		µs
G = 100			992		µs
G = 200			1816		µs
Slew Rate					
G = 5 to 100			9		mV/µs

Continued at: http://www.analog.com/static/imported-files/data_sheets/AD8236.pdf

Burr-Brown Products
from Texas Instruments

OPA333
OPA2333

SBOS351C – MARCH 2006 – REVISED MAY 2007

1.8V, *micro*POWER CMOS OPERATIONAL AMPLIFIERS Zerø-Drift Series

FEATURES

- LOW OFFSET VOLTAGE: 10µV (max)
- ZERO DRIFT: 0.05µV/°C (max)
- 0.01Hz to 10Hz NOISE: 1.1μV_{PP}
- QUIESCENT CURRENT: 17µA
- SINGLE-SUPPLY OPERATION
- SUPPLY VOLTAGE: 1.8V to 5.5V
- RAIL-TO-RAIL INPUT/OUTPUT
- *micro*SIZE PACKAGES: SC70 and SOT23

APPLICATIONS

- TRANSDUCER APPLICATIONS
- TEMPERATURE MEASUREMENTS
- ELECTRONIC SCALES
- MEDICAL INSTRUMENTATION
- BATTERY-POWERED INSTRUMENTS
- HANDHELD TEST EQUIPMENT

DESCRIPTION

The OPA333 series of CMOS operational amplifiers uses a proprietary auto-calibration technique to simultaneously provide very low offset voltage (10µV max) and near-zero drift over time and temperature. These miniature, high-precision, low quiescent current amplifiers offer high-impedance inputs that have a common-mode range 100mV beyond the rails and rail-to-rail output that swings within 50mV of the rails. Single or dual supplies as low as +1.8V (±0.9V) and up to +5.5V (±2.75V) may be used. They are optimized for low-voltage, single-supply operation.

The OPA333 family offers excellent CMRR without the crossover associated with traditional complementary input stages. This design results in superior performance for driving analog-to-digital converters (ADCs) without degradation of differential linearity.

The OPA333 (single version) is available in the SC70-5, SOT23-5, and SO-8 packages. The OPA2333 (dual version) is offered in DFN-8 (3mm × 3mm), MSOP-8, and SO-8 packages. All versions are specified for operation from –40°C to +125°C.

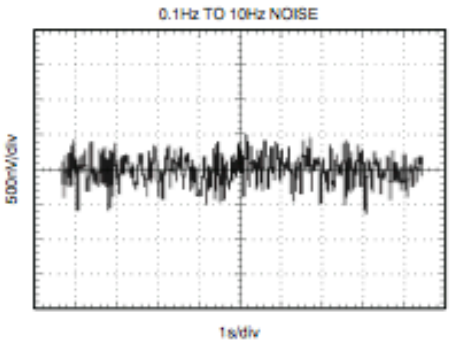

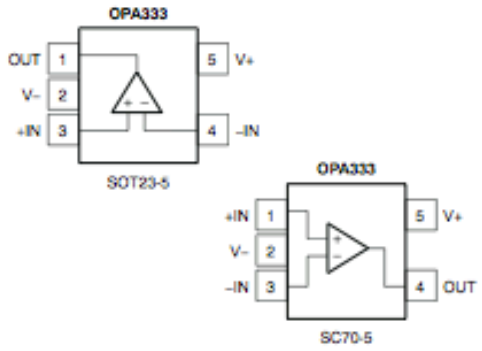

ELECTRICAL CHARACTERISTICS: V_S = +1.8V to +5.5V

Boldface limits apply over the specified temperature range, T_A = –40°C to +125°C.
At T_A = +25°C, R_L = 10kΩ connected to V_S/2, V_{CM} = V_S/2, and V_{OUT} = V_S/2, unless otherwise noted.

PARAMETER		TEST CONDITIONS	OPA333, OPA2333 MIN	OPA333, OPA2333 TYP	OPA333, OPA2333 MAX	UNIT
OFFSET VOLTAGE						
Input Offset Voltage	V_{OS}	V_S = +5V		2	10	µV
vs Temperature	**dV_{OS}/dT**			**0.02**	**0.05**	**µV/°C**
vs Power Supply	**PSRR**	**V_S = +1.8V to +5.5V**		**1**	**5**	**µV/V**
Long-Term Stability[1]				See [1]		
Channel Separation, dc				0.1		µV/V
INPUT BIAS CURRENT						
Input Bias Current	I_B			±70	±200	pA
over Temperature				**±150**		**pA**
Input Offset Current	I_{OS}			±140	±400	pA
NOISE						
Input Voltage Noise, f = 0.01Hz to 1Hz				0.3		μV_{PP}
Input Voltage Noise, f = 0.1Hz to 10Hz				1.1		μV_{PP}
Input Current Noise, f = 10Hz	i_n			100		$fA/\sqrt{Hz}$
INPUT VOLTAGE RANGE						
Common-Mode Voltage Range	V_{CM}		(V–) – 0.1		(V+) + 0.1	V
Common-Mode Rejection Ratio	**CMRR**	**(V–) – 0.1V < V_{CM} < (V+) + 0.1V**	**106**	**130**		**dB**
INPUT CAPACITANCE						
Differential				2		pF
Common-Mode				4		pF
OPEN-LOOP GAIN						
Open-Loop Voltage Gain	**A_{OL}**	**(V–) + 100mV < V_O < (V+) – 100mV, R_L = 10kΩ**	**106**	**130**		**dB**
FREQUENCY RESPONSE						
Gain-Bandwidth Product	GBW	C_L = 100pF		350		kHz
Slew Rate	SR	G = +1		0.16		V/µs
OUTPUT						
Voltage Output Swing from Rail		R_L = 10kΩ		30	50	mV
over Temperature		**R_L = 10kΩ**			**70**	**mV**
Short-Circuit Current	I_{SC}			±5		mA
Capacitive Load Drive	C_L			See Typical Characteristics		
Open-Loop Output Impedance		f = 350kHz, I_O = 0		2		kΩ
POWER SUPPLY						
Specified Voltage Range	V_S		1.8		5.5	V
Quiescent Current Per Amplifier	I_Q	I_O = 0		17	25	µA
over Temperature					**28**	**µA**
Turn-On Time		V_S = +5V		100		µs
TEMPERATURE RANGE						
Specified Range			–40		+125	°C
Operating Range			–40		+150	°C
Storage Range			–65		+150	°C
Thermal Resistance	θ_{JA}					°C/W
SOT23-5				200		°C/W
MSOP-8, SO-8				150		°C/W
DFN-8				50		°C/W
SC70-5				250		°C/W

(1) 300-hour life test at +150°C demonstrated randomly distributed variation of approximately 1µV.

Continued at: http://www.ti.com/lit/ds/symlink/opa2333.pdf

High Stability Thin Film Flat Chip Resistor

VISHAY

TNPW e3

Vishay

High Stability Thin Film Flat Chip Resistor
≤ 0.05 % (1000 h rated power at 70 °C)

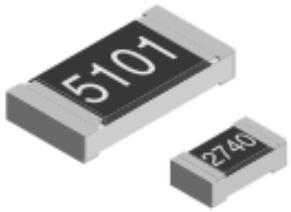

TNPW e3 Precision Thin Film Flat Chip Resistors are the perfect choice for most fields of modern electronics where highest reliability and stability is of major concern. Typical applications include automotive, telecommunication, industrial, medical equipment, precision test and measuring equipment.

FEATURES

- Superior moisture resistivity ≤ 0.25 % (85 °C; 56 days; 85 % RH)
- Lead (Pb)-free solder contacts, RoHS compliant
- AEC-Q200 compliant (sizes 0402 to 1206)
- Low temperature coefficient and tight tolerances (± 0.1 %; ± 10 ppm/K)
- Waste gas resistant

RoHS COMPLIANT

APPLICATIONS

- Test and measuring equipment
- Telecommunication
- Medical equipment
- Industrial equipment
- Instrumentation
- Automotive

STANDARD ELECTRICAL SPECIFICATIONS

DESCRIPTION	TNPW0402	TNPW0603	TNPW0805	TNPW1206	TNPW1210 (1)	TNPW2010	TNPW2512 (1)
Metric size	RR 1005M	RR 1608M	RR 2012M	RR 3216M	RR 3225M	RR 5025M	RR 6332M
Resistance range	10 Ω to 100 kΩ	10 Ω to 332 kΩ	10 Ω to 1 MΩ	10 Ω to 2 MΩ	10 Ω to 3.01 MΩ	10 Ω to 4.99 MΩ	10 Ω to 8.87 MΩ
Resistance tolerance	± 1 %; ± 0.5 %; ± 0.1 %						
Temperature coefficient	± 50 ppm/K; ± 25 ppm/K; ± 15 ppm/K; ± 10 ppm/K					± 50 ppm/K; ± 25 ppm/K	
Climatic category (LCT/UCT/days)	55/125/56	55/125/56	55/125/56	55/125/56	55/125/56	55/125/56	55/125/56
Rated dissipation, P_{70} (2)	0.063 W	0.1 W	0.125 W	0.25 W	0.33 W	0.4 W	0.5 W
Operating voltage, $U_{max.}$ AC/DC	50 V	75 V	150 V	200 V	200 V	300 V	300 V
Maximum permissible film temperature	155 °C	155 °C	155 °C	155 °C	155 °C	155 °C	155 °C
Thermal resistance (3)	870 K/W	550 K/W	440 K/W	220 K/W	170 K/W	140 K/W	110 K/W
Max. resistance change at P_{70}; $\Delta R/R$	10 Ω to 100 kΩ	10 Ω to 332 kΩ	10 Ω to 1 MΩ	10 Ω to 2 MΩ	10 Ω to 3.01 MΩ	10 Ω to 4.99 MΩ	10 Ω to 8.87 MΩ
1000 h	≤ 0.05 %	≤ 0.05 %	≤ 0.05 %	≤ 0.05 %	≤ 0.05 %	≤ 0.05 %	≤ 0.05 %
8000 h	≤ 0.10 %	≤ 0.10 %	≤ 0.10 %	≤ 0.10 %	≤ 0.10 %	≤ 0.10 %	≤ 0.10 %
225 000 h	≤ 0.30 %	≤ 0.30 %	≤ 0.30 %	≤ 0.30 %	≤ 0.30 %	≤ 0.30 %	≤ 0.30 %
Insulation voltage:							
U_{rms} 1 min	75 V	100 V	200 V	300 V	300 V	300 V	300 V
Continuous	75 V	75 V	75 V	75 V	75 V	75 V	75 V
$FIT_{observed}$	≤ 0.1 x 10^{-9}/h	≤ 0.1 x 10^{-9}/h	≤ 0.1 x 10^{-9}/h	≤ 0.1 x 10^{-9}/h	≤ 0.1 x 10^{-9}/h	≤ 0.1 x 10^{-9}/h	≤ 0.1 x 10^{-9}/h
Weight/1000 pieces	0.65 g	2 g	5.5 g	10 g	16 g	28 g	39 g

Notes

(1) Size not specified in EN 140401-801

(2) Rated voltage $\sqrt{P \times R}$. The power dissipation on the resistor generates a temperature rise against the local ambient, depending on the heat flow support of the printed-circuit board (thermal resistance). Using advanced temperature level may require special considerations towards the choice of circuit board and solder material. The rated dissipation applies only if the permitted film temperature is not exceeded.

(3) Measuring conditions in accordance with EN 140401-801

- TNPW 0402 without marking

Continued at: http://www.vishay.com/docs/28758/tnpw_e3.pdf

Surface Mount Multilayer Ceramic Chip Capacitors (SMD MLCCs)

X7R Dielectric, 6.3VDC-250VDC (Commercial Grade)

The Capacitance Company
KEMET
CHARGED.

Overview

KEMET's X7R dielectric features a 125°C maximum operating temperature and is considered "temperature stable." The Electronics Components, Assemblies & Materials Association (EIA) characterizes X7R dielectric as a Class II material. Components of this classification are fixed, ceramic dielectric capacitors suited for bypass and decoupling applications or for frequency discriminating circuits where Q and stability of capacitance characteristics are not critical. X7R exhibits a predictable change in capacitance with respect to time and voltage and boasts a minimal change in capacitance with reference to ambient temperature. Capacitance change is limited to ±15% from -55°C to +125°C.

Benefits

- -55°C to +125°C operating temperature range
- Pb-Free and RoHS compliant
- Temperature stable dielectric
- EIA 0402, 0603, 0805, 1206, 1210, 1808, 1812, 1825, 2220 and 2225 case sizes
- DC voltage ratings of 6.3V, 10V, 16V, 25V, 50V, 100V, 200V and 250V
- Capacitance offerings ranging from 150pF to 47µF
- Available capacitance tolerances of ±5%, ±10% and ±20%
- Non-polar device, minimizing installation concerns
- 100% pure matte tin-plated termination finish allowing for excellent solderability
- SnPb termination finish option available upon request (5% min)

Applications

Typical applications include decoupling, bypass, filtering and transient voltage suppression.

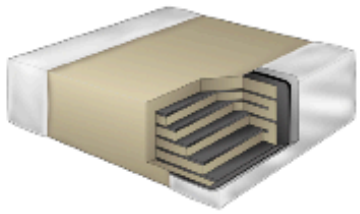

Ordering Information

C	1206	C	106	M	4	R	A	C	TU
Ceramic	Case Size (L" x W")	Specification/ Series	Capacitance Code (pF)	Capacitance Tolerance	Voltage	Dielectric	Failure Rate/ Design	Termination Finish[1]	Packaging/Grade (C-Spec)[2]
	0402 0603 0805 1206 1210 1808 1812 1825 2220 2225	C = Standard	2 Sig. Digits + Number of Zeros	J = ±5% K = ±10% M = ±20%	9 = 6.3 8 = 10V 4 = 16V 3 = 25V 6 = 35V 5 = 50V 1 = 100V 2 = 200V A = 250V	R = X7R	A = N/A	C = 100% Matte Sn	Blank = Bulk TU = 7" Reel Unmarked TM = 7" Reel Marked

[1] *Additional termination finish options may be available. Contact KEMET for details.*
[2] *Additional reeling or packaging options may be available. Contact KEMET for details.*

Continued at:
http://www.kemet.com/kemet/web/homepage/kechome.nsf/vapubfiles/KEM_C1002_X7R_SMD.pdf/$file/KEM_C1002_X7R_SMD.pdf

Microchip - MSP430AFE2x2

MIXED SIGNAL MICROCONTROLLER

FEATURES

- Low Supply Voltage Range: 1.8 V to 3.6 V
- Ultra-Low Power Consumption
  - Active Mode: 220 µA at 1 MHz, 2.2 V
  - Standby Mode: 0.5 µA
  - Off Mode (RAM Retention): 0.1 µA
- Five Power-Saving Modes
- Ultra-Fast Wake-Up From Standby Mode in Less Than 1 µs
- 16-Bit RISC Architecture, up to 12-MHz System Clock
- Basic Clock Module Configurations
  - Internal Frequencies up to 12 MHz With Two Calibrated Frequencies
  - Internal Very-Low-Power Low-Frequency (LF) Oscillator
  - High-Frequency (HF) Crystal up to 16 MHz
  - Resonator
  - External Digital Clock Source
- Up to Three 24-Bit Sigma-Delta Analog-to-Digital (A/D) Converters With Differential PGA Inputs
- 16-Bit Timer_A With Three Capture/Compare Registers
- Serial Communication Interface (USART), Asynchronous UART or Synchronous SPI Selectable by Software
- 16-Bit Hardware Multiplier
- Brownout Detector
- Supply Voltage Supervisor/Monitor with Programmable Level Detection
- Serial Onboard Programming, No External Programming Voltage Needed Programmable Code Protection by Security Fuse
- On-Chip Emulation Module
- Family Members are Summarized in Table 1.
- For Complete Module Descriptions, See the *MSP430x2xx Family User's Guide*, Literature Number SLAU144

DESCRIPTION

The Texas Instruments MSP430™ family of ultra-low-power microcontrollers consists of several devices featuring different sets of peripherals targeted for various applications. The architecture, combined with five low-power modes, is optimized to achieve extended battery life in portable measurement applications. The device features a powerful 16-bit RISC CPU, 16-bit registers, and constant generators that contribute to maximum code efficiency. The digitally controlled oscillator (DCO) allows wake-up from low-power modes to active mode in less than 1 µs.

The MSP430AFE2x3 devices are ultra-low-power mixed signal microcontrollers integrating three independent 24-bit sigma-delta A/D converters, one 16-bit timer, one 16-bit hardware multiplier, USART communication interface, watchdog timer, and 11 I/O pins.

The MSP430AFE2x2 devices are identical to the MSP430AFE2x3, except that there are only two 24-bit sigma-delta A/D converters integrated.

The MSP430AFE2x1 devices are identical to the MSP430AFE2x3, except that there is only one 24-bit sigma-delta A/D converter integrated.

Available family members are summarized in Table 1.

Table 1. Family Members[1]

Device	Flash (KB)	SRAM (Byte)	EEM	SD24_A Converters	16-Bit MPY	Timer_A[2]	USART (UART/ SPI)	Clocks	I/O	Package Type[3]
MSP430AFE253IPW	16	512	1	3	1	3	1	HF, DCO, VLO	11	24-TSSOP
MSP430AFE233IPW	8	512	1	3	1	3	1	HF, DCO, VLO	11	24-TSSOP
MSP430AFE223IPW	4	256	1	3	1	3	1	HF, DCO, VLO	11	24-TSSOP
MSP430AFE252IPW	16	512	1	2	1	3	1	HF, DCO, VLO	11	24-TSSOP
MSP430AFE232IPW	8	512	1	2	1	3	1	HF, DCO, VLO	11	24-TSSOP
MSP430AFE222IPW	4	256	1	2	1	3	1	HF, DCO, VLO	11	24-TSSOP
MSP430AFE251IPW	16	512	1	1	1	3	1	HF, DCO, VLO	11	24-TSSOP
MSP430AFE231IPW	8	512	1	1	1	3	1	HF, DCO, VLO	11	24-TSSOP
MSP430AFE221IPW	4	256	1	1	1	3	1	HF, DCO, VLO	11	24-TSSOP

(1) For the most current package and ordering information, see the Package Option Addendum at the end of this document, or see the TI web site at www.ti.com.
(2) Each number in the sequence represents an instantiation of Timer_A with its associated number of capture compare registers and PWM output generators available. For example, a number sequence of 3, 5 would represent two instantiations of Timer_A, the first instantiation having 3 and the second instantiation having 5 capture compare registers and PWM output generators, respectively.
(3) Package drawings, thermal data, and symbolization are available at www.ti.com/packaging.

Development Tool Support

All MSP430™ microcontrollers include an Embedded Emulation Module (EEM) that allows advanced debugging and programming through easy-to-use development tools. Recommended hardware options include:

- Debugging and Programming Interface
  - MSP-FET430UIF (USB)
  - MSP-FET430PIF (Parallel Port)
- Debugging and Programming Interface with Target Board
  - MSP-TS430PW24
- Production Programmer
  - MSP-GANG430

Continued at: http://www.ti.com/lit/ds/symlink/msp430afe221.pdf

CC1101

Low-Power Sub-1 GHz RF Transceiver

Applications

- *Ultra low-power wireless applications operating in the 315/433/868/915 MHz ISM/SRD bands*
- *Wireless alarm and security systems*
- *Industrial monitoring and control*
- *Wireless sensor networks*
- *AMR – Automatic Meter Reading*
- *Home and building automation*
- *Wireless MBUS*

Product Description

CC1101 is a low-cost sub-1 GHz transceiver designed for very low-power wireless applications. The circuit is mainly intended for the ISM (Industrial, Scientific and Medical) and SRD (Short Range Device) frequency bands at 315, 433, 868, and 915 MHz, but can easily be programmed for operation at other frequencies in the 300-348 MHz, 387-464 MHz and 779-928 MHz bands.

The RF transceiver is integrated with a highly configurable baseband modem. The modem supports various modulation formats and has a configurable data rate up to 600 kbps.

CC1101 provides extensive hardware support for packet handling, data buffering, burst transmissions, clear channel assessment, link quality indication, and wake-on-radio.

The main operating parameters and the 64-byte transmit/receive FIFOs of **CC1101** can be controlled via an SPI interface. In a typical system, the **CC1101** will be used together with a microcontroller and a few additional passive components.

The **CC1190** 850-950 MHz range extender [21] can be used with **CC1101** in long range applications for improved sensitivity and higher output power.

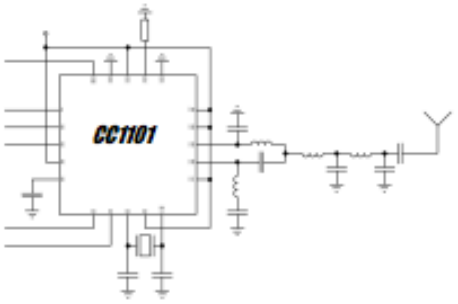

This product shall not be used in any of the following products or systems without prior express written permission from Texas Instruments:

(i) implantable cardiac rhythm management systems, including without limitation pacemakers, defibrillators and cardiac resynchronization devices,

(ii) external cardiac rhythm management systems that communicate directly with one or more implantable medical devices; or

(iii) other devices used to monitor or treat cardiac function, including without limitation pressure sensors, biochemical sensors and neurostimulators.

Please contact low-medical-approval@list.ti.com if your application might fall within the category described above.

Key Features

RF Performance

- High sensitivity
  - -116 dBm at 0.6 kBaud, 433 MHz, 1% packet error rate
  - -112 dBm at 1.2 kBaud, 868 MHz, 1% packet error rate
- Low current consumption (14.7 mA in RX, 1.2 kBaud, 868 MHz)
- Programmable output power up to +12 dBm for all supported frequencies
- Excellent receiver selectivity and blocking performance
- Programmable data rate from 0.6 to 600 kbps
- Frequency bands: 300-348 MHz, 387-464 MHz and 779-928 MHz

Analog Features

- 2-FSK, 4-FSK, GFSK, and MSK supported as well as OOK and flexible ASK shaping
- Suitable for frequency hopping systems due to a fast settling frequency synthesizer; 75 µs settling time
- Automatic Frequency Compensation (AFC) can be used to align the frequency synthesizer to the received signal centre frequency
- Integrated analog temperature sensor

Digital Features

- Flexible support for packet oriented systems; On-chip support for sync word detection, address check, flexible packet length, and automatic CRC handling
- Efficient SPI interface; All registers can be programmed with one "burst" transfer
- Digital RSSI output
- Programmable channel filter bandwidth
- Programmable Carrier Sense (CS) indicator
- Programmable Preamble Quality Indicator (PQI) for improved protection against false sync word detection in random noise
- Support for automatic Clear Channel Assessment (CCA) before transmitting (for listen-before-talk systems)
- Support for per-package Link Quality Indication (LQI)
- Optional automatic whitening and de-whitening of data

Low-Power Features

- 200 nA sleep mode current consumption
- Fast startup time; 240 µs from sleep to RX or TX mode (measured on EM reference design [1] and [2])
- Wake-on-radio functionality for automatic low-power RX polling
- Separate 64-byte RX and TX data FIFOs (enables burst mode data transmission)

General

- Few external components; Completely on-chip frequency synthesizer, no external filters or RF switch needed
- Green package: RoHS compliant and no antimony or bromine
- Small size (QLP 4x4 mm package, 20 pins)
- Suited for systems targeting compliance with EN 300 220 (Europe) and FCC CFR Part 15 (US)
- Suited for systems targeting compliance with the Wireless MBUS standard EN 13757-4:2005
- Support for asynchronous and synchronous serial receive/transmit mode for backwards compatibility with existing radio communication protocols

Improved Range using CC1190

- The ***CC1190*** [21] is a range extender for 850-950 MHz and is an ideal fit for ***CC1101*** to enhance RF performance
- High sensitivity
  - -118 dBm at 1.2 kBaud, 868 MHz, 1% packet error rate
  - -120 dBm at 1.2 kBaud, 915 MHz, 1% packet error rate
- +20 dBm output power at 868 MHz
- +27 dBm output power at 915 MHz
- Refer to AN094 [22] and AN096 [23] for more performance figures of the ***CC1101*** + ***CC1190*** combination

Continued at: http://www.ti.com/lit/ds/symlink/msp430afe221.pdf

Antenna – 0868AT43A0020

High Frequency Ceramic Solutions

868MHz Antenna **P/N 0868AT43A0020**

Detail Specification: 07/26/2010 Page 1 of 3

Recommended Application ISM

General Specifications

Part Number	0868AT43A0020
Frequency Range	858 - 878 Mhz
Peak Gain	-1.0 dBi typ. (XZ-total)
Average Gain	-4.0 dBi typ. (XZ-total)
Return Loss	9.5 dB min.

Input Power	3W max.
Impedance	50 Ω
Operating Temperature	-40 to +85°C
Reel Quanity	1,000
MSL	1

No.	Function
1	Feeding Point
2	NC

Terminal Configuration

Mechanical Dimensions

	In	mm
L	0.276 ± 0.008	7.00 ± 0.20
W	0.079 ± 0.008	2.00 ± 0.20
T	0.031 +.004/-.008	0.80 +0.1/-0.2
a	0.020 ± 0.012	0.50 ± 0.30

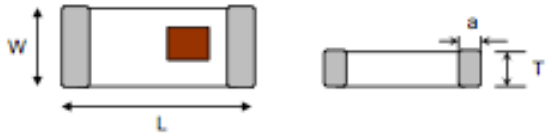

Mounting Considerations

Mount these devices with brown mark facing up. Units: mm

* Line width should be designed to provide 50 Ω impedance matching characteristics.

With Matching Circuit

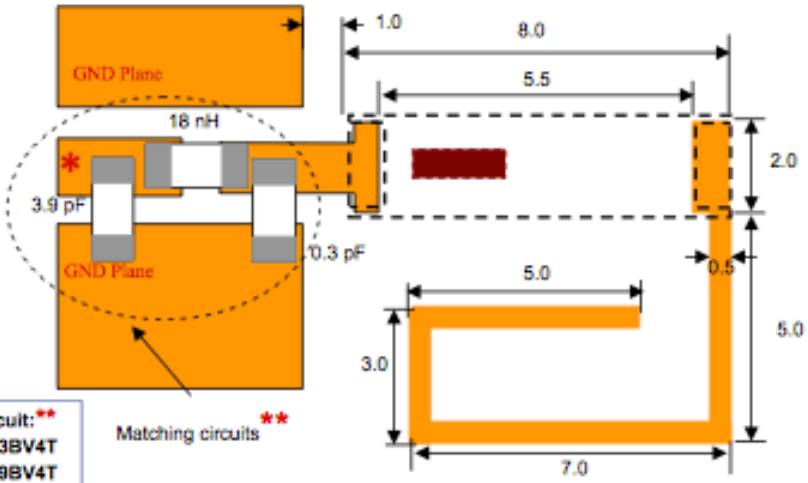

JTI P/N for Matching Circuit:**
Cap (0.3pF): 500R07S0R3BV4T
Cap (3.9pF): 500R07S3R9BV4T
Inductor (18nH): L-07C18NSV6T

Matching circuits **

** matching circuit and component values will depend on PCB layout, thickness, material, etc.

JOHANSON TECHNOLOGY

www.johansontechnology.com
4001 Calle Tecate • Camarillo, CA 93012 • TEL 805.389.1166 FAX 805.389.1821

868MHz Antenna **P/N 0868AT43A0020**
Detail Specification: 07/26/2010 Page 2 of 3

Mounting Considerations

Test Board

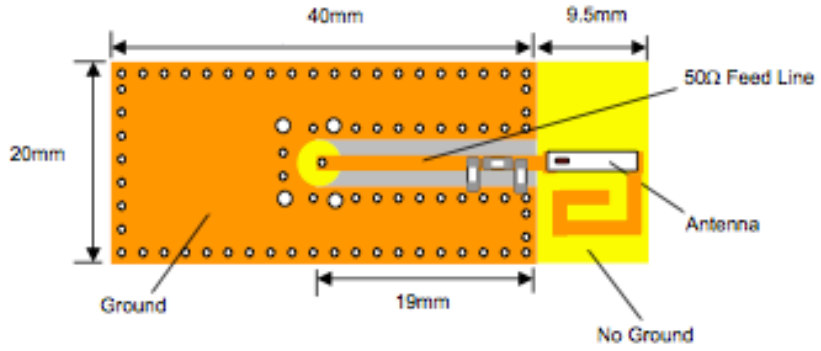

Return Loss (with matching)

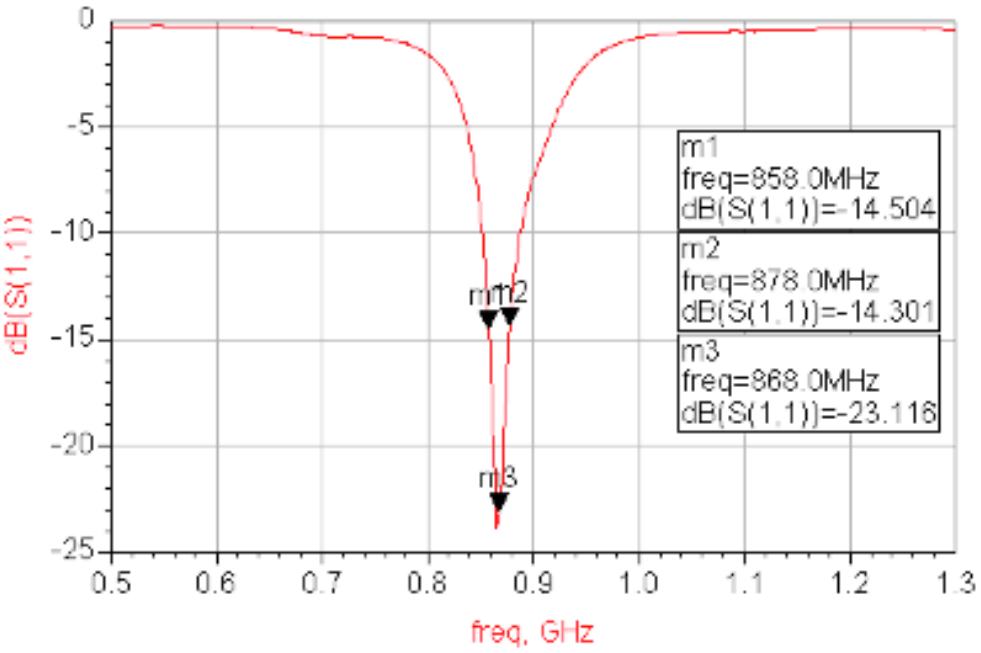

JOHANSON TECHNOLOGY
www.johansontechnology.com
4001 Calle Tecate • Camarillo, CA 93012 • TEL 805.389.1166 FAX 805.389.1821

868MHz Antenna **P/N 0868AT43A0020**
Detail Specification: 07/26/2010 Page 3 or 3

Typical Radiation Patterns

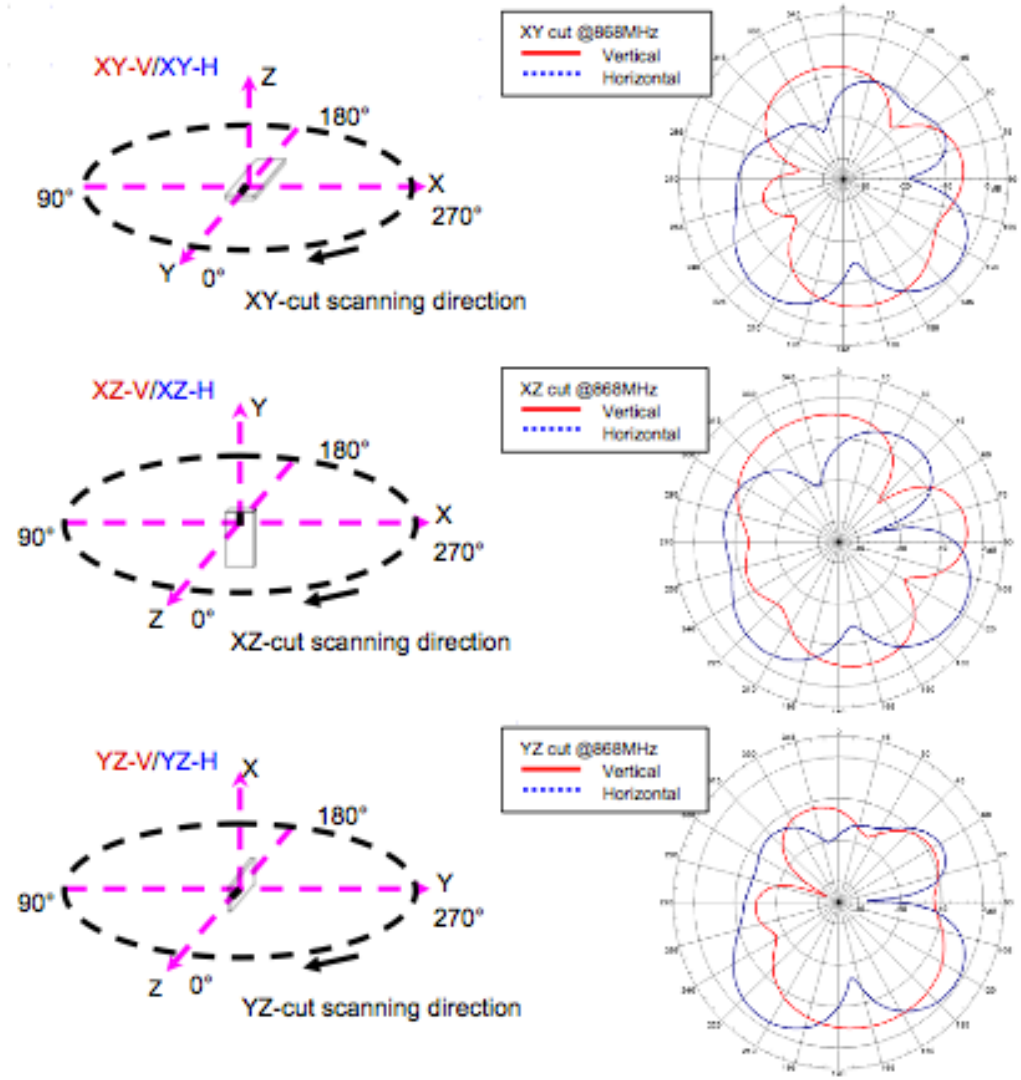

JOHANSON TECHNOLOGY
www.johansontechnology.com
4001 Calle Tecate • Camarillo, CA 93012 • TEL 805.389.1166 FAX 805.389.1821

Li-Ion Battery – QL0200IA

Rechargeable Lithium-ion Batteries

QL0200I-A

PERFORMANCE
- Lithium ion rechargeable cell
- High power design

CHEMISTRY
- LNCAO

MAIN APPLICATIONS
- Medical Implants
- Sensors

KEY FEATURES
- Zero-Volt™ enabled
- Implantable
- Highly reliable
- Domestically produced
- UL1642 certified
- Biocompatibility
- Low self discharge/long calendar life at elevated temperature
- Extended cycle life
- Compact and light weight
- Hermetically sealed

SPECIFICATIONS

ELECTRICAL CHARACTERISTICS

Nominal Capacity	200 mAh
Nominal Voltage	3.6 V
Maximum Recommended Continuous Discharge Current	200 mA
Operating Discharge Temperature	32°C to 42°C

PHYSICAL CHARACTERISTICS

Width	17 mm
Height	35 mm
Thickness	5.5 mm
Weight	8 g
Volume	3.27 cc

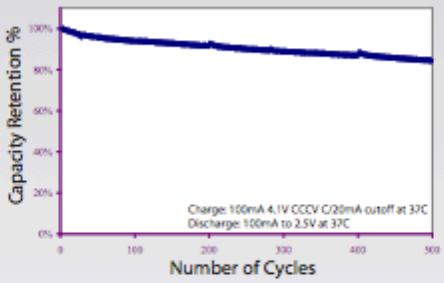

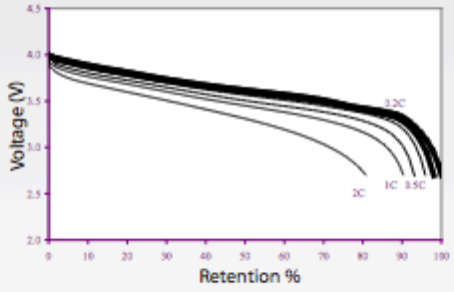

FOR MORE INFORMATION
Contact Paul Beach
paulb@quallion.com
818.833.2000

www.quallion.com

QUALLION
Powering Life.

Quallion LLC | 12744 San Fernando Road | Sylmar, CA 91342 | Info@quallion.com

ALLOY Data

Titanium Alloy Ti 6Al-4V ELI

Type Analysis

Carbon (Maximum)	0.08 %	**Titanium**	Balance
Aluminum	5.50 to 6.50 %	**Vanadium**	3.50 to 4.50 %
Nitrogen (Maximum)	0.05 %	**Iron (Maximum)**	0.25 %
Oxygen (Maximum)	0.130 %	**Hydrogen (Maximum)**	0.013 %
Other, Total (Maximum)	0.40 %		

* Other, Each (Maximum) = 0.1%

** For AMS 4930 rev. D, Hydrogen = 0.0125% and Yttrium = 0.005%

General Information

Description

Pure titanium undergoes an allotropic transformation from the hexagonal close-packed alpha phase to the body-centered cubic beta phase at a temperature of 882.5°C (1620.5°F). Alloying elements can act to stabilize either the alpha or beta phase. Through the use of alloying additions, the beta phase can be sufficiently stabilized to coexist with alpha at room temperature. This fact forms the basis for the creation of titanium alloys that can be strengthened by heat treating.

Titanium alloys are generally classified into three main categories: alpha alloys, which contain neutral alloying elements (such as Sn) and/or alpha stabilizers (such as Al, O) only and are not heat treatable; alpha + beta alloys, which generally contain a combination of alpha and beta stabilizers and are heat treatable to various degrees; and beta alloys, which are metastable and contain sufficient beta stabilizers (such as Mo, V) to completely retain the beta phase upon quenching, and can be solution treated and aged to achieve significant increases in strength.

Ti 6Al-4V ELI is a higher-purity ("extra-low interstitial") version of Ti 6Al-4V, with lower specified limits on iron and the interstitial elements C and O. It is an alpha+beta alloy.

Ti 6Al-4V ELI has been the material of choice for many medical and dental applications due to its excellent biocompatibility. The ELI grade has superior damage tolerance (fracture toughness, fatigue crack growth rate) and better mechanical properties at cryogenic temperatures compared to standard grade Ti 6Al-4V.

Applications

Ti 6Al-4V ELI may be considered in any biomedical application, particularly for implantable components, because of its biocompatibility, good fatigue strength, and low modulus. It could also be considered for any application where a combination of high strength, light weight, good corrosion resistance, and high toughness are required, especially at cryogenic temperatures. Some typical applications where this alloy has been used successfully include joint replacements, bone fixation devices, surgical clips, and cryogenic vessels.

Corrosion Resistance

Ti 6Al-4V ELI spontaneously and immediately forms a stable, continuous, tightly adherent oxide film upon exposure to oxygen in air or water. This accounts for its excellent corrosion resistance in a variety of media. Ti 6Al-4V ELI is highly resistant to general corrosion in most aqueous solutions, as well as in oxidizing acids, chlorides (in the presence of water), and alkalis. Part of the reason for Ti 6Al-4V ELI's good biocompatibility is its corrosion resistance. Body fluids are basically chloride brines with a pH range from about 7.4 to acidic, other

organic compounds-conditions under which Ti 6Al-4V ELI is highly immune to corrosion.

Stress-corrosion cracking (SCC) and crevice corrosion have been associated with exposure to halide ions at elevated temperatures; for this reason, it is general practice to avoid chlorinated solvents and chlorinated cutting fluids in processing titanium.

Titanium and its alloys, including Ti 6Al-4V ELI, are susceptible to hydrogen embrittlement. It is important to minimize hydrogen pickup during processing, particularly heat treating and acid pickling. Specifications for Ti 6Al-4V ELI (ASTM F 136) mill products typically specify a maximum hydrogen limit of 120 ppm.

Important Note: *The following 5-level rating scale is intended for comparative purposes only. Corrosion testing is recommended; factors which affect corrosion resistance include temperature, concentration, pH, impurities, aeration, velocity, crevices, deposits, metallurgical condition, stress, surface finish and dissimilar metal contact.*

Sulfuric Acid	Moderate	Acetic Acid	Excellent
Sodium Hydroxide	Moderate	Salt Spray (NaCl)	Excellent
Sea Water	Excellent	Humidity	Excellent

Medium	Concentration %	Temperature		Corrosion Rate	
		°C	°F	mm/yr	mils/yr
Implanted in Canine Mandibular Bone	-	-	-	nil	nil
Hydrochloric Acid	2	37.8	100	nil - .030	nil - 1.2
Hydrochloric Acid	10	37.8	100	0.508 - 1.02	20.0 - 40.0
Hydrochloric Acid	vapors	37.8	100	8.33 - 1.04	328 - 408
Nitric Acid	65	boiling	boiling	0.076 - 0.13	3.0 - 5.0
Sulfuric Acid	2	37.8	100	0.396 - 0.549	15.6 - 21.6
Sodium Hydroxide	25	boiling	boiling	0.046 - 0.051	1.8 - 2.0

Properties

Physical Properties

One advantage of Ti 6Al-4V ELI over other materials in implantable devices such as joint replacements is its low elastic modulus, which is more similar to that of bone than other biocompatible materials. This is shown in the hyperlink entitled "Elastic Modulus of Some Material."

Density

--	0.1600 lb/in³

Continued at: http://cartech.ides.com/datasheet.aspx?i=101&E=268